Innovative Solutions for Aquaculture: Spatial Impacts and Carrying Capacity – Further Developing, Refining and Validating Existing Models of Environmental Effects of Finfish Farming

Prepared for PIRSA Aquaculture and FRDC

2007

Dr Jason E. Tanner, Dr Timothy D. Clark, Dr Milena Fernandes and Quinn Fitzgibbon

FRDC Project No. 2003/222

SARDI Aquatic Sciences Publication No.F2007/000537

SARDI

SOUTH AUSTRALIAN RESEARCH AND DEVELOPMENT INSTITUTE

This Publication may be cited as:
Tanner, J.E., Clark, T.D., Fernandes, M. and Fitzgibbon, Q. (2007) Innovative Solutions for Aquaculture: Spatial Impacts and Carrying Capacity – Further Developing, Refining and Validating Existing Models of Environmental Effects of Finfish Farming. South Australian Research and Development Institute (Aquatic Sciences), Adelaide, 126pp. SARDI Aquatic Sciences Publication Number F2007/000537

South Australian Research and Development Institute
SARDI Aquatic Sciences
2 Hamra Avenue
West Beach, SA 5024

Telephone: (08) 8207 2400
Facsimile: (08) 8207 5481
http://www.sardi.sa.gov.au

Printed in Adelaide July 2007

SARDI Aquatic Sciences Publication Number F2007/000537
SARDI Research Report Series Number 218

Author(s): J.E. Tanner, T.D. Clark, M. Fernandes and Q. Fitzgibbon
Reviewers: Simon Bryars and John Carragher
Approved: Dr. M. Doroudi

Signed:
Date: 11 July 2007
Distribution: FRDC, PIRSA Aquaculture, SARDI Aquatic Sciences Library
Circulation: Restricted – needs approval from PIRSA Aquaculture

Table of Contents

2003/222 Innovative Solutions for Aquaculture: Spatial Impacts and Carrying Capacity – Further Developing, Refining and Validating Existing Models of Environmental Effects of Finfish Farming

PRINCIPAL INVESTIGATOR: Dr J.E. Tanner
ADDRESS: SARDI Aquatic Sciences
PO Box 120
Henley Beach, SA. 5022.
Telephone: 08 8207 5489
Fax: 08 8207 5481

OBJECTIVES:

1. To develop an understanding of yellowtail kingish metabolism, with specific regard to determining the proportions of feed inputs that end up as dissolved/particulate waste vs respired CO_2.
2. To gain a basic understanding of nutrient flows around yellowtail kingfish cages, and thus further develop and refine an existing model of nutrient outputs to the environment.
3. To validate the outputs of both models against field data, to confirm their validity for estimating potential carrying capacities in aquaculture production areas.

NON TECHNICAL SUMMARY:

OUTCOMES ACHIEVED TO DATE

The models developed in this project provide a much greater understanding of how carbon, nitrogen and phosphorus are dispersed into the environment from yellowtail kingfish farming in Fitzgerald Bay. For the first time, they give us a good estimate of the total amount of nitrogen and phosphorus released into the water column in a soluble form, and the sediments in an insoluble form, allowing direct comparisons to other input sources. The carbon model also gives a visual indication of how organic matter is likely to be deposited around cages, and where the areas of greatest accumulation are likely to occur.

As aquaculture continues to grow, both in South Australia and elsewhere, it is becoming increasingly necessary to understand how wastes are circulated through the environment, both to minimize environmental impacts, and to minimize feedbacks that may reduce production. This information will also allow direct comparisons of nutrient inputs to the marine environment between aquaculture and other industries. In this project, we

develop budgets for both nitrogen and phosphorus derived from feed inputs into a yellowtail kingfish pen in Fitzgerald Bay. These are then used as the basis for a 'carrying capacity' model, which can be used to predict the extent of increased nutrient loadings that will be observed with increases in production. In addition, we refine a model of carbon deposition, and apply it to the same location, to examine likely patterns of aquaculture-derived sediment on the seafloor. To underpin both the nutrient budgets and the models, we also conducted a series of laboratory experiments on fish metabolism (focusing on yellowtail kingfish, but with some work on mulloway), and undertook field investigations of nutrient cycling at Fitzgerald Bay.

The physiological work focused on determining the oxygen consumption of both yellowtail kingfish and mulloway under a variety of environmental conditions. To do this, an existing flume tank was modified into a flume respirometer, that allowed fish of up to 3 kg in weight to be swum against a constant current in an airtight environment, allowing decreases in water oxygen concentrations to be measured. This drop in oxygen then allowed the amount of energy the fish was using to swim at a given speed to be calculated. Using this information, it was also possible to determine how much energy the fish needed simply to maintain itself in a resting state. This information is important for the modeling, as it allows us to estimate how much of the feed inputs are actually metabolized by the fish and released into the water as carbon dioxide, versus how much is released as either dissolved nutrients or solid wastes. Because of problems with the original flume, a second smaller flume was obtained to conduct more detailed studies on YTK. As well as oxygen consumption, these experiments allowed the maximum sustainable swimming speed of both species to be calculated, and for mulloway, the response of fish to lowered oxygen levels was assessed. This experiment showed that mulloway could survive at very low oxyen levels (<20% of saturation), although their metabolic performance suffered when saturation levels dropped below 50%.

The nutrient budget work showed that an annual production of 2,000 tonnes of YTK in Fitzgerald Bay will lead to the release of ~ 400 tonnes of nitrogen and 100 tonnes of phosphorus into the environment. Most of the nitrogen released is in the dissolved form, while most phosphorus is released in particulate form. The nitrogen figure compares to a discharge of ~1,100 tonnes of N from southern bluefin tuna farming off Port Lincoln, 48 tonnes from the Whyalla wastewater treatment plant, and 210 tonnes from the Whyalla steelworks. The carrying capacity model suggests that an additional 1463 tonnes of YTK can be produced in Fitzgerald Bay annually, on top of current production levels of ~2,000 tonnes, before existing water quality guidelines are breached.

The carbon deposition model predicts that areas of high sedimentation are very localized around individual pens. The majority of wastes are dispersed in a north-south direction, with southward dispersal being predominant. There is very little dispersal in an east-west direction. As a result of the tight deposition patterns, increased sedimentation rates outside of leases would only be appreciable if pens are located very close to the lease boundary.

KEYWORDS: Aquaculture, carrying capacity, nitrogen budget, phophorus budget, sedimentation, oxygen consumption, yellowtail kingfish, mulloway.

Acknowledgments

This project was funded as part of the Innovative Solutions for Aquaculture joint initiative by PIRSA Aquaculture and FRDC. SARDI Aquatic Sciences and Adelaide University provided additional support to this project. The authors would like to thank Simon Bryars and John Carragher for their comments on an earlier version of this report. In particularl, we would also like to thank staff of PIRSA Aquaculture for the various involvement in, and comments on, the project throughout its life, including Michael Deering, Colin Johnston, Emily Mellor, Stephen Madigan and Peter Lauer.

Background

The aquaculture industry in South Australia is in the process of undergoing rapid expansion. In response to this, PIRSA Aquaculture have been in the process of revising the management plans for a number of key aquaculture areas. As part of this revision, SARDI Aquatic Sciences have undertaken a series of comprehensive field surveys, and developed preliminary models to assess the environmental effects of finfish farming. These models provide some indication of potential carrying capacities, but also highlight a number of deficiencies in our knowledge of the interaction between aquaculture and the environment. As a result of these deficiencies, it is not currently possible to provide a good estimate of the potential stocking capacity for either finfish or shellfish in any given area, and thus the revised management plans are likely to default to a cautious approach of allowing only limited incremental increases in production.

The current planning process has highlighted the need to further develop the existing models. In particular, there is a need to examine some of the assumptions underlying them and some of the inputs used to parameterise them, in order to facilitate planning over a longer time period and to provide certainty of access to the aquaculture industry. Without increased certainty, substantial investment opportunities could be lost, resulting in decreased growth rates in the aquaculture sector in South Australia. As a result, PIRSA Aquaculture have asked SARDI Aquatic Sciences to develop a project to further refine the current models and their inputs and validate them against field data from select existing aquaculture areas. The data collected and their summation within select models will provide for an integrated approach to enhancing the scientific basis underpinning the management process. It is not intended to use the refined model to predict carrying capacity per se, but rather to integrate our knowledge on the environmental effects of finfish aquaculture, allowing us to compare

alternative management strategies, and to identify important areas in which our knowledge is deficient.

For finfish, there are currently 2 models in use. The first examines local-scale effects of waste deposition around individual pontoons or clusters of pontoons, while the second looks at regional-scale nutrient enrichment. The waste deposition model looks at the amount of carbon waste produced, and using information on settling rates and the current regime, tracks where it is deposited, and by making assumptions about how quickly it is processed by the benthos it also tracks waste accumulation on the sea-floor. The nutrient model looks at outputs of NO_3, NO_2, NH_4 and PO_4, and calculates regional scale enrichment of these ions based on regional flushing rates.

For both models, the key input is feeding rate, which it should be easy to gain an understanding of from farm management data. The processes encapsulated in the models are more problematic, however, as we have a limited understanding of how food inputs are converted to fish waste, or of what happens to the waste once it is produced. For example, the nutrient model assumes that all waste N is released as the form being examined, as we currently do not know how it is partitioned between nitrate, nitrite and ammonia. Similarly, for the waste deposition model, we have had to make an educated guess on how much carbon is released as CO_2 through respiration, rather than being deposited on the seafloor, as our knowledge of the physiology of key species is limited. The Aquafin CRC is funding a major project to look at these questions for tuna, but it is unlikely that the results will be applicable to other species, given the well-known difference between tuna physiology and that of most other finfish species. It is thus important that we gain a basic understanding of the wastes produced in the aquaculture of other species, especially yellowtail kingfish, and how the environment processes these wastes. This will build on the work being undertaken for tuna, in order to both conduct this work most efficiently, and to produce results that can be compared to the results for tuna, with the potential to then be able to gain a greater understanding of what is happening than would be obtained by studying one species in isolation.

Need

Aquaculture is a rapidly growing industry in Australia, and as such there are substantial resource allocation issues. South Australia is at the forefront of this development with a range of innovative aquaculture industries, an active group in PIRSA Aquaculture addressing policy and management issues, and another in SARDI Aquatic Sciences providing the scientific and

technical background information for such matters through targeted research and development (R&D). As such, South Australia provides an ideal model for other states.

While a reasonable level of information exists and, through the Aquafin CRC, continues to grow for tuna farming, this is not the case for most of the other marine aquaculture industry sectors. A fundamental concern in managing these industry sectors is determining the level of production that a given area can sustain without undue effects on the environment. This can be done in two broad ways, the first is by experimentally increasing production and assessing the response of the environment through an environmental monitoring program. The second is through the use of comprehensive models to determine the expected nutrient inputs, under a given level of production in combination with pre-defined trigger points for the nutrients which we believe represent levels above which an environmental impact will occur. The second method is the focus of this project and its advantage is that it allows us to predict the optimal level of production in relation to the principles of ecologically sustainable development. The development and refinement of such models will provide tools to assess the consequences of management responses, allowing a more considered approach to the expansion of the aquaculture industry. Another result will be greater certainty of resource access for industry, which should encourage investment in South Australian aquaculture.

This project will build upon and support the project “Innovative solutions for aquaculture planning and management – Project 5, Environmental audit of aquaculture developments in South Australia”. Both projects will provide much of the scientific and technical data for input into the project “Innovative solutions for aquaculture planning and management – Project 1, Decision support system for aquaculture development”, where “Decision support system” is defined as a computer based, integrated method for supporting management decisions. Decision support systems must incorporate rigorous and scientifically sound decision criteria and, as such they require a good understanding of the potential environmental impacts that may result from aquaculture, as well as the characteristics of existing or future farm sites and the ecosystem in which they exist

Objectives

1. To develop an understanding of yellowtail kingfish metabolism, with specific regard to determining the proportions of feed inputs that end up as dissolved/particulate waste vs respired CO_2.

2. To gain a basic understanding of nutrient flows around yellowtail kingfish cages, and thus further develop and refine an existing model of nutrient outputs to the environment.
3. To validate the outputs of both models against field data, to confirm their validity for estimating potential carrying capacities in aquaculture production areas.

Objective 1:

A series of preliminary experiments were conducted at Adelaide University to examine the metabolic activity of yellowtail kingfish using a large flume respirometer. While there were a number of problems encountered in these experiments, they provided a useful first indication of YTK metabolism, and this work is discussed in chapter 1. While waiting for more fish to become available, a similar series of experiments were conducted with mulloway, with much greater success (see chapter 3). The YTK experiments were followed up with experiments in a second flume, which proved to give much more reliable results. This work is documented in chapter 2.

Objective 2:

Chapter 4 discusses the work conducted to develop nitrogen and phosphorus budgets for two YTK pens in Fitzgerald Bay. These budgets indicate how much of each element is lost to the environment, and whether it is lost in the dissolved or solid form. The values for the two pens are expressed both on a daily basis, and for an entire growout period (close to 1 year). These values have then been scaled up to give an indication of nutrient inputs into the whole of Fitzgerald Bay from YTK farming, and these values are placed into the context of other local inputs. Chapter 5 integrates the data obtained from the experimental work in chapters 2 & 4 into a model of carbon deposition around a group of YTK pens. Chapter 6 integrates the nutrient budgets into a 'carrying capacity' model, which is then used to predict how great an increase in production can be sustained before ANZECC/ARMCANZ water quality guidelines are breached.

Objective 3:

The output of the carbon deposition model is compared to actual sedimentation rates measured in the field in chapter 5. While the model predicts greater carbon deposition than was measured, if a few assumptions are made about how the laboratory data used in developing the model are likely to differ from actual rates in the field, these discrepancies can be explained. It was not possible to validate the carrying capacity model. The original intention was to use changes in nutrient levels in a new farming area off Port Giles to do this validation, however, this farm was not established. The second

option was to rely on a substantial increase in production at Fitzgerald Bay, but again, this did not happen.

Chapter 1: Initial examination of the metabolism and energetics of yellowtail kingfish (*Seriola lalandi*): review of literature and methodology development

Q. P. Fitzgibbon

School of Earth and Environmental Sciences,
University of Adelaide,
Adelaide, South Australia, 5005

1.1 Abstract

Aquaculture of yellowtail kingfish (YTK - *Seriola lalandi*) is rapidly growing in South Australia, however, there is no information on their metabolic physiology. Gaining an understanding of a species metabolism is essential in order to improve aquaculture efficiency, as precise metabolic data are required for calculations of aquaculture system oxygen requirements, fish energy requirements, environmental impact assessment, and species-specific physiological thresholds. This chapter reviews fish metabolism with reference to aquaculture, YTK, and metabolic research on active fish. It outlines the development of a water tunnel respirometer from an existing flume tank. Initial testing of this respirometer showed that YTK acclimatized to the respirometer within 6 h of introduction. The standard metabolic rate (R*s*) (77 mg h^{-1}, normalized to a mass of 1 kg, n=6) was found to be similar to other active fish species and scaled with respect to mass (mass scaling exponent *b*=0.85), like most teleost species examined. In a subsequent experiment, the critical swimming velocity was found to be 1.57 $\pm$ 0.18 body-lengths s^{-1} (mean $\pm$ SE, n=10), corresponding to an active metabolic rate of 506 $\pm$ 44 mg kg^{-1} h^{-1}. However, in this experiment, the fish failed to fully acclimatize to the respirometer, resulting in the elevation of R*s* (274 $\pm$31 mg kg^{-1} h^{-1}, n=10). Furthermore, several individuals failed to recover from handling and transport stress. It is hypothesized that this stress susceptibility was related to culture deformities of the particular cohort of YTK examined. Techniques to improve YTK metabolic research success are discussed.

1.2 Introduction

The marine farming of yellowtail kingfish (YTK - *Seriola lalandi*) is a rapidly growing aquaculture sector in South Australia. Species of the genus *Seriola* are circumglobal, and are important to commercial and recreational fisheries in many countries. For many years, the culture of yellowtail (*Seriola*

quinqueradiata) has supported a large and profitable aquaculture industry in Japan, where the flesh is highly regarded for raw consumption as sushi and sashimi (Poortenaar *et al.*, 2001). Driven by a high demand and price for *Seriola spp*. in international seafood markets, countries including Australia, Ecuador, Japan and several in Europe are striving to produce these fish commercially (Benetti *et al.*, 2001). Presently, there are several YTK marine sea-cage farms in South Australia and YTK farming is considered a growth industry for the state. The rapid development of the YTK aquaculture industry has highlighted the need for, and lack of, physiological information for the species. Gaining an understanding of the basic physiology is essential in order to improve YTK aquaculture efficiency. Precise metabolic data are required for calculations of aquaculture system oxygen requirements, fish energy requirements, environmental impact assessment, and species-specific physiological thresholds.

1.2.1 Fish metabolism and energetics

From an energy budget perspective, fish, like all organisms, use energy obtained from the ingestion of food (U) for the synthesis of tissues (P), and as fuel in the metabolic process (R), with some energy being lost as waste products (W) (Calow, 1985; Jobling, 1994). The metabolic process powers the synthesis of tissues and all other physiochemical work required by the organism. As oxygen is required in the enzymatic steps involved with the metabolic process, oxygen consumption ($\dot{M}_{O_2}$) has almost universally been used to determine metabolic rate in fish through indirect calorimetry (Fry, 1971; Brett, 1972). Aerobic metabolism (R) in fish can be broken into 3 main categories (reviewed by Calow, 1985; Priede, 1985; Jobling, 1994; Korsmeyer *et al*., 1996; Korsmeyer and Dewar, 2001): (i) standard metabolic rate (R*s*) is the resting and fasting metabolic rate and is theoretically the minimal metabolic rate of the animal, (ii) metabolism due to locomotory activity (R*a*), which is typically swimming in fish, and finally, (iii) the metabolic rate attributed to the activities of food digestion and assimilation (R*f*), also often referred to as “specific dynamic action”. The relationship between the above parameters may be represented as follows:

$$U = P + R + W \quad (1.1)$$

where:

$$R = Rs + Ra + Rf \quad (1.2)$$

*R*s – *Standard metabolic rate*

Common methods of measuring R*s* include: (i) recording the $\dot{M}_{O_2}$ of a motionless resting fish (Fu *et al.*, 2005b), (ii) extrapolating the relationship

between $\dot{M}_{O_2}$ and swimming velocity back to zero velocity (Dewar and Graham, 1994; Sepulveda and Dickson, 2000), or (iii) measurement of $\dot{M}_{O_2}$ of immobilized specimens (neuromuscular or spinal block) (Brill, 1979; 1987). Use of the last two techniques is most common for active fish species. Validation for both techniques was recorded by Brill (1987), who found that the R*s* of aholehole (*Kuhlia sanduicensis*) and rainbow trout (*Oncorhynchus mykiss*) measured by neuromuscular blocking, was not significantly different from published data of R*s* measured by extrapolating the $\dot{M}_{O_2}$/swimming velocity relationship back to zero velocity.

Ra – Aerobic locomotion

In order to further explain the aerobic cost of locomotion, some terminology must be outlined (Brett, 1972; Korsmeyer and Dewar, 2001). Routine metabolic rate (RMR), refers to the average aerobic metabolism associated with spontaneous activity and may occur over a wide range of values. Active metabolic rate (AMR) refers to the maximum sustained rate (for 1 h by definition) of aerobic metabolism without fatigue. The difference between AMR and R*s* represents an animal's aerobic capacity or metabolic scope. In fish, $\dot{M}_{O_2}$ increases exponentially with swimming speed until it reaches the "critical velocity" (U_{crit}) corresponding to the AMR of the animal. Higher speeds can be achieved, but they must involve anaerobic metabolism and result in an oxygen debt and fatigue. This is often referred to as burst swimming, and in fish, oxygen demand during these events can exceed oxygen supply by an order of magnitude (Brett, 1972).

Rf – Specific dynamic action

R*f* is defined as the increase in metabolic rate following the ingestion of food and represents the metabolic expenditures for ingestion, digestion and absorption (Jobling, 1981). As the energetic cost of mechanical food ingestion and digestion has been found to be small in fish (Tandler and Beamish, 1979; Jobling and Davis, 1980; Jobling, 1981), R*f* is considered mostly a post-absorptive effect attributed to catabolism events such as amino acid deamination (Beamish and Trippel, 1990; Cho and Kaushik, 1990) or anabolic processes like protein synthesis (Brown and Cameron, 1991a; b; Lyndon *et al.*, 1992). In poikilothermic (cold-blooded) species, this is most commonly measured as the post-prandial (i.e. post-feeding) increase in $\dot{M}_{O_2}$ (Jobling and Davis, 1980; Jobling, 1981; Fu *et al.*, 2005a; Fu *et al.*, 2006). In fish, $\dot{M}_{O_2}$ generally peaks soon after ingestion, followed by a gradual decline to the pre-feeding or resting level (Jobling, 1981). The magnitude of this effect is measured by calculating the total $\dot{M}_{O_2}$ above the resting level, and commonly includes quantification of the peak and duration. The peak level of post-prandial $\dot{M}_{O_2}$ in fish is generally twice the

resting level and, in most fish species tested, the magnitude represents 9-20% of the ingested energy (reviewed by Jobling, 1981).

1.2.2 The effect of body mass and temperature

In general, the relationship between metabolism and weight in fish can be described by the equation (Fry, 1971; Clarke and Johnston, 1999):

$$R = aW^b \quad (1.3)$$

where "R" is the rate of metabolism, "W" is fish body weight, "a" is a constant and "b" is the scaling component. Clark and Johnson (1999) collated the published R*s* - mass relationship for 69 teleost species and found that, of the 110 studies examined, 80% reported a scaling component of b=0.65 – 0.95, with a total study mean of b=0.79. More recently, White and Seymour (2005) found a teleost interspecific exponent of *b*=0.88. As this coefficient is less than 1.0, fish mass-specific R*s* declines proportionately as an animal gets larger.

The relationship between environmental temperature and R*s* in fish is curvilinear (Brett, 1972). The data from published studies examining the relationship between R*s* and temperature for teleost fish shows that an Arrhenium model best describes the relationship as follows (Clarke and Johnston, 1999):

$$R = A \exp(-\mu / GT) \quad (1.4)$$

Where: "A" is a constant, "μ" the Arrhenius constant, "G" the universal gas constant and "T" the absolute temperature. When Clarke & Johnston (1999) applied this model to the more commonly used Q_{10}, they found that the mean of the 69 species was 1.83, but the within-species median was 2.40 (the frequency distribution being negatively skewed). This implies that the metabolic rate of fish approximately doubles with increasing temperature of 10^oC.

1.2.3 Metabolism and aquaculture

The basic principle of bioenergetics involves the energy budget equation stated earlier (eqn 1.1). Put simply, energy consumed is used in the metabolic process, deposited as new body tissue, or lost as wastes (Calow, 1985; Jobling, 1994). Therefore, bioenergetic studies are principally concerned with the physiological basis behind the relationship between feeding and growth. As feed costs represent a considerable component of aquaculture expense, and tissue growth is the ultimate aim of aquaculture farms, understanding and optimizing this relationship is critical for fish farming. Defining and evaluating the energy cost associated with

metabolism is an essential component of bioenergetic studies, therefore metabolic data obtained in the present experiments will greatly help the further examination of bioenergetics in YTK.

Metabolism also represents a considerable proportion of energy losses from the system, and R*a* and R*f* are of particular importance to aquaculture. R*s* has little direct relevance to fish farming, however, it is often important as a baseline for metabolic state comparisons. Swimming activity (R*a*) represents a major component of energy expenditure of fish, especially for highly active species. Specific dynamic action (R*f*) can also represent a considerable proportion of energy losses, accounting for up to 20% of the ingested energy (Jobling, 1981).

1.2.4 Common fish metabolic physiology technologies and techniques

The majority of recent aerobic metabolism studies of active fish have been conducted in water tunnel respirometers (Brett, 1972; Dewar and Graham, 1994; Grottum and Sigholt, 1998; Sepulveda *et al.*, 2003). These respirometers generally work by encouraging a fish to swim against a current of water pumped through a stationary swimming chamber. The advantage of tunnel respirometers is that the activity of the fish can be accurately controlled and manipulated (Jobling, 1994). The basic design of the most commonly used respirometers is shown in Figure 1.1.

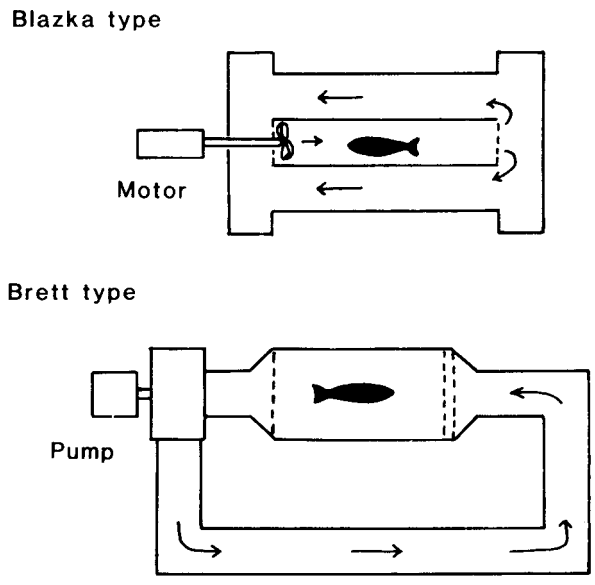

Figure 1.1: Common tunnel respirometer used for fish metabolism experiments, the Brett and Blazka type respirometers (Jobling, 1994).

Even, rectangular flow, through the swim chamber is critical to the design of a respirometer. Driving the water through horizontal cylinders and grids of

various sizes will facilitate the production of a rectangular plane of uniform turbulence (Beamish, 1978). Once the flow chamber is constructed, uniform flow should be visually assessed by dye flow patterns (Sepulveda and Dickson, 2000).

Oxygen consumption ($\dot{M}_{O_2}$) of the fish can be calculated by the equation:

$$\dot{M}_{O_2} = Vr \bullet \Delta O_2 w / \Delta t \bullet BW \qquad (1.5)$$

where "Vr" is the total water volume of the respirometer, "$\Delta O_2 w$" is the change in oxygen concentration of the water, "Δt" is the corresponding time period and "BW" is the fish's body weight. During each trial, it is important to avoid large changes in oxygen concentration and accumulation of CO_2 or excretory products, as this may affect the $\dot{M}_{O_2}$ of the fish (Steffensen, 1989).

Before introduction to the swimming chamber, it is customary to starve the fish to ensure that it is in the post-absorptive state. The starvation time required varies between species and studies, however, a period of between 24 and 72 hours is generally accepted (Gooding *et al.*, 1981; Dewar and Graham, 1994; Jobling, 1994; Grottum and Sigholt, 1998). A sufficient acclimation period is also required to allow the fish to recover from handling, and to become familiar with its new environment. A period greater than 12 hours is generally accepted (Beamish, 1978), however for some active fish species studied, this time can be considerably less (Tsukamoto and Chiba, 1981; Dewar and Graham, 1994). During this period, slow water flow should be generated to provide orientation and to avoid oxygen depletion. Also during this period, the fish should be kept from external disturbances and low ambient light levels often accelerate acclimation. In most respirometer experiments on active fish, the swim chamber is covered with light limiting material (such as cloth) to reduce outside disturbances (Graham and Laurs, 1982; Dewar and Graham, 1994; Sepulveda and Dickson, 2000).

Respiratory trials generally consist of measuring the $\dot{M}_{O_2}$ of the fish at steady swimming velocities over 1 h periods (Brett, 1972). This is followed by a consistent stepwise increase in velocity until the critical velocity (U_{crit}) is reached. The U_{crit} is usually visually assessed as the speed at which the fish is unable to maintain its position with steady, continuous tail beats assumed to be powered by the slow-twitch, oxidative mytotomal muscle (Sepulveda and Dickson, 2000). Passing the U_{crit} normally results in the fish resorting to irregular burst swimming or falling back into the downstream screen. At this stage, the trial is generally terminated and the exact critical speed calculated by the equation (Beamish, 1978):

$$U_{crit} = Ui + (Ti / Tii \bullet Uii) \quad (1.6)$$

Where: "Ui" is the highest velocity maintained for the entire prescribed period, "Uii" the velocity increments, "Ti" is the time the fish swam at the fatigue velocity and "Tii" the prescribed swimming period. At this stage, $\dot{M}o_2$ at a previously tested reduced velocity can be used to evaluate the passing of the U_{crit}. If $\dot{M}o_2$ is greater than previously measured, it can be assumed that the fish had acquired an oxygen debt. Also, analysis of the data should indicate the U_{crit}, as $\dot{M}o_2$ should increase exponentially until the critical velocity where $\dot{M}o_2$ will plateau.

1.2.5 Metabolism of yellowtail kingfish

The metabolic parameters of YTK have never been assessed, however Tsukamoto and Chiba (1981) examined the $\dot{M}o_2$ of a closely related *Seriola* species, the yellowtail. In that study, 700-800 g fish were swum for 30-60 min at four test-swimming velocities (24, 36, 49 and 62 cm s^{-1}). Oxygen consumption was found to increase with velocity, with a remarkable increase as the velocity changed from 49 to 62 cm s^{-1}. However, the rate of increase did not prove to be exponential. Tsukamoto and Chiba (1981) hypothesized that the lack of an exponential increase in oxygen consumption with swimming speed was due to the fish passing the U_{crit} between 49 and 62 cm s^{-1}. Thus, soon after 49 cm s^{-1}, $\dot{M}o_2$ failed to increase with swimming velocity, but instead plateaued at the AMR, after which an oxygen debt began to accumulate. This hypothesis was supported by a study that measured electrical activity and lactate production in red and white muscle in relation to swimming velocity with similar sized yellowtail (Tsukamoto, 1981). In that study, electrical discharge was only recorded from the anaerobic white muscle when the swimming velocity was increased past 49 cm s^{-1}. There was also a corresponding marked increase in blood lactate levels at this swimming speed. Tsukamoto and Chiba (1981) concluded that the U_{crit} was 53 cm s^{-1}, corresponding to an AMR of 600-800 mg kg^{-1} h^{-1}. Extrapolation of the $\dot{M}o_2$ relationship back to zero velocity showed an R*s* of 200 mg kg^{-1} h^{-1}. However, in a subsequent study with equivalent sized yellowtail, R*s* was found to be considerably less than this value. Yamamoto and Itazawa (1981) measured oxygen consumption of lightly anaesthetized yellowtail (750-1245 g) in a small flow-through cylindrical chamber (44×12 cm) at a "resting" swimming velocity (1.62 L min^{-1}). In that study, R*s* was estimated to be approximately half (103 mg kg^{-1} h^{-1}) of that predicted by Tsukamoto and Chiba (1981). The reason for this discrepancy is unclear, although it is most probably due to the considerable difference in experimental protocols.

In order to make relevant comparisons with the above-published metabolic rates, it is essential to represent swimming velocity in body lengths s^{-1} (BL s^{-1}). Tsukamoto and Chiba (1981) did not publish the length data for the fish used, however, in a similar Japanese study that used equivalent sized yellowtail (750-1245 g), lengths were given (395-483 mm) (Yamamoto and Itazawa, 1981). As the yellowtail were bought at a similar time from Japanese commercial fish farms, it is unlikely that the condition factor of the fish would greatly vary between the experiments. Therefore, to aid in experimental design, an average length of 395 mm has been assigned to the average 750 g yellowtail used in Tsukamoto and Chiba (1981), thus giving a experimental velocity range of 0.6-1.6 BL s^{-1} with a critical velocity of 1.3 BL s^{-1}.

At present, the magnitude and duration of R*f* in *Seriola* species is unknown. However, Shimeno *et al.* (1993) measured the rate that yellowtail digest 2% of body weight (%BW) rations of either formulated fish pellets or fresh fish. They found that both diets were digested at similar rates and were nearly all digested within 24 h of feeding. In fish, it is hypothesized that there is a close relationship between the rate of digestion and R*f*. Jobling and Davies (1980) found that R*f* in plaice (*Pleuronectes platessa*) was observed for just a slightly longer period than the passage of food through the gut. Furthermore, De La Gandara *et al*. (2002) found that oxygen consumption of groups of Mediterranean yellowtail (*Seriola dumerili*) in open tanks fell to basal levels within 24 h of feeding. These studies suggest that the duration of R*f* in YTK is likely to be approximately 24 h. However, species differences and the effects of ration, feed composition and temperature, are likely to greatly influence R*f* in YTK.

1.2.6 Direction of research

As YTK are known to be a highly active species, it was believed that a Brett-type water tunnel respirometer would be best to examine their metabolic physiology. Water tunnel respirometry allows control of the swimming velocity, thus facilitating the evaluation of R*s*, cost of R*a* and the metabolic scope. Unfortunately there was not a water tunnel sufficient in size and velocity range within South Australia or known within Australia. There was, however, a large flume tank sufficient in size at the University of Adelaide. The following description outlines the transformation of this flume into a functioning Brett-type water tunnel respirometer. Furthermore, it discusses the validation of this flume as a functioning respirometer and the development of techniques required for YTK metabolic research.

1.3 Materials and Methods

1.3.1 Flume tank modifications and preliminary testing

In order to transform the flume tank at the School of Earth and Environmental Sciences, University of Adelaide, into a functioning Brett-type water tunnel respirometer, some major modifications were required. Principally this involved the design and construction of a sealed lid, temperature control mechanism and saltwater delivery facility. The completed respirometer is shown in Figure 1.2 and modifications performed were as follows. (i) Construction of a three-piece sealed perspex lid with a hinged access hatch and sealed stainless steel bearing around the engine shaft. This lid is sealed on neoprene gaskets and contains sixteen air release valves to allow removal of trapped air. (ii) Installation of a new engine shaft with enlarged propeller to increase flume water flow velocity capabilities. (iii) Installation of a temperature control unit to maintain water temperatures within $\pm 0.2^{o}$C. (iv) Construction and installation of perspex water flow diverters to induce a uniform water flow distribution through-out the working section. (v) Design and installation of a saltwater delivery pipeline to allow the flume to be gravity filled with saltwater that is delivered in a water transport vessel. (vi) Installation of dissolved oxygen analysis equipment that includes; two Cameron Instruments Co. oxygen electrodes, a peristaltic pump that perfuses a consistent even stream of sampled water over the electrode surfaces, a computer that logs all recorded data in real time using Sable Systems Co. data acquisition software and a water bath to maintain the oxygen electrodes at a consistent temperature. (vii) Shade cloth covering to induce dark ambient conditions within the working section.

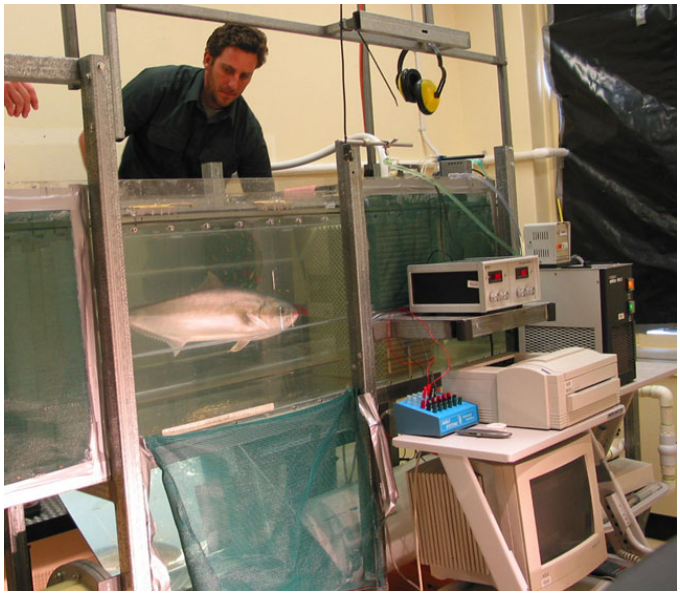

Figure 1.2**.** The completed water tunnel respirometer at the end of a preliminary experiment with a 3.04 kg yellowtail kingfish. Also shown is the dissolved oxygen data collection and logging equipment (oxygen electrodes and meter, computer for real time data logging, water bath to maintain electrode temperature and peristaltic pump to pass sampled water over the electrode surface).

The completed respirometer held a total of 850 L and was predominantly constructed from acrylic plastic and large diameter unplasticised polyvinyl chloride storm-water pipe. Water flow was driven by a single 20 cm propeller powered by a 1.5 kW CMG Electric motor with Nord AC® variable speed controller, enabling a maximum water flow velocity of 60-70 cm s^{-1}. Circulating water passes through flow-resistance tubes (1 cm internal diameter × 25 cm long) to induce even laminar flow before entry into the working section. Laminar flow was verified by video observation of neutrally buoyant particles (wet cotton wool balls) drifting through the working section with a MotionScope® PCI High Speed Video System. The working section is 100 × 40 × 40 cm (length × width × height). Water velocity calibrations were made with a Sontek (ADV) Acoustic Doppler velocimeter (mean 25hz for 10 s), from 10 positions (five horizontal × two vertical intervals) in the active working section. The coefficient of variation between mean flow velocity and sample position was found to be low (<6.1%, n=10). The integrity of the respirometer seal was examined in an experiment that involved dropping the internal dissolved oxygen content to 5.2 mg L^{-1} (70% saturation) with sodium sulphite (combined with cobalt chloride to catalyse the reaction). Passive oxygen diffusion back into the respirometer was found to be less than 1% per h.

1.3.2 Experimental animals

Yellowtail kingfish were randomly selected from 2,000 L flow-through (3 mm gravel filtered seawater) tanks at the South Australian Research and Development Institute, Aquatic Sciences, West Beach facility. Fish were maintained at ambient light and water temperature. Fish were fed Skretting Nova® marine diet to satiation once a day, but were starved for a minimum of 36 h before the beginning of any experimental trials.

1.3.3 General procedures

For each experimental trial, individual fish were scoop-netted from the stock tank and immediately transferred into a 2,000 L fish transport container filled with seawater and transported 13 km to the University of Adelaide campus where all respiratory trials were conducted. Seawater from the transport container was used to gravity fill the respirometer. Fish were introduced into the working section through a hinged hatch, which was sealed immediately, and the up-stream half covered to limit visual disturbance. At introduction, water flow velocity was set at near maximum (60 cm s^{-1}) as it was found that fish were less likely to panic and turn if given a fast water flow to swim against. In the subsequent 3 h, water flow velocity was gradually reduced to ~0.6 BL s^{-1} to facilitate steady swimming and stayed at this speed for the remainder of the acclimation period. This speed was the start point velocity for all experimental trials. Fish generally maintained position within the shaded forward half of the working section, only falling back to the visible

rear section when unable to maintain position against the water current. Once sealed, water level was topped-up by gravity feed from the fish transport vessel and gas bled from the system through the sixteen bleeder valves. Water dissolved oxygen was manipulated by bubbling air or oxygen through a large air stone in-between $\dot{M}_{O_2}$ measurements and was maintained above 5.6 mg L^{-1} (~75 % saturation) for all experimental trials. During the acclimation period, gently bubbled air maintained dissolved oxygen above 7 mg L^{-1}. During all experiments, respirometer water temperatures were maintained between 21.8 and 22.2°C. Following experimental trials, fish were anaesthetized in 0.05 mg L^{-1} clove oil, and fork length (BL) and mass (M) recorded.

1.3.4 Experimental protocols

Fish $\dot{M}_{O_2}$ was recorded over a 1 h period before the swimming velocity was changed and the next swim trial begun. This procedure continued until the U_{crit} or the maximum water flow velocity was reached and the experiment terminated. U_{crit} was defined as when the fish resorted to burst and glide swimming and brushed its tail up against the back screen more than three times in 30 s. U_{crit} was calculated using the equation (Brett, 1964):

$$U_{crit} = U_c + [(T_f / T_i) \bullet U_i] \qquad (1.7)$$

where U_c is the last speed at which the fish swam the entire 1 h period, T_f is the time the fish swam at the final speed, T_i is the time interval at each speed (1 h), and U_i is the velocity increments.

At the end of the experiment the fish was removed from the respirometer and background respiration measured. Although background respiration was found to be small, all fish oxygen consumption results were adjusted accordingly. Three experiments were conducted:

1. Acclimation experiment: In order to establish the required acclimation period, three YTK (2.65, 1.03 and 3.04 kg) were individually swum at a constant swimming velocity of ~0.6 BL s^{-1} for 24 h and $\dot{M}_{O_2}$ recorded over a 1 h period at 6, 10, 14, 18 and 22 h after introduction. Fish were introduced in the late afternoon and dissolved oxygen maintained near normoxia by bubbling air between $\dot{M}_{O_2}$ measurements.

2. Standard metabolic rate (Rs) and effect of body mass: The $\dot{M}_{O_2}$ of YTK of varying size (0.948-4.32 kg) was determined when swimming velocity was increased by increments of 5-10 cm s^{-1} until the U_{crit} or the maximum water flow velocity was reached.

3. Critical swimming velocity (U_{crit}) and active metabolic rate (AMR): The $\dot{M}_{O_2}$ of YTK of similar size (0.769 ± 0.049 kg) was determined when swimming velocity was increased by increments of 10 cm s^{-1} until the U_{crit} was reached.

1.3.5 Data Analysis

Fish oxygen consumption rate was determined by the following equation:

$$\dot{M}_{O_2} \text{ (mg kg}^{-1} \text{ h}^{-1}) = ((O - B) \bullet V)/ M \qquad (1.8)$$

where O is the fish oxygen consumption recorded (mg L^{-1} h^{-1}), B is the recorded relevant background respiration rate for the trial (mg L^{-1} h^{-1}), V is the respirometer volume (L) and M is the fish mass (kg). The relationship between $\dot{M}_{O_2}$ and swimming velocity was then assessed using exponential regression. Standard metabolic rate was determined by extrapolation of the $\dot{M}_{O_2}$ exponential relationship back to a swimming velocity of 0.0 cm s^{-1}. Statistical differences represented are Analysis of Variance with Tukey Post-Hoc analysis ($P<0.05$) performed using Microsoft StatistiXL software. Values are mean ±SE.

1.4 Results

1.4.1 Acclimation experiment:

At a constant swimming velocity of ~0.6 BL s^{-1}, the $\dot{M}_{O_2}$ of the three fish examined was similar (255 ± 11.8, 235 ± 13.0, 226 ± 8.59 mg kg^{-1} h^{-1}, for fish 1,2, and 3 respectively, n=5) (Figure 1.3) and there was no significant difference in $\dot{M}_{O_2}$ with acclimation time (ANOVA: $F_{4,10} = 0.894$, $P=0.502$). These results demonstrate that a minimum period of at least 6 h was sufficient time for YTK acclimation.

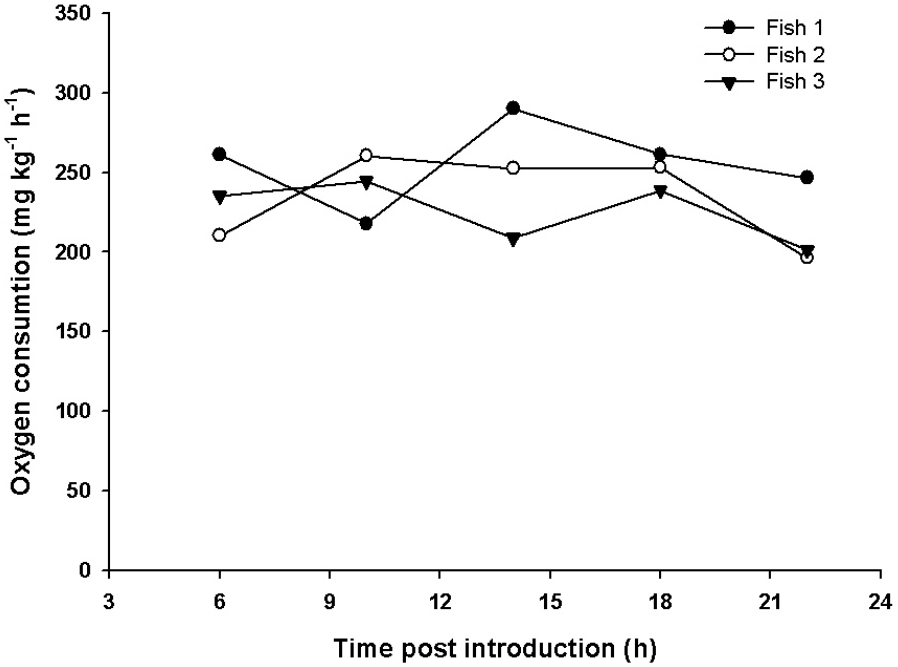

Figure 1.3. Oxygen consumption of three yellowtail kingfish (2.65kg, 3.04 kg and 1.03 kg for fish 1,2 and 3 respectively) for 22 h after introduction into the respirometer at a constant swimming velocity of 0.6 BL s^{-1}.

1.4.2 Standard metabolic rate (Rs) and effect of body mass

Five out of eleven YTK swim trials were unsuccessful. These trials generally resulted in the YTK turning and panicking within the flume. On most occasions this panic event would occur within the first hour after introduction, however, it could occur at any stage within the experiment.

Of the six successful trials, the swimming velocity range (U) achieved was variable and largely dependent on fish size (Table 1.1). The minimum comfortable swimming velocity was found to be ~0.6 BL s^{-1}, and thus in cm s^{-1} was greater for large fish than for small fish. Below this velocity, the fish's swimming would become more erratic and it would become prone to turning within the respirometer. U_{crit} was not achieved in any of the trials, as the fish used were able to maintain their position within the flume at the maximum velocity achievable. For the smallest fish (0.948 kg), it was likely that the maximum velocity examined (65 cm s^{-1}) was close to the U_{crit}, as at this velocity the fish resorted to burst and glide swimming. This inference is supported by the apparent flattening in $\dot{M}_{O_2}$ at this velocity (Fig 1.4b). Also, immediately following this trial, $\dot{M}_{O_2}$ was elevated (327 mg h^{-1}) when fish were swum at a slow velocity (15 cm s^{-1}), suggesting that the fish had

acquired an oxygen debt. If 65 cm s^{-1} is taken to be the U_{crit} for this individual it would correspond to 1.5 BL s^{-1}.

Table 1.1: Mass (M), body length (BL), swim velocity range (U) and exponential relationship between $\dot{M}_{O_2}$ and swimming velocity ($\dot{M}O_2$ (mg h^{-1}) = a•e^{bU}).

M (kg)	BL (cm)	U (cm s^{-1})	Exponential Relationship		R^2
			Scaling factor (a)	Exponent (b)	
0.948	42.2	25-65	70	0.033	0.96
1.627	48.0	35-65	117	0.025	0.99
2.812	57.0	35-55	235	0.018	0.93
2.958	57.5	45-55	168	0.024	0.99
3.370	61.0	45-65	250	0.017	0.99
4.360	67.0	40-60	228	0.030	0.56

In all experiments $\dot{M}_{O_2}$ increased exponentially with swimming velocity (Table 1.1). The standard metabolic rate (R*s*) derived by extrapolation of the swimming velocity/$\dot{M}_{O_2}$ relationship to a velocity of zero (scaling factor in Table 1) ranged between 70 and 250 mg h^{-1}. When these R*s* values are plotted against mass, a strong allometric relationship (R^2=0.90) was found (Fig 1.4a), corresponding to a study R*s* of 77.2 mg h^{-1} (normalized to a mass of 1 kg) with a scaling exponent of 0.85.

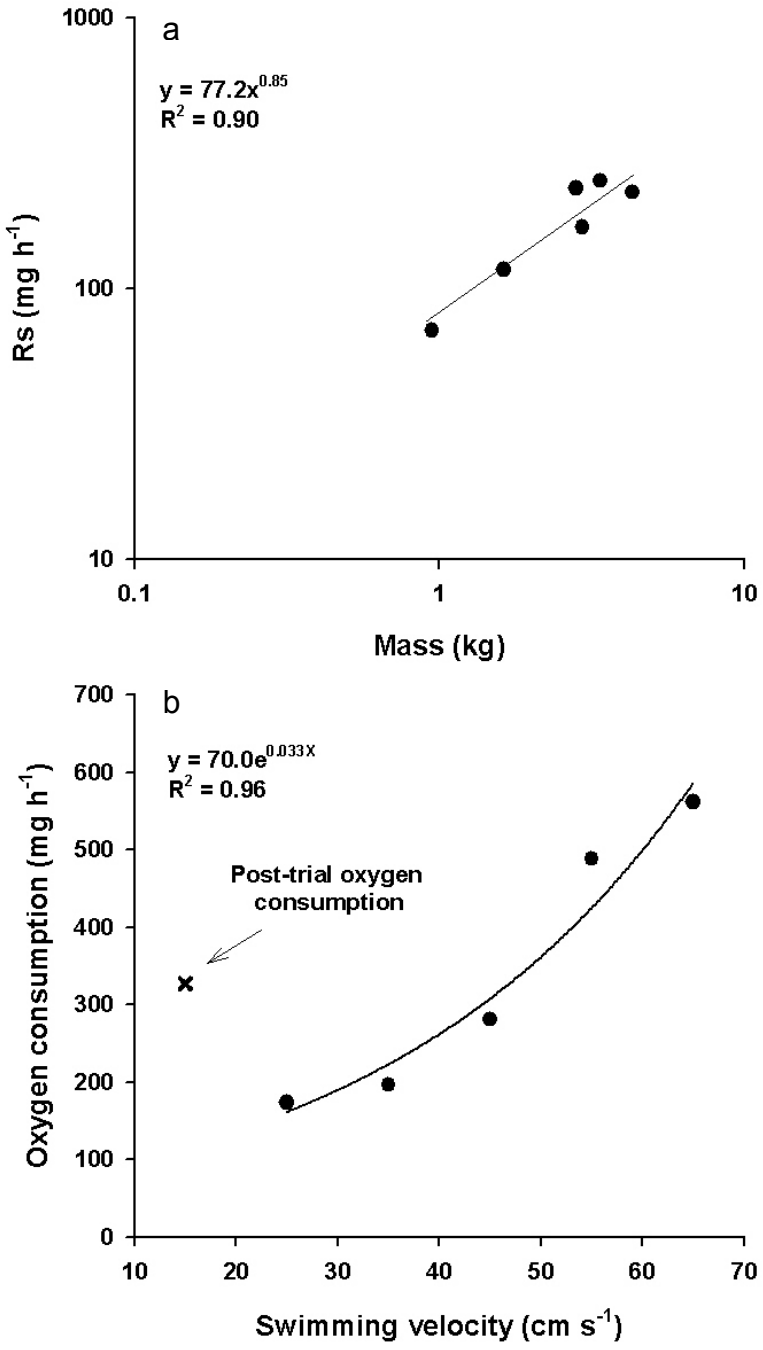

Figure 1.4. (a) The standard metabolic rates (R_s) of the six yellowtail kingfish plotted on logarithmic axes with fitted allometric relationship (R^2 = 0.90). and **(b)** The relationship between swimming velocity and oxygen consumption ($\dot{M}_{O_2}$) for a single yellowtail kingfish (mass=0.948 kg) at 22°C, showing the exponential increase in $\dot{M}_{O_2}$ with velocity (R^2=0.96) including oxygen consumption rate recorded immediately following measurement at the fastest swim velocity (×)

1.4.3 Critical swimming velocity (U_{crit}) and active metabolic rate (AMR)

This cohort of YTK proved to be very difficult to work with, as they often failed to acclimatize to the flume environment. They infrequently recovered from the transport stress and on introduction to the flume would collapse with exhaustion and fail to recover. Fish that did survive the acclimation period would often collapse at seemingly gentle velocities well before the predicted termination of the experiment. From twenty-eight attempts, successful data collection was only achieved from ten fish.

To increase the likelihood that the U_{crit} would be reached within the water velocity range of the respirometer, a cohort of small YTK (0.79 $\pm$0.49 kg) was used (Table 1.2). All experiments were terminated when the fish resorted to burst and glide swimming and brushed its tail up against the back screen more than three times in 30 s. This was defined as the U_{crit}, which ranged between 1.03 and 1.76 BL s^{-1} (Table 1.2).

Table 1.2. Mass (M), body length (BL), swimming velocity range (U) and critical swimming velocity (U_{crit}) of the ten yellowtail kingfish swum for 1 h periods at progressively higher swimming velocities by increments of 10 cm s^{-1} at 22°C.

Fish	M (kg)	BL (cm)	U (cm s^{-1})	U_{crit} (BL s^{-1})
1	0.624	34.0	20-60	1.76
2	0.563	34.0	20-50	1.47
3	0.748	35.5	20-60	1.72
4	0.805	39.1	20-60	1.48
5	0.66	35.9	20-60	1.61
6	0.668	35.5	20-60	1.69
7	0.927	38.9	20-40	1.03
8	1.00	41.5	20-70	1.60
9	0.848	37.1	20-70	1.89
10	1.12	41.5	20-60	1.45
Mean	**0.796**	**37.3**	**-**	**1.57**
SE	**0.049**	**0.821**	**-**	**0.180**

Mean $\dot{M}_{O_2}$ increased exponentially with swimming velocity (R^2=0.92) (Fig 1.5). At the highest swimming velocities, $\dot{M}_{O_2}$ appeared to flatten with

swimming velocity suggesting that the maximum aerobic metabolism (AMR) had been reached, corresponding to 506 ± 44 mg kg^{-1} h^{-1} (n=10). By extrapolation of the swimming velocity / $\dot{M}_{O_2}$ relationship to a velocity of zero, an R*s* of 274 ± 31 mg kg^{-1} $h^{-1}$was calculated.

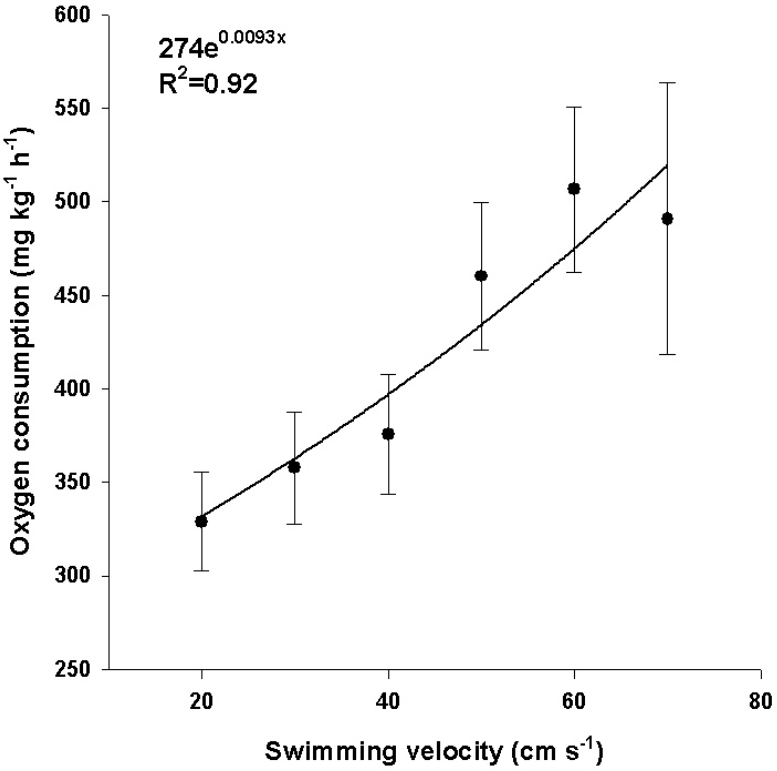

Figure 1.5. The relationship between oxygen consumption and swimming velocity of ten yellowtail kingfish (0.796 ±0.049 kg) swum at 22°C for 1 h periods at progressively higher swimming velocities until the critical swimming velocity was reached. Values are means ±SE (n=10).

1.5 Discussion

1.5.1 Flume modifications and initial testing

The University of Adelaide flume tank was never designed for teleost research. Instead, it was constructed mainly for the examination of surface swimming of terrestrial mammals (see Fish and Baudinette, 1999; Fish *et al.*, 2001). For these reasons, substantial modifications were required. The first and most significant modification was to seal the system to create an aquatic respirometer. This was achieved with a three-piece lid with hinged access hatch that proved to stop nearly all passive oxygen diffusion. The hydrodynamics of the flume were also poor for teleost research, as the flow velocity was not even throughout the cross-sectional area. Uneven flow creates slow points in which fish can rest, and thus swimming velocity cannot be defined. Several modifications were required to even-out the flow, including the inclusion of a large flow-resistance tube grid. Unfortunately this reduced the water velocity range, which was partially corrected for by increasing the propeller size. Other major modifications included the construction of a saltwater delivery system and temperature control unit. Initial YTK tests were promising, with fish performing well and appearing to acclimate to the respirometer within 6 h of introduction.

1.5.2 Standard metabolic rate (Rs) and effect of mass

When the YTK R*s* (Fig 1.4b) is normalized to a study temperature of 25^{o}C with Q_{10}=1.65 (White and Seymour, 2005), giving a value of 89.7 mg kg$^{-0.85}$ h^{-1}, it is found to be very similar to other active fish species such as sockeye salmon (113 mg kg$^{-0.88}$ h^{-1}, *Oncorhynchus nerka*, Brett, 1964), Atlantic cod (106 mg kg$^{-0.88}$ h^{-1}, *Gadus morhua*, Schurmann and Steffensen, 1997), yellowtail (133 mg kg$^{-0.88}$ h^{-1}, Yamamoto and Itazawa, 1981), and rainbow trout (51.9 mg kg$^{-0.88}$ h^{-1}, Brill, 1987). However it is considerably less than for tuna species (258-292 mg kg$^{-0.88}$ h^{-1}, Brill, 1987; Dewar and Graham, 1994) and dolphin fish *(Coryphaena hippurus*, 178.2 mg kg$^{-0.88}$ h^{-1}, Benetti *et al.*, 1995). Elevated R*s* for tuna species is associated with physiological adaptations, such as a large gill surface area, that allow them to achieve great aerobic scopes. The gill surface area of YTK is unknown, however other cardiovascular parameters of yellowtail appear to be more similar to those of rainbow trout than to tuna (Brill and Bushnell, 2001).

The slope of YTK R*s* mass scaling presented in Fig 1.4a (b = 0.85, se=0.145) is similar to the intraspecific scaling exponent of sockeye salmon R*s* (b=0.88) (Brett and Glass, 1973) nor to the interspecific R*s* exponent for 82 species of fish (b=0.88) (White and Seymour, 2005). This suggests that YTK R*s* scales with respects to mass no differently to other teleosts,

however more data over a wider range of fish mass are required to completely define the relationship and strengthen the allometric regression.

1.5.3 Critical swimming velocity (U_{crit}) and active metabolic rate (AMR)

The critical swimming velocity (U_{crit}) is defined as the maximum swimming velocity a fish can maintain for a defined period. However, the U_{crit} will vary depending on the velocity increment and the amount of time spent at each speed (Bushnell *et al.*, 1984). Furthermore, body mass and study temperature will affect the maximum sustainable swimming velocity of an individual. For these reasons, interspecific comparisons of U_{crit} are problematic. In the present study, U_{crit} of YTK was 1.6 BL s^{-1}(Table 2). This is similar to U_{crit} recorded with yellowtail (1.3 BL s^{-1}, 15^{o}C, Tsukamoto and Chiba, 1981), Atlantic cod (1.9 BL s^{-1}; 0.30 kg, 15^{o}C, Schurmann and Steffensen, 1997), and rainbow trout (1.8 BL s^{-1}; 0.25-0.35 kg, 15^{o}C, Bushnell *et al.*, 1984). However, it is considerably lower than the U_{crit} recorded for more active species such as sockeye salmon (2.9 BL s^{-1}; 0.746 kg, 15^{o}C, Brett, 1965), chub mackerel (3.8-5.8 BL s^{-1}; *Scomber japonicus*, 0.03-0.16 kg, 24^{o}C, Sepulveda and Dickson, 2000), and kawakawa tuna (3.4 BL s^{-1}; *Euthynnus affinis*, 0.02-0.27 kg, 24^{o}C, Sepulveda and Dickson, 2000). This is surprising as YTK are known to be active pelagic fish, and thus would be expected to have similar swimming capacity to other marine pelagic fish such as sockeye salmon.

The $\dot{M}_{O_2}$ at the U_{crit} corresponds to an animal's maximum aerobic metabolism (AMR). For the YTK examined this corresponded to 506 mg kg^{-1} h^{-1}, which is similar to equivalent sized active species such as yellowtail, (600-800 mg kg^{-1} h^{-1}, 15^{o}C, Tsukamoto and Chiba, 1981) and sockeye salmon (730 mg kg^{-1} h^{-1}; 15^{o}C, Brett, 1965), but is considerably more than less active species such as Atlantic cod (206 mg kg^{-1} h^{-1}; 0.30 kg, 15^{o}C, Schurmann and Steffensen, 1997) and rainbow trout (318 mg kg^{-1} h^{-1}; 0.25-0.35 kg, 15^{o}C, Bushnell *et al.*, 1984). The R*s* derived in our experiment (274 mg kg^{-1} h^{-1}) was, however, considerably greater than that of the previous trials (77 mg kg^{-1} h^{-1}), and that of subsequent YTK experiments (93 mg kg^{-1} h^{-1}, Clark, Chapter 2). This suggests that the YTK examined did not fully acclimatize to the flume environment, resulting in the elevation of $\dot{M}_{O_2}$ at slow swimming velocities. Poor acclimation was also evident by the low rate of trial success. Close to two thirds of individual fish tested failed to recover from transport, and never regained steady swimming within the respirometer. Several modifications in procedures and technologies were attempted to improve recovery, including; (i) increasing acclimation period to 16 h, (ii) increasing water oxygen saturation of the flume when fish were introduced, (iii) inclusion of a mirror to give the impression of a second fish within the flume, (iv) modified lighting and shading, (v) modification of water flow velocity at time of fish introduction, (vi) reduction of the working section

area, and (vii) reducing flume vibrations and noise. However, none of these modifications improved swimming success rates. The reason why this cohort of YTK performed so differently to previous fish is unknown. It was hypothesized these small fish may have felt more vulnerable when isolated from the school. However, introduction of more than one fish into the respirometer could compromise results due to individual variation and swim slipstreaming. There is also a suggestion that developmental abnormalities may have increased the animal's susceptibility to stress. Approximately 50% of experimental animals had obvious external deformities (bent spines or jaws). These types of external abnormalities are also commonly associated with further internal abnormalities such as incomplete gas bladder formation. In aquaculture, YTK with abnormalities are known to be more sensitive to stressors such as net changes (S. Shiilg, personal communication). Poor swimming performance of individual hatchery cohorts of coho salmon (*Oncorhynchus kisutus*) has been reported previously (Davis *et al.*, 1963). In that case, poor performance was hypothesized to be due to anemia as a result of disease.

Due to the problems experienced, respirometer procedures were reviewed before continuation of research with a new cohort of YTK. It appeared clear that YTK can be greatly susceptible to stress and measures should be taken to reduce its effect. One obvious way was to move the respirometer to the location that the YTK were being held (SARDI Aquatic Sciences). This would alleviate the need for transport, which took > 1.5 h from fish capture until time of introduction into the respirometer. Having the respirometer connected to a constant saltwater supply would also give greater flexibility in experimental protocol, allowing water exchanges to occur if experiments were required to be extended to allow sufficient acclimation. Furthermore, it was apparent that the University of Adelaide flume had some limitations for YTK metabolic physiology research. Its large working section was originally thought to be an advantage, as it would reduce the effects of confinement stress. However, it became clear that this large cross-sectional area allowed the fish to turn against the water flow. When this happened, the fish would crash into the down-stream grid, often resulting in the fish panicking until exhaustion. Also, a respirometer with a greater water flow velocity range would allow the examination of the AMR of larger individuals. For these reasons it was decided to repeat the experiment with a newly constructed respirometer from LaTrobe University that had a smaller cross-sectional area, greater velocity range and could be based at SARDI Aquatic Sciences (reported on by T. D. Clark in the next chapter). Experimentation continued with the University of Adelaide flume on another important aquaculture species in South Australia, Australian mulloway (*Argyrosomus japonicus*), which was found to be much less susceptible to transport stress than YTK (reported on by Fitzgibbon *et al*., in chapter 3).

1.6 Acknowledgements

This work received funds from PIRSA Aquaculture and the Fisheries R&D Corporation. QPF would like to thank Russel Baudinette for his initiation of this work, the University of Adelaide Physics Department workshop for their assistance in flume tank modifications, Arron Strawbridge and Jane Skinner for there dedicated technical assistance.

1.7 References

Beamish, F. W. H. & Trippel, E. A. (1990). Heat Increment: A static or dynamic dimension in bioenergetic models. *Transactions of the American Fisheries Society* **119,** 649-661.

Benetti, D. D., Brill, R. W. & Kraul Jr, S. A. (1995). The standard metabolic rate of dolphin fish. *Journal of Fish Biology* **46,** 987-996.

Benetti, D. D., Nakada, M., Minemoto, Y., Hutchinson, W., Shotton, S. & Tindale, A. (2001). Aquaculture of yellowtail amberjacks *Carangidea*: Current status, progress and constraints. *Aquaculture 2001: Book of Abstracts* 56.

Brett, J. R. (1964). The respiratory metabolism and swimming performance of young sockeye salmon. *Journal of Fisheries Research Board of Canada* **21,** 1184-1226.

Brett, J. R. (1965). The relation of size to rate of oxygen consumption and sustained swimming speed of sockeye salmon (*Oncorhynchus nerka*). *Journal of Fisheries Research Board of Canada* **22,** 1491-1501.

Brett, J. R. (1972). The metabolic demand for oxygen in fish, particularly salmonids, and a comparison with other vertebrates. *Respiration Physiology* **14,** 151-170.

Brett, J. R. & Glass, N. R. (1973). Metabolic rates and critical swimming speeds of sockeye salmon (*Oncorhynchus nerka*) in relation to size and temperature. *Journal of Fisheries Research Board of Canada* **30,** 379-387.

Brill, R. W. (1979). The effect of body size on the standard metabolic rate of skipjack tuna, *Katsuwonus pelamis*. *Fishery Bulletin* **77,** 494-498.

Brill, R. W. (1987). On the standard metabolic rates of tropical tunas, including the effect of body size and acute temperature change. *Fishery Bulletin* **85,** 25-35.

Brown, C. R. & Cameron, J. N. (1991a). The relationship between specific dynamic action (SDA) and protein synthesis rates in the channel catfish. *Physiological Zoology* **64,** 298-309.

Brown, C. R. & Cameron, J. N. (1991b). The induction of specific dynamic action in channel catfish by infusion of essential amino acids. *Physiological Zoology* **64,** 276-297.

Bushnell, P. G., Steffensen, J. F. & Johansen, K. (1984). Oxygen consumption and swimming performance in hypoxia-acclimated rainbow trout *Salmo gairdneri*. *Journal of Experimental Biology* **113,** 225-235.

Cho, C. Y. & Kaushik, S. J. (1990). Nutritional Energetics in fish: Energy and protein utilization in rainbow trout (*Salmo gairdneri*). *World Review of Nutrition and Dietetics* **61,** 132-172.

Clarke, A. & Johnston, N. M. (1999). Scaling of metabolic rate with body mass and temperature in teleost fish. *Journal of Animal Ecology* **68,** 893-905.

Davis, G. E., Foster, J., Warren, C. & Doudoroff, P. (1963). The influence of oxygen concentration on the swimming performance of juvenile Pacific salmon at various temperatures. *Transactions of the American Fisheries Society* **92,** 111-124.

De La Gandara, F., Garcia-Gallego, M. & Jover, M. (2002). Effect of feeding frequency on the daily oxygen consumption in young Mediterranean yellowtails (*Seriola dumerili*). *Aquacultural Engineering* **26,** 27-39.

Dewar, H. & Graham, J. B. (1994). Studies of tropical tuna swimming performance in a large water tunnel I. Energetics. *Journal of Experimental Biology* **192,** 13-31.

Fish, F. E. & Baudinette, R. V. (1999). Energetics of locomotion by the Australian water rat (*Hydromys chrysogaster*): A comparison of swimming and running in a semi-aquatic mammal. *Journal of Experimental Biology* **202,** 353-363.

Fish, F. E., Frappell, P. B., Baudinette, R. V. & MacFarlane, P. M. (2001). Energetics of terrestrial locomotion of the platypus *Ornithorhynchus anatinus*. *Journal of Experimental Biology* **204,** 797-803.

Fry, F. E. J. (1971). The effect of environmental factors on the physiology of fish. In *Fish Physiology* (Hoar, W. S. & Randall, D. J., eds), pp. 1-99: Academic Press

Fu, S. J., Xie, X. J. & Cao, Z. D. (2005a). Effect of meal size on postprandial metabolic response in southern catfish (*Silurus meridionalis*). *Comparative Biochemistry and Physiology a-Molecular & Integrative Physiology* **140,** 445-451.

Fu, S. J., Xie, X. J. & Cao, Z. D. (2005b). Effect of fasting on resting metabolic rate and postprandial metabolic response in *Silurus meridionalis*. *Journal of Fish Biology* **67,** 279-285.

Fu, S. J., Cao, Z. D. & Peng, J. L. (2006). Effect of meal size on postprandial metabolic response in Chinese catfish (*Silurus asotus* Linnaeus). *Journal of Comparative Physiology* **B176,** 489-495.

Gooding, R. M., Neill, W. H. & Dizon, A. E. (1981). Respiration rates and low-oxygen tolerance limits in skipjack tuna, *Katsuwonus pelamis*. *Fishery Bulletin* **79,** 31-48.

Graham, J. B. & Laurs, R. M. (1982). Metabolic rate of the albacore tuna *Thunnus alalunga*. *Marine Biology* **72,** 1-6.

Grottum, J. A. & Sigholt, T. (1998). A model for oxygen consumption of Atlantic salmon (*Salmo salar*) based on measurements of individual fish in a tunnel respirometer. *Aquacultural Engineering* **17,** 241-251.

Jobling, M. & Davis, J. C. (1980). Effect of feeding on the metabolic rate, and the specific dynamic action in plaice, *Pleuronectes platessa* L. *Journal of Fish Biology* **16,** 629-638.

Jobling, M. (1981). The influences of feeding on the metabolic rate of fishes: a short review. *Journal of Fish Biology* **18,** 385-400.

Korsmeyer, K. E. & Dewar, H. (2001). Tuna metabolism and energetics. In *Fish Physiology: Tuna Physiology, Ecology, and Evolution* (Block, B. A. & Stevens, E. D., eds), pp. 35-78: Academic Press

Lyndon, A. R., Houlihan, D. F. & Hall, S. J. (1992). The effect of short-term fasting and single meal on protein synthesis and oxygen consumption in cod, *Gadus morhua*. *Journal of Comparative Physiology B* **162,** 209-215.

Poortenaar, C. W., Hooker, S. H. & Sharp, N. (2001). Assessment of yellowtail kingfish (*Seriola lalandi lalandi*) reproductive physiology, as a basis for aquaculture development. *Aquaculture* **201,** 271-286.

Schurmann, H. & Steffensen, J. F. (1997). Effects of temperature, hypoxia and activity on the metabolism of juvenile Atlantic cod. *Journal of Fish Biology* **50,** 1166-1180.

Sepulveda, C. & Dickson, K. A. (2000). Maximum sustainable speeds and cost of swimming in juvenile kawakawa tuna (*Euthynnus affinis*) and chub mackerel (*Scomber japonicus*). *Journal of Experimental Biology* **203,** 3089-3101.

Sepulveda, C., Dickson, K. A. & Graham, J. B. (2003). Swimming performance studies on the eastern Pacific bonito *Sarda chiliensis*, a close relative of the tunas (family *Scombridae*). *Journal of Experimental Biology* **206,** 2739-2748.

Shimeno, S., Takeda, M., Takii, K. & Ono, T. (1993). Post-feeding changes of digestion and plasma constituents in young yellowtail fed with raw fish and formulated diets. *Nippon Suisan Gakkaishi* **59,** 507-513.

Steffensen, J. F. (1989). Some errors in respirometry of aquatic breathers: how to avoid and correct for them. *Fish Physiology and Biochemistry* **6,** 49-45.

Tandler, A. & Beamish, F. W. H. (1979). Mechanical and biochemical components of apparent specific dynamic action in largemouth bass, *Micropterus salmoides* Lacepede. *Journal of Fish Biology* **14,**

Tsukamoto, K. (1981). Direct evidence for functional and metabolic differences between dark and ordinary muscle in free-swimming yellowtail, *Seriola quinqueradiata*. *Bulletin of the Japanese Society of Scientific Fisheries* **47,** 573-575.

Tsukamoto, K. & Chiba, K. (1981). Oxygen consumption of yellowtail *Seriola quinqueradiata* in relation to swimming speed. *Bulletin of the Japanese Society of Scientific Fisheries* **47,** 673.

White, C. R. & Seymour, R. S. (2005). The scaling and temperature dependence of vertebrate metabolism. *Biology Letters*

Yamamoto, K.-i. & Itazawa, Y. (1981). Gas exchange in the gills of yellowtail, *Seriola quinqueradiata* under resting and normoxic condition. *Bulletin of the Japanese Society of Fisheries* **47,** 447-451.

Chapter 2: Energy expenditure of the yellowtail kingfish (*Seriola lalandi*) at different swimming speeds: developing a bioenergetics model for Australian aquaculture.

Timothy D. Clark
Roger S. Seymour

Earth and Environmental Sciences,
University of Adelaide,
South Australia 5005, Australia.

List of symbols and abbreviations

BL	body length (e.g. BL s^{-1} refers to the number of body lengths swum per second)
GCOT	gross aerobic cost of transport (the total amount of oxygen used to swim at a given speed)
NCOT	net aerobic cost of transport (the amount of oxygen used above SMR to swim at a given speed)
min	a modifier to indicate the minimum value obtained for a given variable (e.g. $GCOT_{min}$ is the minimum gross aerobic cost of transport obtained)
max	a modifier to indicate the maximum value obtained for a given variable (e.g. $\dot{M}_{O_2\,max}$ is the maximum rate of oxygen consumption obtained at the highest swimming speeds)
M_b	body mass
$\dot{M}_{O_2}$	rate of oxygen consumed from the water by an animal
SMR	standard metabolic rate - the minimum metabolic rate attainable by an animal (i.e. $\dot{M}_{O_2}$ when at complete rest, not digesting etc)
U	swimming velocity (e.g. U_{opt} is optimal swimming velocity, U_{max} is maximal swimming velocity)

2.1 Abstract

In recent years, members of the genus *Seriola* (amberfishes, amberjacks, and yellowtails) have been identified as potentially valuable aquaculture species in the Australasian region. The yellowtail kingfish (*S. lalandi*) is of particular interest to Australian aquaculturalists, yet there are no data relating to the energetics of this species. The present study utilized a

swimming respirometer to measure oxygen consumption rates ($\dot{M}_{O_2}$; ~ energy expenditure) of ~ 2 kg *S. lalandi* when exposed to different swimming speeds at two temperatures. The standard aerobic metabolic rate (SMR) of *S. lalandi* ranged from 1.55 mg min^{-1} kg^{-1} at 20°C to 3.31 mg min^{-1} kg^{-1} at 25°C. At both temperatures, $\dot{M}_{O_2}$ increased exponentially with swimming speed to reach maximum values of 10.9 mg min^{-1} kg^{-1} at 20°C and 13.3 mg min^{-1} kg^{-1} at 25°C (swimming at 2.3 BL s^{-1}). All data were combined to formulate a bioenergetics model for *S. lalandi* based on swimming speed and water temperature. It was predicted that 1000 kg of *S. lalandi* in 20°C water would consume 4839 mg of dissolved oxygen per minute (290,364 mg per hour) when swimming at their optimum swimming speed, which corresponds to an energy usage of 68 kJ per minute (4094 kJ per hour). The same mass of *S. lalandi* when swimming in 25°C water would consume 9063 mg of dissolved oxygen per minute (543,774 mg per hour), which corresponds to an energy usage of 128 kJ per minute (7667 kJ per hour). This bioenergetics model should be useful to estimate energy usage, oxygen usage and stocking densities of *S. lalandi* when under aquaculture conditions.

2.2 Introduction

The genus *Seriola* (amberfishes, amberjacks, and yellowtails) has a circumglobal distribution and comprises several species of highly active predatory marine fish, which may exceed 2 m in length and a body mass (M_b) of around 80 kg (Gillanders et al., 2001; Poortenaar et al., 2001). In recent years, members of this genus have been identified as potentially valuable aquaculture species in the Australasian region (Poortenaar et al., 2001), yet little is known of their energetics. The limited energetics data that exist for the *Seriola* genus have been obtained exclusively from studies on *S. quinqueradiata* (commonly referred to as 'yellowtail'), which is an inhabitant of the northwestern Pacific Ocean. This species has been reported to have a standard metabolic rate (SMR) greater than most other fishes, and approaching that of the tunas (Yamamoto et al., 1981; Korsmeyer and Dewar, 2001), although these data may have been affected by stress due to heavy instrumentation and confinement to a small static respirometer.

Given these previous findings for *S. quinqueradiata*, it appears that members of this genus may have enhanced metabolic expenditure which may have repercussions for their use as an aquaculture species. The present study utilizes an important species for the Australian aquaculture industry, the yellowtail kingfish (*S. lalandi*), to investigate aerobic energy expenditure ($\dot{M}_{O_2}$) while swimming at two different temperatures. The main aims of this study were to determine (1) the minimal energy expenditure (i.e. SMR) and maximal energy expenditure ($\dot{M}_{O_2\,max}$) attainable for this species,

(2) the speed at which the ratio between energy expenditure and swimming speed is lowest (i.e. U_{opt}; which provides an indication of daily energy usage under aquaculture conditions), and (3) a model for predicting energy expenditure of a group of fish under aquaculture conditions.

2.3 Materials and Methods

2.3.1 Animals

Ten yellowtail kingfish were studied between 10 November 2005 and 10 January 2006. Fish eggs were originally purchased from Clean Seas Aquaculture (Arno Bay, South Australia) in February 2004 and transported to the South Australian Research and Development Institute where they were hatched. The larvae were weaned in larval tanks, and eventually relocated to a 40,000 l holding tank where they were raised on commercial pellets (Skretting, Cambridge, Tasmania) to a body mass of approximately 2 kg. At least three days prior to commencing experiments, the fish were moved to 1,000 l indoor tanks at the same water temperature to which they were exposed outdoors (approximately 20^{o}C), and on a light:dark cycle (13 h:11 h) that resembled day length patterns for the time of year. Fish were fed once per day, but were fasted for at least 30 h prior to use in experiments, to eliminate the influence of digesting metabolism on the measurements.

2.3.2 Swimming respirometer

Measurements of $\dot{M}_{O_2}$ at different swimming velocities were performed in a constant temperature room using an upright Brett-type swimming respirometer (water volume 137 L), which was constructed at La Trobe University in Melbourne, Australia. The entire respirometer sat within an aerated waterbath (length 1500 mm, width 300 mm, height 1200 mm; replaced with fresh seawater at 2 L min^{-1}) which provided thermal stability and a source of oxygenated water to flush the respirometer between measurements. Water velocity through the respirometer was regulated by a 245 mm diameter propeller, which was positioned at one end of the respirometer and connected via a stainless steel shaft to a computer-driven DC motor (Baldor, VPT 34550; interfaced with 0 – 10 V external Penta Drive Regenerative speed controller) mounted above the waterbath. A submersible pump with a one-way valve, positioned at the bottom of the respirometer, provided the only interface between the water in the respirometer and that in the waterbath, and computer control of the submersible pump (using a voltage output from PowerLab; see below) allowed the respirometer to be automatically flushed and sealed continuously at predefined intervals. The volume of water pumped into the respirometer by the submersible pump was released through a pipe at the top of the respirometer that extended above the water line of the waterbath. Water temperature and oxygen saturation in the respirometer were continuously monitored using a calibrated sensor (sc100 LDO, Hach, USA),

and outputs from this, and a measure of the voltage supplied to the propeller motor and submersible flushing pump, were collected at 100 Hz (PowerLab/4SP and Chart software, ADInstruments, Sydney, Australia).

2.3.3 Swimming protocol

Resting values for each individual at 20 ± 0.5°C were obtained only following at least 24 h of recovery in the respirometer, when $\dot{M}_{O_2}$ had stabilized. Rates of oxygen consumption were repeatedly measured as the fish was exposed to incremental changes in water velocity. Some fish were incremented beyond their maximum sustainable swimming velocity (characterized by vigorous burst episodes and subsequent resting against the grid at the posterior end of the respirometer; typically ≥ 2.3 BL s^{-1}). Each $\dot{M}_{O_2}$ measurement was performed over a 10 min period so that oxygen saturation in the respirometer never fell below 75%, and the respirometer was flushed for 20 min between each measurement with oxygenated water from the waterbath. Fish were maintained at each swimming velocity for at least 60 min (i.e. two measurement cycles) to ensure that all variables had reached a steady state (this excludes speeds greater than 2.3 BL s^{-1} where fish were unable to maintain position for more than ~10 min). Several fish struggled immediately when water velocity was increased above that used to obtain resting values (i.e. 0.3 – 0.7 BL s^{-1}). In such circumstances, water velocity was rapidly increased to a high, yet sustainable level, to encourage a greater level of exercise, and fish were maintained at this velocity until $\dot{M}_{O_2}$ plateaued. Some individuals swam at intermediate speeds in later attempts (after a sufficient recovery period), but the number of steady state data points able to be obtained from each individual (minimum 3 velocities, maximum 6 velocities) was reliant upon how well they adjusted to swimming in the respirometer (sample sizes indicated in tables and figures).

To examine the effect of temperature on energy expenditure, two fish were maintained at 0.3 – 0.7 BL s^{-1} in the respirometer after the 20°C swimming protocol while the water was heated from 20°C to 25 ± 0.5°C (taking approximately 3 h). Fish were given at least 2 h to acclimate to the new temperature (also to ensure complete recovery from the previous swim at 20°C), then the same swimming protocol was performed as outlined above.

2.3.4 Data analysis and statistics

Rates of oxygen consumption were calculated using the rate of decline in oxygen saturation in the respirometer over the final 7 min of each 10 min measurement. Calculations took account of the effect of temperature on the oxygen capacitance of the water (Dejours, 1975). The respirometer was regularly sealed without containing a fish, to determine background respiration rates and subsequently correct $\dot{M}_{O_2}$ measurements of the fish,

although the reduction in oxygen saturation during these trials was in all cases negligible.

Gross aerobic cost of transport (GCOT) was calculated by dividing each $\dot{M}_{O_2}$ value by the swimming velocity (*U*) at which the measurement was obtained, and net aerobic cost of transport (NCOT) was calculated from ($\dot{M}_{O_2}$ – SMR)/*U*. Least squares regressions were used where appropriate, and comparisons of slopes and elevations were performed using ANCOVA. Significance was considered at $P<0.05$. Data are presented as mean ± SE of the mean. Minimum and maximum values are denoted by the subscripts $_{min}$ and $_{max}$, respectively, where the acronym SMR is equivalent to $\dot{M}_{O_2\,min}$. *N* = number of animals, *n* = number of data points.

2.4 Results

2.4.1 Zero swimming velocity

Two individuals at 20°C opted to rest on the bottom of the respirometer when exposed to a slow water velocity (0.42 BL s^{-1} on both occasions), rather than gently swimming against the water flow as did all other individuals. Consequently, the resting $\dot{M}_{O_2}$ data points from these two animals can be included in the regression as zero swimming velocity at 20°C, thus alleviating the need to extrapolate this regression to the vertical axis, as was the case with data at 25°C (Fig. 2.1, Table 2.1). It should be noted that these two individuals were in perfect health and swam just as well as all other fish when water velocity was increased. The rate of oxygen consumption at 0 BL s^{-1} (i.e. SMR) increased 2.1-fold (Q_{10} = 4.5) from 1.55 mg min^{-1} kg^{-1} at 20°C to 3.31 mg min^{-1} kg^{-1} at 25°C (Fig. 2.1a, Table 2.2).

Table 2.1. Regression equations describing the relationship between oxygen consumption rate ($\dot{M}_{O_2}$ mg min^{-1} kg^{-1}) and swimming velocity (U BL s^{-1}).

Temperature (°C)	*N*	*n*	*a*	*b*	*LL of a*	*UL of a*	S_b	r^2	*P*
20	10	32	1.55	0.85	1.48	1.63	0.04	0.94	<0.01
25	2	9	3.31	0.61	3.21	3.42	0.03	0.99	<0.01

Relationships determined over a velocity range of approximately 0.0 – 2.3 BL s^{-1} at 20°C and 0.3 – 2.3 BL s^{-1} at 25°C. Regression equations expressed as $y = a \bullet e^{bU}$. Error intervals for *a* were asymmetric, thus lower limits (*LL*) and upper limits (*UL*) are given; S_b = SE of *b*. *P* values determined by ANOVA.

Table 2.2. Values of oxygen consumption rates ($\dot{M}_{O_2}$) for *S. lalandi* at zero and maximum (U_{max}; 2.3 BL s^{-1}) swimming velocities.

Variable	Swimming velocity (body lengths per second)					
	20°C			25°C		
	0 BL s^{-1}	2.3 BL s^{-1}	Factorial change	0 BL s^{-1}	2.3 BL s^{-1}	Factorial change
$\dot{M}_{O_2}$ (mg min^{-1} kg^{-1})	1.55	10.93	7.0	3.31#	13.32#	4.0

Values calculated from regression equations given in Table 2.1. U_{max} was taken to be 2.3 BL s^{-1} at both temperatures. #significantly different from the corresponding measurement at 20°C (P<0.05).

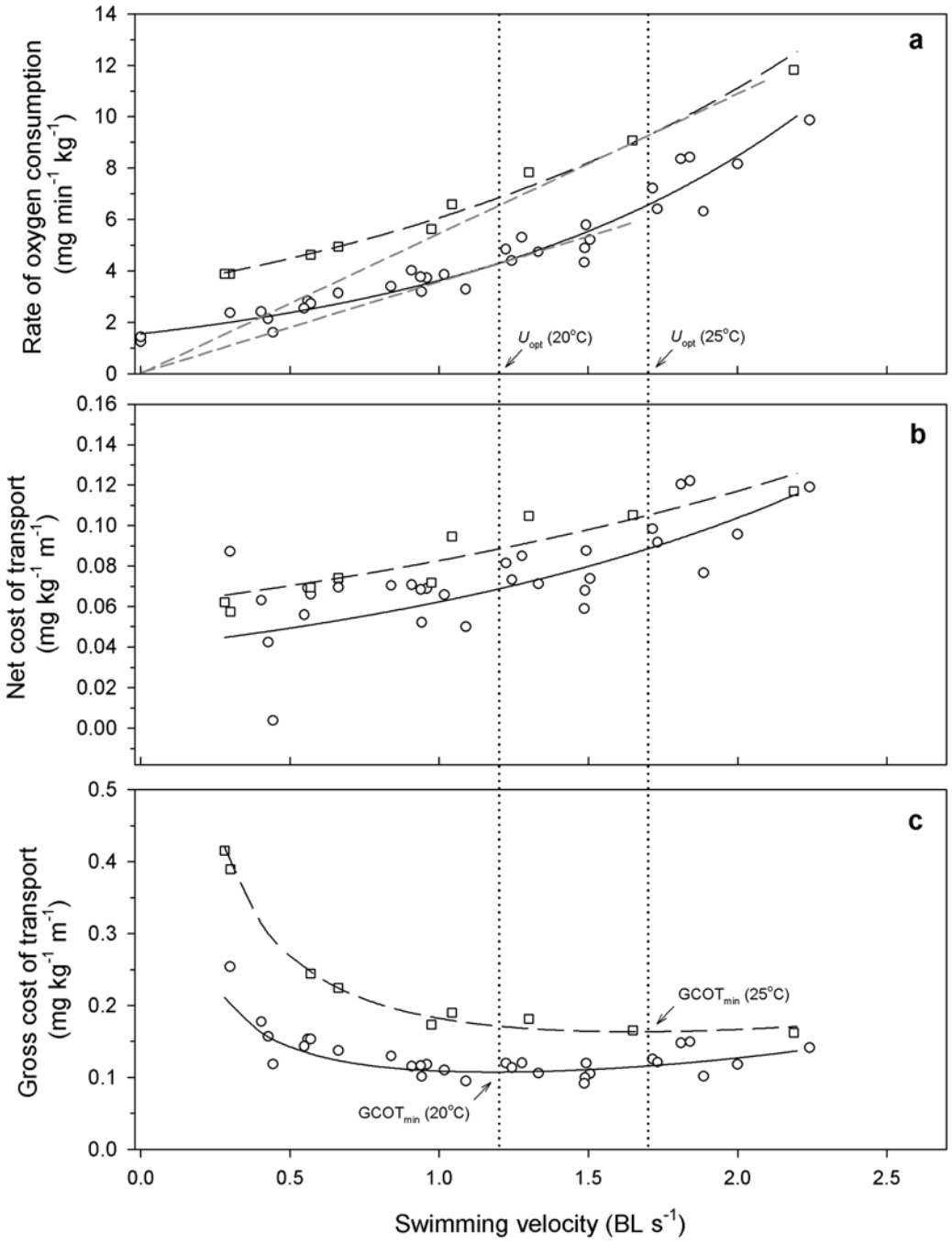

Figure 2.1 Relationship of (a) rate of oxygen consumption ($\dot{M}_{O_2}$), (b) net aerobic cost of transport (NCOT), and (c) gross aerobic cost of transport (GCOT) as a function of swimming velocity (up to 2.3 BL s^{-1}) for *Seriola lalandi* at 20°C and 25°C. Circles and solid regressions represent animals at 20°C ((a) *N*=10, (b)-(c) *N*=4), while squares and dashed regressions represent animals at 25°C (*N*=2). In (a), the slope at the tangent to the curve from the origin (pale dashed lines) is equal to the optimum swimming velocity (U_{opt}), which occurs where GCOT is at a minimum (GCOT$_{min}$).

2.4.2 Effects of exercise

At 20°C, $\dot{M}_{O_2}$ increased exponentially with swimming velocity up to approximately 2.3 BL s^{-1} (Fig 2.1a), after which $\dot{M}_{O_2}$ tended to plateau ($\dot{M}_{O_2\,max}$) and swimming often became more erratic and interspersed with burst episodes. Fish at 25°C displayed a similar exponential pattern of increasing $\dot{M}_{O_2}$ with swimming velocity, however this was elevated in comparison with fish at 20°C (P<0.01). Although it was not determined if fish at 25°C were capable of sustained swimming at velocities in excess of 2.3 BL s^{-1}, behavioural observations indicated that this was unlikely and, consequently, the maximum sustainable swimming velocity (U_{max}) is considered herein to be 2.3 BL s^{-1} at both temperatures. The absolute aerobic scope ($\dot{M}_{O_2\,max}$ – SMR; that is the absolute amount that $\dot{M}_{O_2}$ can be increased when going from a resting to an exercising state) remained essentially unchanged across temperature at approximately 9.5 mg min^{-1} kg^{-1}, hence the factorial aerobic scope ($\dot{M}_{O_2\,max}$ / SMR; that is the proportional amount that $\dot{M}_{O_2}$ can be increased when going from a resting to an exercising state) decreased substantially from 7.0 at 20°C to 4.0 at 25°C (Table 2.2).

2.4.3 Aerobic cost of transport

The gross aerobic cost of transport (GCOT), expressed here on a per meter basis, was always higher at 25°C, but at both temperatures changed in a somewhat shallow U-shaped relationship with swimming velocity (Fig. 2.1c). Nevertheless, minimum values of GCOT ($GCOT_{min}$) occurred at the optimal swimming velocities (U_{opt}) of 1.2 BL s^{-1} at 20°C and 1.7 BL s^{-1} at 25°C. Some of the variation in GCOT with temperature is likely attributable to the effect of temperature on SMR, although, even when accounting for SMR by calculating the net aerobic cost of transport (NCOT), the efficiency of swimming was still greater at the cooler temperature (Fig. 2.1b).

2.4.4 Bioenergetics model

A multiple linear regression was used to determine the effects of swimming speed and water temperature on $\dot{M}_{O_2}$, with the intention of formulating a bioenergetics model for use under aquaculture conditions. The regression indicated that swimming speed was the primary variable to use when predicting $\dot{M}_{O_2}$ (r^2 = 0.76), though the addition of temperature to the model improved the regression (r^2 = 0.93). The resultant model for predicting $\dot{M}_{O_2}$ of *S. lalandi* is:

$$\dot{M}_{O_2} = (3.657 \bullet U) + (0.479 \bullet T) - 9.129 \qquad (2.1)$$

where $\dot{M}_{O_2}$ is oxygen consumption rate in mg O_2 min^{-1} kg^{-1}, U is swimming speed in body lengths s^{-1}, and T is water temperature in °C.

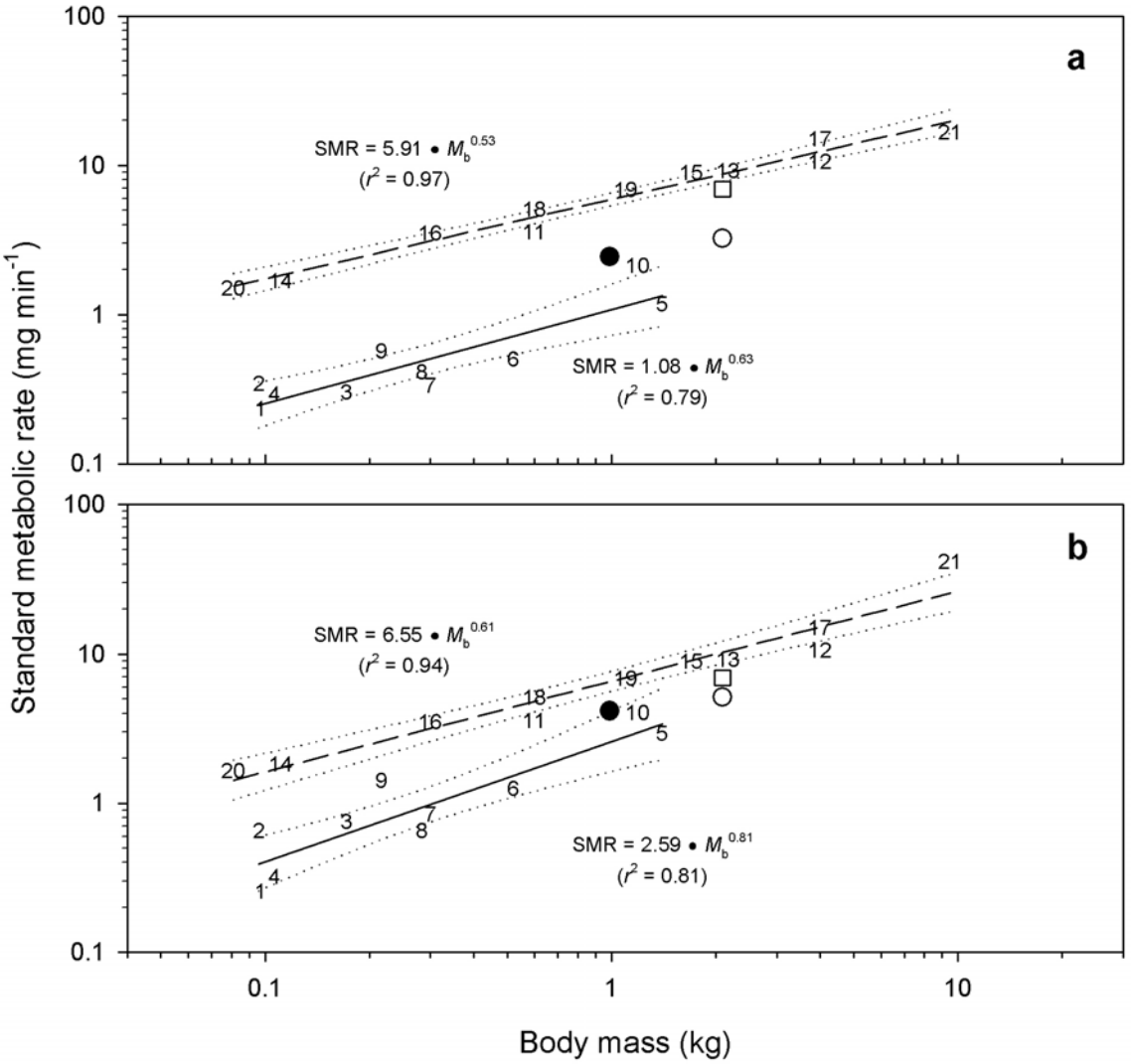

Figure 2.2 Interspecific comparison for teleosts of standard metabolic rate (SMR) versus body mass (M_b) at (a) the temperature at which the measurement was made, and (b) 25°C (corrected using Q_{10} = 2.5). Numbers from 1 – 10 and solid regression represent non-tuna species considered to be of high performance, and numbers from 11 – 21 and dashed regression represent species of tuna (dotted lines indicate 95% confidence intervals for each regression). 1 – 3, mackerel, *Scomber japonicus* measured at [1]24°C (Sepulveda and Dickson, 2000), [2]18°C (Dickson et al., 2002) and [3]15°C (Shadwick and Steffensen, 2000); 4 – 5, salmon, *Oncorhynchus nerka* measured at [4]24°C (Brett and Glass, 1973) and [5]15°C (Brett, 1965); 6 – 7, rainbow trout, *Oncorhynchus mykiss* measured at [6-7]15°C (Bushnell et al., 1984; Brill, 1987); 8, menhaden, *Brevoortia tyrannus* measured at 20°C (Macy et al., 1999); 9, bluefish, *Pomatomus saltatrix* measured at 15°C (Freadman, 1979); 10, bonito, *Sarda chiliensis* measured at 18°C (Sepulveda et al., 2003); 11 – 14, yellowfin, *Thunnus albacares* measured at [11-13]25°C (Brill, 1987; Dewar and Graham, 1994) and [14]24°C (Sepulveda and Dickson, 2000); 15 – 17, skipjack, *Katsuwonus pelamis* measured at [15-17]25°C (Brill, 1979; Dewar and Graham, 1994); 18 – 20, kawakawa, *Euthynnus affinis* measured at [18-19]25°C (Brill, 1987) and [20]24°C (Sepulveda and Dickson, 2000); 21, albacore, *Thunnus alalunga* measured at 15°C (Graham et al., 1989). Closed circle represents *Seriola quinqueradiata* measured at 19°C (Yamamoto et al., 1981), and open symbols represent data for *Seriola lalandi* from the present study measured at 20°C (open circle) and 25°C (open square). For comparative purposes, data for species of *Seriola* were not included in formulating the regressions.

Table 2.3. Comparison of variables for *Seriola* with those of the most extensively studied active teleost, rainbow trout, and the exceptionally high performance teleosts, the tunas.

Variable	*Seriola*[#]				Rainbow trout	Tunas
Activity level	Rest		Rest		Rest	Routine
Temperature (°C)	~ 20	(20)	25	(25)	10 – 15	25
Body mass (kg)	1.0 – 1.4	(~ 2.0)	~ 1.0	(1.9)	0.4 – 1.5	~ 1.0 – 2.0
$\dot{M}_{O_2}$ (mg min^{-1} kg^{-1})	2.5	(1.6)	–	(3.3)	0.8	12.9 – 16.2

[#] values given in parenthesis are from the present study for *S. lalandi*, whereas all other values are for *S. quinqueradiata* (~ 20°C data compiled from Yamamoto et al., 1981; Yamamoto, 1991; Lee et al., 2003c; 25°C data compiled from Ishimatsu et al., 1990, 1997; Lee et al., 2003b); data for rainbow trout compiled from Holeton and Randall, 1967; Randall et al., 1967; Stevens and Randall, 1967; Kiceniuk and Jones, 1977; Brill and Bushnell, 1991, 2001; Farrell and Jones, 1992; Altimiras and Larsen, 2000; data for tunas (skipjack and yellowtail) compiled from Bushnell et al., 1990; Brill and Bushnell, 1991, 2001; Jones et al., 1993; Bushnell and Jones, 1994; Dewar and Graham, 1994; Korsmeyer et al., 1997a,b.

2.5 Discussion

2.5.1 Standard metabolic rate

Standard metabolic rate is defined as the resting and fasting metabolism at a given temperature and is theoretically the minimum sustainable metabolic rate (Dejours, 1975; Korsmeyer and Dewar, 2001). The mass-specific SMR of *S. lalandi* at 20°C (1.55 mg kg^{-1} min^{-1}) is lower than that reported previously for the closely related *S. quinqueradiata* at a similar temperature (2.45 mg kg^{-1} min^{-1}; Table 2.3). It seems, however, that SMR of the *Seriola* genus is somewhat enhanced in comparison with that of many other active species, and it thus approaches values reported for tunas (Fig. 2.2a).

The temperature sensitivity of SMR determined for *S. lalandi* between 20°C and 25°C (Q_{10} = 4.5) is greater than typically documented for biological rate processes (Q_{10} = 2 – 3; Schmidt-Nielsen, 1990), although similar findings have been reported (Q_{10} = 6.8 for SMR in the bat ray, *Myliobatus californica*, following an acute temperature change; Hopkins and Cech, 1994). It is plausible that the acute nature of the temperature change used in the present study was causal to the large temperature sensitivity, thus a longer period of acclimation to 25°C may have resulted in a depression in SMR (O'Steen and Bennett, 2003; MacNutt et al., 2004). Nevertheless, the time course used here (from 20°C to 25°C in ~3 h) was chosen to simulate ecologically relevant changes in temperature that may be experienced during relatively rapid horizontal or vertical migrations, and the enhanced temperature sensitivity of SMR may be of functional significance in such circumstances.

2.5.2 Aerobic metabolic scope

It has been widely theorised that the high SMR for pelagic fish species supports the biochemical and anatomical framework enabling heightened rate processes and expansion of their aerobic metabolic scope (Dewar and Graham, 1994). Maximum values of $\dot{M}_{O_2}$ determined for *S. lalandi* (Fig. 2.1; Table 2.2) are in the upper range of other active fish such as salmon (typically <14 mg min^{-1} kg^{-1}; Brett, 1965; Lee et al., 2003a), yet they are well below the $\dot{M}_{O_2\,max}$ predicted for tunas (27 – 45 mg min^{-1} kg^{-1}; Brill and Bushnell, 1991, 2001). The absolute aerobic scope of *S. lalandi* remained at approximately 9.5 mg min^{-1} kg^{-1} across the temperature range and, subsequently, the factorial aerobic scope decreased 1.8-fold with increasing temperature (Table 2.2). This contrasts with several other species of teleosts, for which an increase in temperature is associated with an increase in the absolute aerobic scope (Webber et al., 1998; Claireaux et al., 2000; Clark et al., 2005). It is possible that *S. lalandi* has a bell-shaped relationship between absolute aerobic scope and water temperature, such as that reported for species of salmon and trout (Dickson and Kramer, 1971; Brett and Glass, 1973; Taylor et al., 1996; Farrell, 2002; Lee et al., 2003a), yet this may only be determined with further experimentation at multiple temperatures. Nevertheless, the data presented for *S. lalandi* indicate that SMR comprises a smaller proportion of the absolute aerobic scope when the fish is at 20^{o}C as opposed to 25^{o}C, such that a greater fraction of the metabolic scope is available for other aerobic processes (e.g. swimming, digesting) when at the cooler temperature. From these data, it may be predicted that *S. lalandi* when fed a given ration would have a higher growth rate at 20^{o}C than at 25^{o}C, although this remains speculative until such experiments are performed.

2.5.3 Aerobic cost of transport

Calculation of U_{opt} and $GCOT_{min}$ of aquaculture species is arguably of more commercial relevance than SMR or $\dot{M}_{O_2\,max}$. Optimum swimming velocity and $GCOT_{min}$ provide estimates of routine activity levels and energy expenditure when under aquaculture conditions. Indeed, U_{opt} is considered a good predictor for routine swimming speeds in a range of species, suggesting that fish usually swim at speeds at which transport costs are minimal (Videler, 1993; Dewar and Graham, 1994; Tanaka et al., 2001; Lowe, 2002).

The U_{opt} for *S. lalandi* was higher at the warmer temperature than at the cooler temperature, which can be attributed to the thermal effects on SMR causing an increase in $GCOT_{min}$ at warmer temperatures. In comparison with the prominent U-shaped relationship that is typically documented for other species (Dewar and Graham, 1994; Lee et al., 2003a; Parsons and Sylvester, 1992), GCOT of *S. lalandi* at both temperatures followed a shallower U-shaped relationship with swimming velocity (Fig. 2.1c), such

that increases in swimming speed above U_{opt} were associated with negligible increases in swimming cost (i.e. the oxygen required to swim 1 m remained relatively constant from U_{opt} to U_{max}, even though GCOT should theoretically increase exponentially with swimming velocity above $GCOT_{min}$ to overcome the exponential increase in hydrodynamic resistance; Brett, 1964; Videler and Nolet, 1990).

The length-specific $GCOT_{min}$ determined for *S. lalandi* at 25°C compares favourably to values obtained for other pelagic teleosts including yellowfin tuna at 25°C and sockeye salmon at approximately 15°C (Table 2.4), although the higher U_{opt} values determined for *S. lalandi* and yellowfin tuna indicate a greater overall efficiency of these species over the salmon. At 20°C, *S. lalandi* displayed remarkable efficiency at U_{opt}, with the $GCOT_{min}$ being substantially lower than predicted for a fish of this body mass (Table 2.4; Brett, 1964), and lower than values obtained from most other species of pelagic teleost (Dewar and Graham, 1994; Lee et al., 2003a).

2.5.4 Bioenergetics model

The proposed bioenergetics model (equation 2.1 in Results) can be utilized to predict the dissolved oxygen usage and energy usage of fish in aquaculture conditions. For example, 1000 kg of *S. lalandi* when swimming in 20°C water at typical cruising speed (U_{opt} = 1.2 BL s^{-1} at 20°C) would consume 4839 mg of dissolved oxygen per minute (290,364 mg per hour), which corresponds to an energy usage of 68 kJ per minute (4094 kJ per hour). The same mass of *S. lalandi* when swimming in 25°C water (where U_{opt} = 1.7 BL s^{-1}) would consume 9063 mg of dissolved oxygen per minute (543,774 mg per hour), which corresponds to an energy usage of 128 kJ per minute (7667 kJ per hour). Care must be taken when applying this model to a population of fish that are greatly different in mass to the ones used in the present study (i.e. ~ 2 kg), given the fact that energy expenditure does not scale isometrically with body mass (White et al., 2005). Aquaculturalists of *S. lalandi* can use the values obtained from this bioenergetics model as a basis for energy expenditure of their fish in the commercial setting, hence subtracting these values from the metabolisable energy present in the feed.

Table 2.4. Comparison of swimming performance variables for *S. lalandi* with those of other similarly sized active teleosts.

Variable	*S. lalandi*		Sockeye salmon	Yellowfin tuna
Temperature (^{o}C)	20	25	~ 15	25
Body mass (kg)	2.1	1.9	3.0	2.2
Body length (m)	0.56	0.55	0.63	0.51
U_{opt} (BL s^{-1})	1.2	1.7	1.0	2.0
$GCOT_{min}$ (mg kg^{-1} m^{-1})	0.107 (0.127)[#]	0.164 (0.130)[#]	0.135	0.158
$GCOT_{min}$ (mg kg^{-1} BL^{-1})	0.062	0.088	0.085	0.081
NCOT at U_{opt} (mg kg^{-1} m^{-1})	0.069	0.105	0.050	0.100
NCOT at U_{opt} (mg kg^{-1} BL^{-1})	0.039	0.058	0.032	0.051

[#] values in parenthesis were predicted using $GCOT_{min}$ (mg kg^{-1} m^{-1}) = 0.1525 • $M_b^{-0.25}$, modified from Brett (1964) (note that this equation was formulated using data from animals at 15^{o}C); data for sockeye salmon are from Lee et al. (2003a); data for yellowfin tuna are from Dewar and Graham (1994).

2.6 Acknowledgements

This project was funded by grants from the Fisheries Research and Development Corporation and PIRSA Aq2uaculture, the Australian Research Council and the University of Adelaide. Our appreciation is extended to Arron Strawbridge (South Australian Research and Development Institute) for assistance with surgical procedures and for all aspects of animal husbandry. Quinn Fitzgibbon (University of Adelaide) is thanked for assistance with raising the fish and animal husbandry. Mick Kent, Laurence Durham and Brian Taylor (La Trobe University) are thanked for constructing the swim respirometer, while Peter Frappell (La Trobe University) is thanked for lending the respirometer to the University of Adelaide in order to perform this study. Craig White (University of Birmingham, UK) provided valuable comments relating to statistical analyses.

2.7 References

Altimiras, J. and Larsen, E. (2000). Non-invasive recording of heart rate and ventilation rate in rainbow trout during rest and swimming. Fish go wireless! *Journal of Fish Biology* **57**, 197-209.

Brett, J. R. (1964). The respiratory metabolism and swimming performance of young sockeye salmon. *Journal of the Fisheries Research Board of Canada* **21**, 1183-1226.

Brett, J. R. (1965). The relation of size to rate of oxygen consumption and sustained swimming speed of sockeye salmon

(*Oncorhynchus nerka*). *Journal of the Fisheries Research Board of Canada* **22**, 1491-1501.

Brett, J. R. and Glass, N. R. (1973). Metabolic rates and critical swimming speeds of sockeye salmon (*Oncorhynchus nerka*) in relation to size and temperature. *Canada Fisheries Research Board Journal* **30**, 379-387.

Brill, R. W. (1979). The effect of body size on the standard metabolic rate of skipjack tuna, *Katsuwonus pelamis*. *Fishery Bulletin* **77**, 494-498.

Brill, R. W. (1987). On the standard metabolic rates of tropical tunas, including the effect of body size and acute temperature change. *Fishery Bulletin* **85**, 25-35.

Brill, R. W. and Bushnell, P. G. (1991). Metabolic and cardiac scope of high energy demand teleosts, the tunas. *Canadian Journal of Zoology* **69**, 2002-2009.

Brill, R. W. and Bushnell, P. G. (2001). The cardiovascular system of tunas. In *Tuna - Physiology, Ecology, and Evolution*, (eds. B. A. Block and E. D. Stevens), pp. 468. San Diego: Academic Press.

Bushnell, P. G. and Jones, D. R. (1994). Cardiovascular and respiratory physiology of tuna - adaptations for support of exceptionally high metabolic rates. *Environmental Biology of Fishes* **40**, 303-318.

Bushnell, P. G., Brill, R. W. and Bourke, R. E. (1990). Cardiorespiratory responses of skipjack tuna (*Katsuwonus pelamis*), yellowfin tuna (*Thunnus albacares*), and bigeye tuna (*Thunnus obesus*) to acute reductions of ambient oxygen. *Canadian Journal of Zoology* **68**, 1857-1865.

Bushnell, P. G., Steffensen, J. G. and Johansen, K. (1984). Oxygen consumption and swimming performance in hypoxia-acclimated rainbow trout, *Salmo gairdneri*. *Journal of Experimental Biology* **13**, 225-235.

Claireaux, G., Webber, D. M., Lagardere, J. P. and Kerr, S. R. (2000). Influence of water temperature and oxygenation on the aerobic metabolic scope of Atlantic cod (Gadus morhua). *Journal of Sea Research* **44**, 257-265.

Clark, T. D., Ryan, T., Ingram, B. A., Woakes, A. J., Butler, P. J. and Frappell, P. B. (2005). Factorial aerobic scope is independent of temperature and primarily modulated by heart rate in exercising Murray cod

(*Maccullochella peelii peelii*). *Physiological and Biochemical Zoology* **78**, 347-355.

Dejours, P. (1975). Principles of Comparative Respiratory Physiology. Amsterdam: North-Holland Publishing Company.

Dewar, H. and Graham, J. B. (1994). Studies of tropical tuna swimming performance in a large water tunnel, 1 - Energetics. *Journal of Experimental Biology* **192**, 13-31.

Dickson, I. W. and Kramer, R. H. (1971). Factors influencing scope for activity and active and standard metabolism of rainbow trout (*Salmo gairdneri*). *Canada Fisheries Research Board Journal* **28**, 587-596.

Dickson, K. A., Donley, J. M., Sepulveda, C. and Bhoopat, L. (2002). Effects of temperature on sustained swimming performance and swimming kinematics of the chub mackerel *Scomber japonicus*. *Journal of Experimental Biology* **205**, 969-980.

Farrell, A. P. (2002). Cardiorespiratory performance in salmonids during exercise at high temperature: insights into cardiovascular design limitations in fishes. *Comparative Biochemistry & Physiology* **132**, 797-810.

Farrell, A. P. and Jones, D. R. (1992). The heart. In *Fish Physiology*, vol. 12A(eds. W. S. Hoar D. J. Randall and A. P. Farrell), pp. 1-88. San Diego: Academic Press.

Freadman, M. A. (1979). Swimming energetics of striped bass (*Morone saxatilis*) and bluefish (*Pomatomus saltatrix*): gill ventilation and swimming metabolism. *Journal of Experimental Biology* **83**, 217-230.

Gillanders, B. M., Ferrell, D. J. and Andrew, N. L. (2001). Estimates of movement and life-history parameters of yellowtail kingfish (*Seriola lalandi*): how useful are data from a cooperative tagging program? *Marine and Freshwater Research* **52**, 179-192.

Graham, J. B., Lowell, W. R., Lai, N. C. and Laurs, R. M. (1989). O_2 tension, swimming-velocity, and thermal effects on the metabolic rate of the Pacific albacore *Thunnus alalunga*. *Experimental Biology* **48**, 89-94.

Holeton, G. F. and Randall, D. J. (1967). The Effect of Hypoxia Upon the Partial Pressure of Gases in the Blood and Water Afferent and Efferent to the Gills of Rainbow Trout. *J Exp Biol* **46**, 317-327.

Hopkins, T. E. and Cech, J. J. (1994). Effect of temperature on oxygen consumption of the bat ray, *Myliobatis californica* (Chondrichthyes, Myliobatidae). *Copeia* **1994**, 529-532.

Ishimatsu, A., Maruta, H., Tsuchiyama, T. and Ozaki, M. (1990). Respiratory, ionoregulatory and cardiovascular responses of the yellowtail *Seriola quinqueradiata* to exposure to the red tide plankton *Chattonella*. *Nippon Suisan Gakkaishi-Bulletin of the Japanese Society of Scientific Fisheries* **56**, 189-199.

Ishimatsu, A., Maruta, H., Oda, T. and Ozaki, M. (1997). A comparison of physiological responses in yellowtail to fatal environmental hypoxia and exposure to *Chattonella marina*. *Fisheries Science* **63**, 557-562.

Jones, D. R., Brill, R. W. and Bushnell, P. G. (1993). Ventricular and arterial dynamics of anaesthetised and swimming tuna. *Journal of Experimental Biology* **182**, 97-112.

Kiceniuk, J. W. and Jones, D. R. (1977). The oxygen transport system in trout (*Salmo gairdneri*) during sustained exercise. *The Journal of Experimental Biology* **69**, 247-260.

Korsmeyer, K. E. and Dewar, H. (2001). Tuna metabolism and energetics. In *Tuna - Physiology, Ecology, and Evolution*, (eds. B. A. Block and E. D. Stevens), pp. 468. San Diego: Academic Press.

Korsmeyer, K. E., Lai, N. C., Shadwick, R. E. and Graham, J. B. (1997a). Heart rate and stroke volume contributions to cardiac output in swimming yellowfin tuna - response to exercise and temperature. *Journal of Experimental Biology* **200**, 1975-1986.

Korsmeyer, K. E., Lai, N. C., Shadwick, R. E. and Graham, J. B. (1997b). Oxygen transport and cardiovascular responses to exercise in the yellowfin tuna *Thunnus albacares*. *Journal of Experimental Biology* **200**, 1987-1997.

Lee, C. G., Farrell, A. P., Lotto, A., MacNutt, M. J., Hinch, S. G. and Healey, M. C. (2003a). The effect of temperature on swimming performance and oxygen consumption in adult sockeye (*Oncorhynchus nerka*) and coho (*O. kisutch*) salmon stocks. *The Journal of Experimental Biology* **206**, 3239-3251.

Lee, K. S., Ishimatsu, A., Sakaguchi, H. and Oda, T. (2003b). Cardiac output during exposure to *Chattonella marina* and environmental hypoxia in yellowtail (*Seriola quinqueradiata*). *Marine Biology* **142**, 391-397.

Lee, K. S., Kita, J. and Ishimatsu, A. (2003c). Effects of lethal levels of environmental hypercapnia on cardiovascular and blood-gas status in yellowtail, Seriola quinqueradiata. *Zoological Science* **20**, 417-422.

Lowe, C. G. (2002). Bioenergetics of free-ranging juvenile scalloped hammerhead sharks (*Sphyrna lewini*) in Kane'ohe Bay, O'ahu, HI. *Journal of Experimental Marine Biology & Ecology* **278**, 141-156.

MacNutt, M. J., Hinch, S. G., Farrell, A. P. and Topp, S. (2004). The effect of temperature and acclimation period on repeat swimming performance in cutthroat trout. *Journal of Fish Biology* **65**, 342-353.

Macy, W. K., Durbin, A. G. and Durbin, E. G. (1999). Metabolic rate in relation to temperature and swimming speed and the cost of filter feeding in Atlantic menhaden, *Brevoortia tyrannus*. *Fishery Bulletin* **97**, 282-293.

O'Steen, S. and Bennett, A. F. (2003). Thermal acclimation effects differ between voluntary, maximum, and critical swimming velocities in two cyprinid fishes. *Physiological & Biochemical Zoology* **76**, 484-496.

Parsons, G. R. and Sylvester, J. L. (1992). Swimming efficiency of the white crappie, *Pomoxis annularis*. *Copeia* **1992**, 1033-1038.

Poortenaar, C. W., Hooker, S. H. and Sharp, N. (2001). Assessment of yellowtail kingfish (*Seriola lalandi lalandi*) reproductive physiology, as a basis for aquaculture development. *Aquaculture* **201**, 271-286.

Randall, D. J., Holeton, G. F. and Stevens, E. D. (1967). The Exchange of Oxygen and Carbon Dioxide Across the Gills of Rainbow Trout. *J Exp Biol* **46**, 339-348.

Schmidt-Nielsen, K. (1990). Animal Physiology: Adaptation and Environment. Cambridge: Cambridge University Press.

Sepulveda, C. and Dickson, K. A. (2000). Maximum sustainable speeds and cost of swimming in juvenile kawakawa tuna (*Euthynnus affinis*) and chub mackerel (*Scomber japonicus*). *Journal of Experimental Biology* **203**, 3089-3101.

Sepulveda, C. A., Dickson, K. A. and Graham, J. B. (2003). Swimming performance studies on the eastern Pacific bonito *Sarda chiliensis*, a close relative of the tunas (family Scombridae), I - Energetics. *Journal of Experimental Biology* **206**, 2739-2748.

Shadwick, R. E. and Steffensen, J. F. (2000). The cost and efficiency of aerobic locomotion in the chub mackerel (*Scomber japonicus*). *American Zoologist* **40**, 2108.

Stevens, E. D. and Randall, D. J. (1967). Changes in gas concentrations in blood and water during moderate swimming activity in trout. *The Journal of Experimental Biology* **46**, 329-337.

Tanaka, H., Takagi, Y. and Naito, Y. (2001). Swimming speeds and buoyancy compensation of migrating adult chum salmon *Oncorhynchus keta* revealed by speed/depth/acceleration data logger. *Journal of Experimental Biology* **204**, 3895-3904.

Taylor, S. E., Egginton, S. and Taylor, E. W. (1996). Seasonal temperature acclimatisation of rainbow trout: cardiovascular and morphometric influences on maximal sustainable exercise level. *The Journal of Experimental Biology* **199**, 835-845.

Videler, J. J. (1993). Fish Swimming. London: Chapman and Hall.

Videler, J. J. and Nolet, N. R. (1990). Cost of swimming measured at optimum speed: scale effects, differences between swimming styles, taxonomic groups, and submerged and surface swimming. *Comparative Biochemistry & Physiology A - Comparative Physiology* **97**, 91-99.

Webber, D. M., Boutilier, R. G. and Kerr, S. R. (1998). Cardiac output as a predictor of metabolic rate in cod *Gadus morhua*. *Journal of Experimental Biology* **201**, 2779-2789.

White, C. R., Phillips, N. F. and Seymour, R. S. (2005). The scaling and temperature dependence of vertebrate metabolism. *Biology Letters*, 1-3.

Yamamoto, K. I. (1991). Increase of arterial O_2 content in exercised yellowtail (*Seriola quinqueradiata*). *Comparative Biochemistry & Physiology A - Comparative Physiology* **98**, 43-46.

Yamamoto, K. I., Itazawa, Y. and Kobayashi, H. (1981). Gas exchange in the gills of yellowtail, *Seriola quinqueradiata* under resting and normoxic condition. *Bulletin of the Japanese Society of Scientific Fisheries* **47**, 447-451.

Chapter 3: Metabolic scope, swimming performance and the effects of hypoxia in the mulloway (*Argyrosomus japonicus*)

Q. P. Fitzgibbon[a]*, A. Strawbridge[b], R. S. Seymour[a]

[a]School of Earth and Environmental Sciences, University of Adelaide, Adelaide, South Australia, 5005. [b]South Australian Research and Development Institute, Henley Beach, South Australia, 5022.

* Corresponding author. Tel.: +61 8 8303 4743; fax: +61 8 8303 4364
E-mail address: quinn.fitzgibbon@adelaide.edu.au

3.1 Abstract

The effects of graded hypoxia on the swimming performance and metabolic scope of the emerging aquaculture species mulloway (*Argyrosomus japonicus),* were investigated. In normoxic conditions (dissolved oxygen = 6.9 ± 0.02 mg L^{-1}, mean ± SE, n=47), mulloway oxygen consumption ($\dot{M}_{O_2}$) increased exponentially with swimming speed to a maximum sustained velocity (critical swimming velocity) of 1.8 body lengths s^{-1} (BL s^{-1}). Active metabolic rate (AMR) was 365 ± 19.7 mg kg^{-1} h^{-1} (n=6) corresponding to a metabolic scope (292 ± 17.6 mg kg^{-1} h^{-1}) of 5 times the standard metabolic rate (SMR; determined by extrapolation of the $\dot{M}_{O_2}$ swimming velocity relationship to a velocity of zero). In all grades of hypoxia (75% saturation =5.2 ± 0.02 (n=44), 50% =3.6 ± 0.03 (n=36), and 25% =1.9 ± 0.02 mg L^{-1} (n=37)), $\dot{M}_{O_2}$ was linearly related to swimming speed. Critical swimming velocity was significantly suppressed at 50% and 25% saturation (1.4 ± 0.04 and 1.4 ±0.02 BL s^{-1} respectively, n=6), however, the metabolic scope was suppressed in all hypoxic grades (209 ± 15.5, 152 ± 9.08 and 149 ± 10.6 mg kg^{-1} h^{-1} for 75%, 50% and 25% saturation respectively, n=6). This demonstrates that though mild hypoxia may not be acutely lethal, it may cause energy budgeting conflicts that will result in reduced production performance. In a further experiment, the critical dissolved oxygen level of mulloway swimming at 0.95 BL s^{-1} was determined to be 1.5 mg L^{-1}. This reveals that mulloway are well adapted to hypoxia, which is probably associated with their natural early life history within estuaries, and gives further evidence to support their suitability for aquaculture expansion.

3.2 Introduction

Metabolism is the physiological engine that powers all activities such as swimming, growth and reproduction (Neill *et al.*, 1994). The potential power that this engine can generate is determined by the metabolic scope, the difference in metabolic rates at the maximum sustained (active metabolic rate; AMR) and minimum metabolism (standard metabolic rate; SMR). The metabolic scope governs the amount of energy available to support activities and the greater the aerobic scope the greater the potential for growth (Fry, 1971). Any environmental condition causing a reduction of metabolic scope leads to energy budgeting conflicts (Lefrancois and Claireaux, 2003). Therefore, maintaining conditions for optimum metabolic scope will result in optimum potential productivity. For this reason metabolic scope is considered to be an integrative measure of environmental quality for aquaculture (Neill and Bryan, 1991).

The environment influences the activity of an organism through metabolism. Fry (1971) categorized the physiological effect of environmental factors as, lethal, controlling, limiting, masking and directive. This conceptual model elucidates how the environment controls the boundaries in which bioenergetic processes must take place (Claireaux and Lagardere, 1999). Dissolved oxygen is considered to be a limiting factor, setting the upper limit of aerobic metabolism and therefore defining the metabolic scope. Although the effect of reduced oxygen uptake capacity of the gills may not be acutely lethal, it can result in a reduction in performance (Priede, 1985).

The mulloway (*Argyrosomus japonicus,* formally *A. hololepidotus)* is a large sciaenid (maximum size 75kg) that has recently become an aquaculture species (Battaglene and Talbot, 1994; Fielder and Bardsley, 1999; Hecht and Mperdempes, 2001). The mulloway is naturally distributed in the coastal waters of the Indian and eastern Pacific oceans and has long been an important commercial fisheries species in Australia and South Africa (Griffiths and Heemstra, 1995; Griffiths, 1997a). Juvenile mulloway reside in estuaries, whilst adults move close offshore and to surrounding surf zones (Gray and McDonal, 1993; Griffiths, 1997a; b). Attributes that make mulloway suitable for aquaculture include its marketability at a relatively high price, high fecundity, fast growth, non-territorial and non-cannibalistic nature, and saline resilience, which make them suitable for both marine cage and on-land saline pond culture.

There is no metabolic information on the mulloway and little on othermembers of the Sciaenidae. This is despite sciaenid species becoming increasingly important to aquaculture world wide (Thomas *et al.*, 1996; Drawbridge, 2001; Holt, 2001). In fact, sciaenid fishes are now the major fish species for artificial propagation in the world's leading producer of

aquaculture products, China (Hong and Zhang, 2003). Consequently, there is a lack of precise metabolic data for calculations of aquaculture system oxygen requirements, environmental impact assessment, and species-specific physiological thresholds.

The following study aims to define some of these metabolic parameters of mulloway. In particular, we examine the relationship between swimming velocity and metabolic rate ($\dot{M}_{O_2}$), SMR, AMR, metabolic scope, and critical swimming velocity (U_{crit}). Furthermore, we will examine the effect of hypoxia on these parameters with the purpose of determining not just the minimum requirements but also hypoxia's potential production-limiting effects through modulation of the metabolic scope.

3.3 Materials and Methods

3.3.1 Experimental Animals

30 juvenile mulloway (340 $\pm$ 8 g, Table 3.1) were randomly selected from 10,000 L flow through (3 mm gravel filtered seawater) stock tanks at the South Australian Research and Development Institute, Aquatic Sciences, West Beach facility. These fish had been raised on site from fertilized eggs supplied by Clean Seas Pty. Ltd., a commercial marine finfish hatchery in Spencer Gulf, South Australia. Fish were maintained at ambient light and water temperature. All experimental trials were conducted between December 2004 and March 2005 when water temperatures remained between 21 and 23^{o}C. Fish were fed Skretting Nova® marine diet to satiation once a day but were starved for a minimum of 36 h before the beginning of any experimental trials.

For each experimental trial, individual fish were scoop-netted from the stock tank and immediately transferred into a 2,000 L fish transport container filled with sea-water and transported 13 km to the University of Adelaide campus where all respiratory trials were conducted. Seawater from the transport container was used to gravity fill the respirometer, and the fish introduced. All fish were introduced into the respirometer late in the afternoon and then left overnight to acclimate for a minimum of 16 h. During the acclimation period, gently bubbled air maintained dissolved oxygen above 7 mg L^{-1} and water flow velocity was set at 7.5 cm s^{-1} (~0.25 body lengths s^{-1}, BL s^{-1}) to facilitate steady swimming and sufficient respirometer mixing. Following experimental trials, fish were anaesthetized in 0.05 mg L^{-1} clove oil, and fork length (BL) and mass (M) recorded.

3.3.2 Experimental apparatus

All respiratory trials were conducted in a large (850 L) Brett-type water tunnel respirometer modified from an existing flume tank. The respirometer was predominantly constructed from acrylic plastic and large diameter unplasticised polyvinyl chloride storm-water pipe. Water flow was driven by a single 20 cm propeller powered by a 1.5 kW CMG electric motor with a Nord AC® variable speed controller, enabling a maximum water flow velocity of 80 cm s^{-1}. Circulating water passed through flow-resistance tubes (1 cm internal diameter × 25 cm long) to induce even laminar flow before entry into the working section. Laminar flow was verified by video observation of neutrally buoyant particles (wet cotton wool balls) drifting through the working section with a MotionScope® PCI High Speed Video System. The working section was 100 × 40 × 40 cm (length × width × height), however, fish were restricted from within 8 cm of the walls by a rigid wire cage (3 cm stay and line wire spacing), to reduce wall flow-resistance effects. Water velocity calibrations were made with a Sontek (ADV) Acoustic Doppler velocimeter (mean 25hz for 10 s), from 10 positions (five horizontal × two vertical intervals) in the active working section. The coefficient of variation between mean flow velocity and sample position was found to be low (<6.1%, n=10).

Fish were introduced into the working section through a hinged hatch, which was sealed immediately, and the up-stream half covered to limit visual disturbance. Fish generally maintained position within the shaded forward half of the working section, only falling back to the visible rear section when unable to maintain position against the water current. Once sealed, water level was topped up by gravity feed from the fish transport vessel and gas bled from the system through twelve bleeder valves. Water dissolved oxygen was manipulated by bubbling air, nitrogen or oxygen through a large air stone. A 2.4 kW pump by-passed respirometer water through a 4 kW chiller and 500 W heater element that maintained respirometer water temperature via a Carel (IR series) digital controller unit. During all experiments, respirometer water temperatures were maintained between 21.8 and 22.2°C.

3.3.3 Dissolved oxygen measurement

Respirometer water was continually sampled and replaced via an Ismatic SA Vario peristaltic pump that passed sampled water through a Microx (FTCH) micro-optode flow-though cell housing, and dissolved oxygen was recorded with a PreSens Microx (TX3) fiber-optic oxygen meter with automatic temperature compensation. Temperature adjusted dissolved oxygen concentration (mg L^{-1}) was logged every 10 s on a personal computer with the Microx TX3 software. The meter was calibrated at the start of each trial according to the manufacturer's instructions, and calibration checked at the end of the trial. Meter drift was never found to be significant. Recorded dissolved oxygen was later adjusted for salinity,

assuming an oxygen solubility of 7.20 mg L^{-1} in oceanic seawater (salinity of 35 ‰) at 22°C. A minimum of 15 min swimming at any velocity was required for oxygen consumption measurements.

3.3.4 Experimental protocols

For all treatments, fish oxygen consumption rate was recorded over a 1 h period before either the swimming velocity or dissolved oxygen was changed and the next swim trial begun. This would continue until the critical swimming velocity (U_{crit}) was reached and the experiment terminated. The critical swimming velocity was defined as when the fish resorted to burst and glide swimming and brushed its tail up against the back screen more than three times in 30 s. Critical swimming velocity was calculated using the equation (Brett, 1964):

$$U_{crit} = U_c + [(T_f / T_i) \times U_i] \quad (3.1)$$

where U_c is the last speed at which the fish swam the entire 1 h period, T_f is the time the fish swam at the final speed, T_i is the time interval at each speed (1 h), and U_i is the velocity increments (7.5 cm s^{-1}).

At the end of the experiment the fish was removed from the respirometer and background respiration measured. Background trials were conducted at the same dissolved oxygen level as in the pertinent respiratory trial, to take into account any changes in passive diffusive qualities of the respirometer depending on experimental oxygen level. Although background respiration was found to be small, all fish oxygen consumption results were adjusted accordingly. Five respiratory experiments were conducted, each using 6 individual fish:

(i) Normoxia
Beginning at a swimming velocity of 7.5 cm s^{-1}, oxygen consumption was recorded for a period of 1 h, before the swimming velocity was then increased in a stepwise fashion by 7.5 cm s^{-1} for periods of 1 h until the critical swimming velocity was reached. Respirometer dissolved oxygen for individual swimming trials was maintained close to normoxia, with a mean start point for trials of 6.9 $\pm$ 0.02 mg L^{-1} (mean $\pm$ SE, n = 47).

(ii) 75%, (iii) 50%, and (iv) 25%
The same procedure was used as for the normoxia trial, except dissolved oxygen was maintained at approximately 75%, 50%, and 25% saturation, with a mean start point of 5.2 $\pm$ 0.02 (n=44), 3.6 $\pm$ 0.03 (n=36), and 1.9 $\pm$ 0.02 mg L^{-1} (n=37) respectively.

(v) Critical dissolved oxygen level (R_{crit})

At a constant water flow velocity of 30 cm s^{-1}, fish oxygen consumption was recorded over periods of 1 h with respirometer dissolved oxygen progressively reduced at the end of each hour. Trials began at approximately 50% (3.6 mg l^{-1}) and stepped down to 40% (2.9 mg L^{-1}), 30% (2.2 mg L^{-1}), 25% (1.8 mg L^{-1}), 20% (1.5 mg L^{-1}), 15% (1.2 mg L^{-1}), 12.5% (0.9 mg L^{-1}) to finally to a minimum of approximately 10% saturation (0.7 mg L^{-1}). Each trial was terminated when the fish could no longer maintain its position against the water flow, and brushed its tail up against the back screen more than three times in 30 s.

3.3.5 Data Analysis

Linear regression was applied to oxygen consumption data and fish oxygen consumption rate determined by the following equation:

$$\dot{M}_{O_2} \text{ (mg kg}^{-1} \text{ h}^{-1}\text{)} = ((O - B) \times V)/ M \qquad (3.2)$$

where O is the fish oxygen consumption recorded (mg L^{-1} h^{-1}), B the recorded relevant background respiration rate for the trial (mg L^{-1} h^{-1}), V the respirometer volume (L) and M the fish mass (kg). Standard metabolic rate was determined by extrapolation of the $\dot{M}_{O_2}$ exponential relationship back to a swimming velocity of 0.0 cm s^{-1}. Statistical differences represented are Analysis of Variance with Tukey Post-Hoc analysis ($P<0.05$) performed using Microsoft StatistiXL software. Values are mean $\pm$ SE.

3.4 Results

In the normoxia experiment, five out of the six fish were capable of swimming at a maximum velocity of 60 cm s^{-1} and an exponential curve best described the relationship between swimming velocity and oxygen consumption (R^2=0.86, Table 3.1, Fig. 3.1a). At 75% saturation, oxygen consumption increased linearly with swimming speed (R^2=0.82) and only two of the six fish were able to maintain sustained swimming at 60 cm s^{-1} (Fig. 3.1b). At 50% saturation, oxygen consumption also appeared to be directly proportional to swimming speed (R^2=0.65), however 52.5 cm s^{-1} was the maximum swimming velocity, which was only achieved by a single fish (Fig. 3.1c). At 25% saturation, the maximum swimming velocity was 45 cm s^{-1}, and oxygen consumption again increased linearly with swimming velocity (R^2=0.85, Fig. 3.1d).

Table 3.1: Fish mass and fork length (BL), trial start point dissolved oxygen (DO), swim velocity range (U) achieved, and relationship between swimming velocity and oxygen consumption ($\dot{M}_{O_2}$),represented as an exponential (Exp.) or linear relationship.

Trial	Mass (kg)	BL (cm)	DO (mg l^{-1})	U (cm s^{-1})	$\dot{M}_{O_2}$ (Exp.)	R^2 (Exp.)	$\dot{M}_{O_2}$ (linear)	R^2 (linear)
100%	0.39 ±0.02	31 ±0.46	6.9 ±0.02	7.5-60	$70.9e^{0.027u}$	0.86	5.19u + 27.0	0.84
75%	0.34 ±0.01	32 ±0.31	5.2 ±0.02	7.5–52.5	$54.1e^{0.026u}$	0.75	3.19u + 36.4	0.82
50%	0.36 ±0.03	32 ±0.85	3.6 ±0.02	7.5–52.5	$38.9e^{0.038u}$	0.58	3.76u + 26.6	0.65
25%	0.33 ±0.01	32 ±0.37	1.9 ±0.02	7.5-45	$25.8e^{0.045u}$	0.75	3.67u + 3.8	0.85
R_{crit}	0.36 ±0.01	32 ±0.37	-	30	-	-	-	-

Values are means ± SE, n=6 for mass and BL, n=47-36 for DO

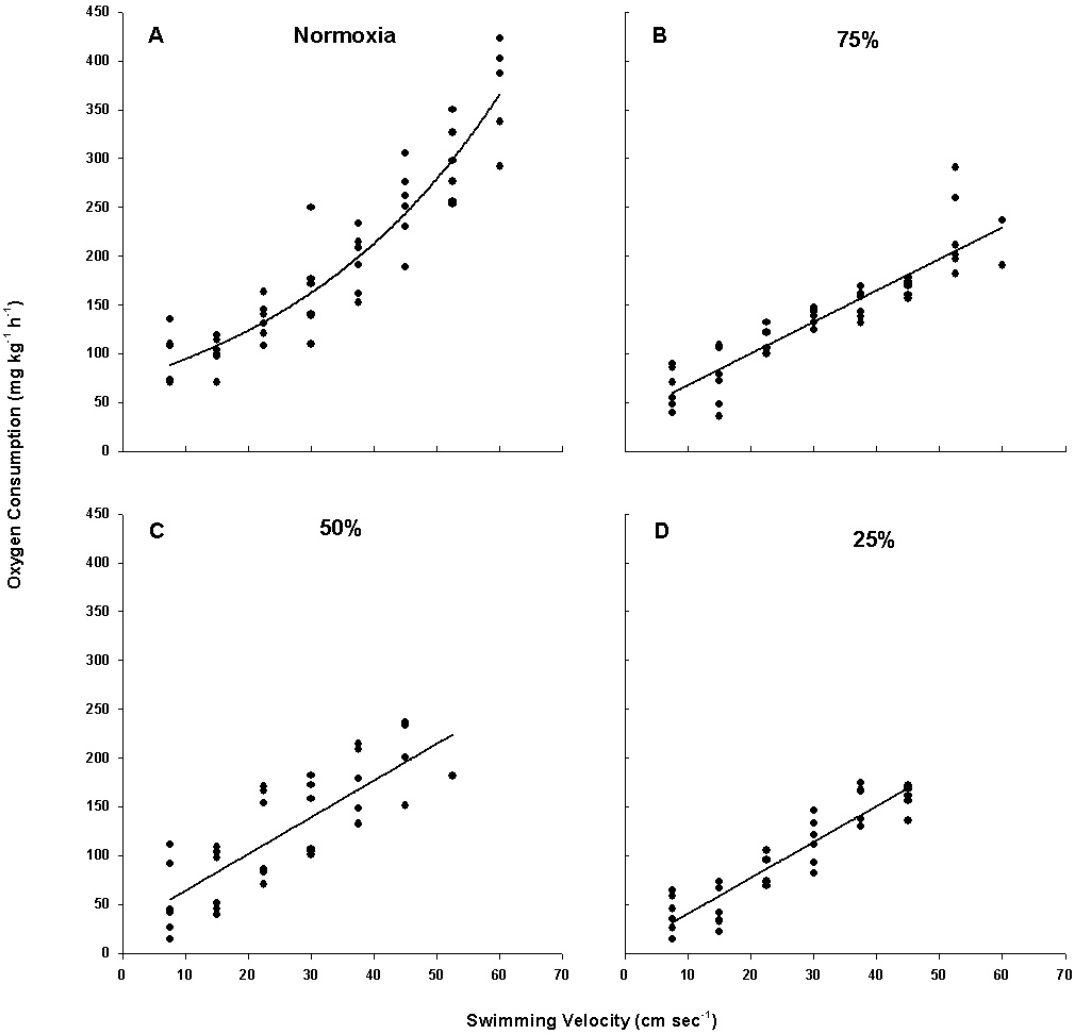

Figure 3.1: The relationship between oxygen consumption and swimming velocity of mulloway (n=6) when swum at progressively increasing velocities (interval of 7.5 cm s^{-1}) for 1 h periods at dissolved oxygen levels of **(a)** 6.9 mg L^{-1} (normoxia), **(b)** 5.2 mg L^{-1} (75%), **(c)** 3.6 mg L^{-1} (50%) and **(d)** 1.9 mg L^{-1} (25%).

Hypoxia reduced U_{crit} (ANOVA: $F_{3,20}$=11.7, p<0.001), AMR (ANOVA: $F_{3,20}$=30.6, p<0.001), and metabolic scope (ANOVA: $F_{3,20}$=23.8, p<0.001) of the mulloway examined. U_{crit} was significantly reduced when dissolved oxygen fell below 50% saturation (Fig 3.2a). Active metabolic rates and metabolic scopes of fish were significantly below those measured during normoxia in all grades of hypoxia (Figs. 3.2b and c respectively).

Dissolved oxygen appeared to have little influence on metabolic rate until the dissolved oxygen level reached 1.5 mg L^{-1} or 20% saturation (Fig. 3.3).

Above this dissolved oxygen level, the oxygen consumption rates of the fish remained close to 120 mg kg^{-1} h^{-1}. Below 1.5 mg L^{-1}, the oxygen consumption rate dropped sharply. One fish lost the ability to sustain swimming at a dissolved oxygen level of approximately 0.9 mg L^{-1} (12.5% saturation), the remaining five fish at 0.7 mg L^{-1}. 1.5 mg L^{-1} was defined as the R_{crit} for the mulloway examined.

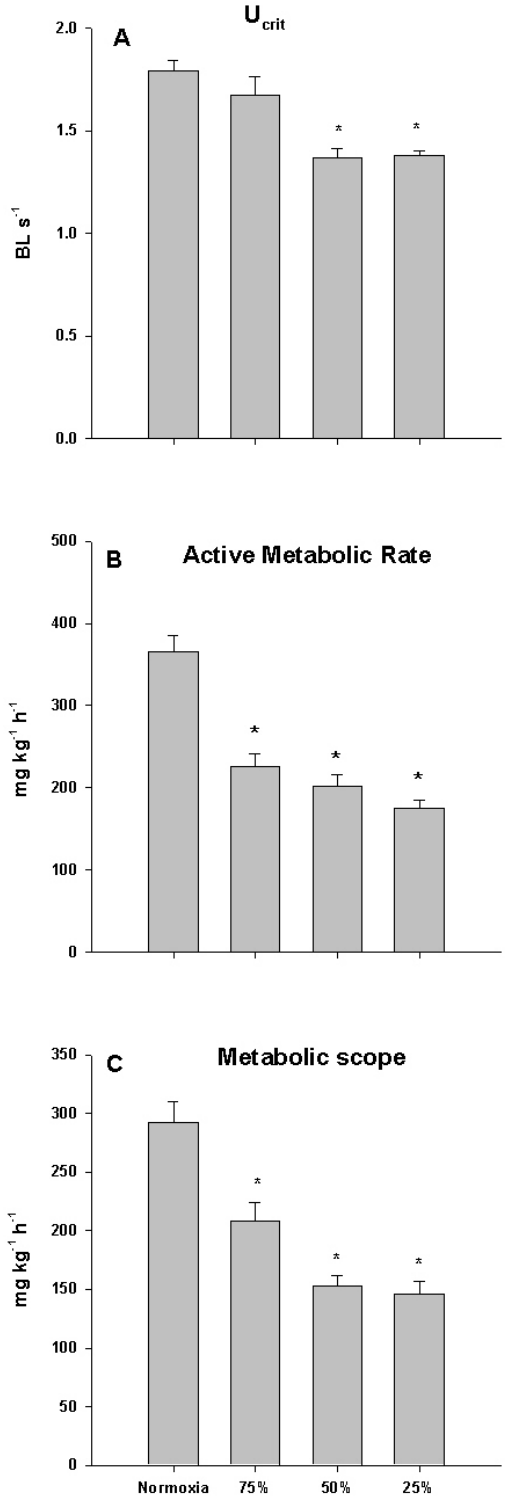

Figure 3.2: (a) Critical swimming velocity (U_{crit}), **(b)** active metabolic rate and **(c)** metabolic scope of mulloway when swum at dissolved oxygen of normoxia, 75, 50 and 25% (details are as for Fig 3.1). * Indicates significant difference from normoxia based on Tukey's post-hoc test ($P<0.05$).

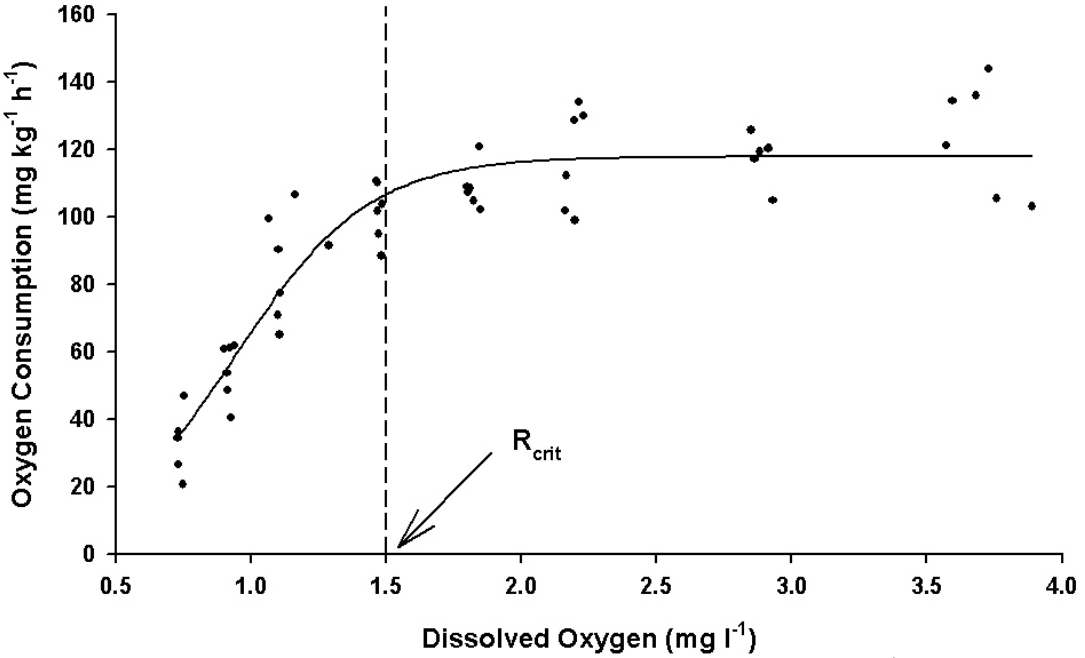

Figure 3.3: Oxygen consumption of mulloway (n=6) swimming at 30 cm s^{-1} for 1 h periods at progressively lower dissolved oxygen levels between 4 and 0.6 mg l^{-1}. The dotted line indicates the determined critical oxygen level (R_{crit}).

3.5 Discussion

3.5.1 Normoxic interspecific comparison

The critical swimming velocity (U_{crit}) is defined as the maximum swimming velocity a fish can maintain for a defined period. However, the U_{crit} will vary depending on the velocity increment and the amount of time spent at each speed (Bushnell *et al.*, 1984). Furthermore, body mass and study temperature will affect the maximum sustainable swimming velocity of an individual. For these reasons interspecific comparisons of U_{crit} are problematic. In the present study, U_{crit} of mulloway was recorded to be 56.3 cm s^{-1}, corresponding to 1.8 BL s^{-1}. This is similar to U_{crit} recorded for the Atlantic cod (1.9 BL s^{-1};*Gadus morhua*, 0.30 kg, 15^{o}C, Schurmann and Steffensen, 1997) and the rainbow trout (1.8 BL s^{-1}; *Oncorhynchus mykiss,* 0.25-0.35 kg, 15^{o}C, Bushnell *et al.*, 1984). However, it is considerably lower than that recorded with more active species such as the sockeye salmon (2.9 BL s^{-1}; *Oncorhynchus nerka*, 0.746 kg, 15^{o}C, Brett, 1965), the chub mackerel (3.8-5.8 BL s^{-1}, *Scomber japonicus*, 0.03-0.16 kg, 24^{o}C, Sepulveda and Dickson, 2000), and the kawakawa tuna (3.4 BL s^{-1};

Euthynnus affinis, 0.02-0.27 kg, 24^{o}C, Sepulveda and Dickson, 2000). It is likely that the limited sustained swimming ability of mulloway is associated with their foraging and predation style. Mulloway are pounce predators, better adapted to sudden bursts of speed rather than rapid sustained swimming. Anatomical adaptations that support close quarter attack include; large, wedge shaped caudal fins and a deep caudal peduncle to enable rapid acceleration, and a large buccal cavity for suction feeding (Griffiths, 1997b).

As with most fish species, an exponential increase best describes the relationship between swimming velocity and $\dot{M}_{O_2}$ of the mulloway. However, at the two slowest velocities (0.24 and 0.48 BL s^{-1}) there is little difference in oxygen consumption rates, with metabolic rate being slightly less at the faster of the two velocities. This is most probably due to an increased energy cost associated with stability control at the low swimming velocities. Indeed, Webb (1998), suggested a J-shaped curve best describes $\dot{M}_{O_2}$ of negatively buoyant fish, and that the elevated metabolic rate of fishes at low velocities should not be dismissed. This could have considerable influence in aquaculture system design, where the fish are required to swim against a defined current. For the mulloway it appears that the optimum swimming speed is between 0.3 and 0.5 BL s^{-1}.

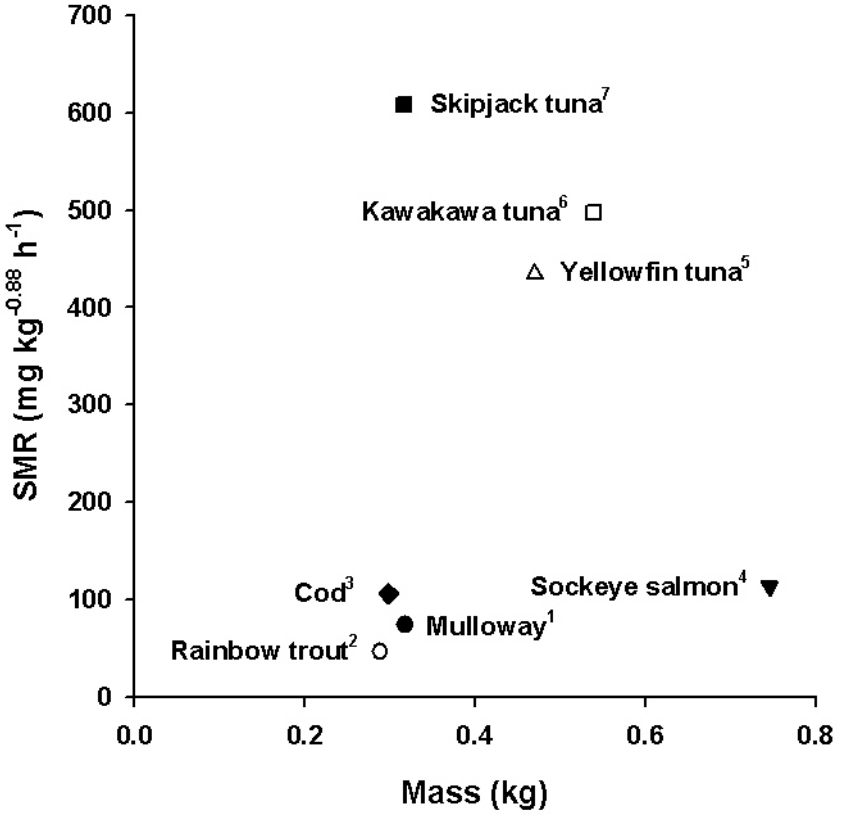

Figure 3.4: The standard metabolic rate plotted independent of mass (assuming a mass scaling exponent of 0.88 and a normalized study temperature of 25°C) of [1]mulloway (present study), [2]rainbow trout (Bushnell et. al, 1984), [3]Atlantic cod (Schurmann and Steffensen, 1997), [4]sockeye salmon (Brett, 1964), [5]yellowfin tuna (Dewar and Graham, 1994), [6]kawakawa tuna (Brill, 1987), and [7]skipjack tuna (Brill, 1979).

For relevant interspecific comparison of metabolic states, the effect of variable study temperature and fish mass must be normalized between studies. Figure 3.4 compares the SMR of mulloway with other active teleost species assuming a mass scaling exponent of 0.88 (Brett and Glass, 1973; White *et al.*, 2006) and normalized study temperature of 25°C with Q_{10}=1.65 (White *et al.*, 2006). As can be seen, the SMR of mulloway is similar to rainbow trout, Atlantic cod, and sockeye salmon (Brett, 1965; Brill, 1987; Schurmann and Steffensen, 1997) but considerably less than that of tuna species (Brill, 1979, 1987; Dewar and Graham, 1994; Fig. 3.4). This suggests that the basal metabolic rate of mulloway is very similar to the majority of active fishes other than the tunas. Tuna are known to be metabolically different to other active teleosts. Their elevated SMR is associated with physiological adaptations such as a large gill surface area that allows tuna to achieve great aerobic scopes (Bushnell and Jones, 1994). Only dolphin fish (*Coryphaena hippurus*) is known to have a similarly

high SMR. The dolphin fish's elevated SMR has been attributed to physiological adaptations similar to that of tuna, such as large gill surface area and fast growth rates.

The AMR recorded for mulloway in the present study (365 ±19.7 mg kg^{-1} h^{-1}, n=6) corresponds to 5 times the SMR (factorial metabolic scope). The factorial metabolic scope ranges widely in fishes from 3.7 for sedentary species such as Murray cod (*Maccullochella peelii peelii*; 14-29°C, Clark *et al.*, 2005) to 15.4 for the active sockeye salmon (*Oncorhynchus nerka,* 15°C, Brett and Glass, 1973). However, in terms of potential power generation, the use of factorial comparisons is limited as they are sensitive to species-specific SMR. For example, though the predicted factorial metabolic scope of tuna (8-9 times SMR) is less than that of sockeye salmon (15 times), tuna's high SMR results in them having a much greater metabolic scope (Brill and Bushnell, 1991; Korsmeyer and Dewar, 2001). In terms of total potential oxygen consumption available, mulloway has a similar available metabolic scope (292 mg kg^{-1} h^{-1}) to that of other more sedentary species such as Atlantic cod (224 mg kg^{-1} h^{-1}, 0.30 kg, 15°C, Schurmann and Steffensen, 1997) and rainbow trout (279 mg kg^{-1} h^{-1}, 0.25-0.35 kg, 15°C, Bushnell *et al.*, 1984).

3.5.2 Critical oxygen level (R_{crit})

All fish have some ability to cope with fluctuations in dissolved oxygen. During mild hypoxia, fish are able to maintain constant metabolic function mainly by increasing respiratory volume (Randall, 1982) and when doing so are referred to as oxygen regulators (Hughes, 1973). However, below a certain dissolved oxygen level (the critical dissolved oxygen level - S_{crit}), the fish is unable to maintain its SMR and oxygen consumption decreases linearly with dissolved oxygen. At this point the fish is now termed an oxygen conformer and if the situation persists, will eventually die. In the present study, instead of evaluating the critical oxygen level based on a resting fish (S_{crit}), it was determined at a routine metabolic state; a swimming velocity of 30 cm s^{-1} (0.95 BL s^{-1}) corresponding to a metabolic load of 45% of the AMR. This was done as it was believed that a critical oxygen level based on fish at a defined routine metabolic rate (R_{crit}) would be more relevant to aquaculture where the fish are likely to have a metabolic load associated with specific dynamic action when hypoxic conditions are experienced. However, it must be acknowledged that the R_{crit} is likely to be an overestimate compared to S_{crit} evaluated based on the SMR. Taking this into account, it appears that the mulloway is well adapted to hypoxia as the R_{crit} recorded (1.5 mg l^{-1}) in the present study is considerably less than that of the S_{crit} of Atlantic cod (2.58 mg l^{-1}, 15°C, Schurmann and Steffensen, 1997) but very similar to that of the rainbow trout (1.6 mg l^{-1}, 20°C, Ott *et al.*, 1980) and only slightly higher than the hypoxia tolerant carp (*Cyprinus*

carpio, 1.1 mg l^{-1}, 25^{o}C, Ott *et al.*, 1980). It is most likely that this hypoxia tolerance is an adaptation to support mulloway's early life history within estuaries, where water quality could be variable, and fluctuations in dissolved oxygen likely. This hypoxia tolerance gives further evidence to support mulloway's suitability for aquaculture expansion.

3.5.3 Effect of hypoxia

The negative effect of hypoxia on fish growth rate is well documented. For the most part, this reduction in growth has been attributed to reduced feed intake and is not a consequence of decreased feed conversion ratio (Chabot and Dutil, 1999; Thetmeyer *et al.*, 1999; Pichavant *et al.*, 2001; Mallekh and Lagardere, 2002). This reduction in feed intake is suggested to be due to energy budgeting conflicts caused by the limiting effect of hypoxia on the metabolic scope. Mallekh and Lagardere (2002) found a linear relationship between turbot (*Scophthalmus maximus*) feed intake and metabolic scope, suggesting that turbot appetite is regulated by their capacity to provide the energy necessary for digestion. Furthermore, this is supported by Claireaux *et al.,* (2000) who found a direct relationship between Atlantic cod hypoxia-related reduced growth rate and metabolic scope. In the present study, mulloway AMR and metabolic scope were significantly suppressed at a dissolved oxygen level of just 75% saturation. This is the same result as recorded for the common sole (*Solea solea*, 4-24^{o}C, Lefrancois and Claireaux, 2003), and similar to that recorded with turbot (6-22^{o}C), where below 78 and 90% air saturation the AMR was suppressed (Mallekh and Lagardere, 2002). This suggests for these species, that even mild hypoxic conditions may cause energy budgeting conflicts that will result in reduced production performance. Such an effect was recorded with Atlantic cod (6-10^{o}C) where 73% air saturation was found to be the critical level of dissolved oxygen below which growth was suppressed (Chabot and Dutil, 1999). This highlights the importance of maintaining dissolved oxygen levels close to air saturation in mulloway culture, as although mild hypoxia will not be acutely lethal, reductions in production performance may be apparent.

3.6 Acknowledgements

This work received funds from PIRSA Aquaculture and the Fisheries R&D Corporation. Authors would like to thank W. Hutchinson for donation of experimental animals and J. Carragher for reviewing this document.

3.6 References

Battaglene, S. C. & Talbot, R. B. (1994). Hormone induction and larval rearing of mulloway, *Argyrosomus hololepidotus* (Pisces: Sciaenidae). *Aquaculture* **126,** 73-81.

Brett, J. R. (1964). The respiratory metabolism and swimming performance of young sockeye salmon. *Journal of Fisheries Research Board of Canada* **21,** 1184-1226.

Brett, J. R. (1965). The relation of size to rate of oxygen consumption and sustained swimming speed of sockeye salmon (*Oncorhynchus nerka*). *Journal of Fisheries Research Board of Canada* **22,** 1491-1501.

Brett, J. R. & Glass, N. R. (1973). Metabolic rates and critical swimming speeds of sockeye salmon (*Oncorhynchus nerka*) in relation to size and temperature. *Journal of Fisheries Research Board of Canada* **30,** 379-387.

Brill, R. W. (1979). The effect of body size on the standard metabolic rate of skipjack tuna, *Katsuwonus pelamis*. *Fishery Bulletin* **77,** 494-498.

Brill, R. W. (1987). On the standard metabolic rates of tropical tunas, including the effect of body size and acute temperature change. *Fishery Bulletin* **85,** 25-35.

Brill, R. W. & Bushnell, P. G. (1991). Metabolic and cardiac scope of high energy demand teleost, the tunas. *Canadian Journal of Zoology* **69,** 2002-2009.

Bushnell, P. G., Steffensen, J. F. & Johansen, K. (1984). Oxygen consumption and swimming performance in hypoxia-acclimated rainbow trout *Salmo gairdneri*. *Journal of Experimental Biology* **113,** 225-235.

Bushnell, P. G. & Jones, D. R. (1994). Cardiovascular and respiratory physiology of tuna: adaptations for support of exceptionally high metabolic rates. *Environmental Biology of Fishes* **40,** 303-318.

Chabot, D. & Dutil, J.-D. (1999). Reduced growth of Atlantic cod in non-lethal hypoxic conditions. *Journal of Fish Biology* **55,** 472-491.

Claireaux, G. & Lagardere, J. P. (1999). Influence of temperature, oxygen and salinity on the metabolism of the European sea bass. *Journal of Sea Research* **42,** 157-168.

Claireaux, G., Webber, D. M., Lagardere, J. P. & Kerr, S. R. (2000). Influence of water temperature and oxygenation on the aerobic metabolic scope of Atlantic cod (*Gadus morhua*). *Journal of Sea Research* **44,** 257-265.

Clark, T. D., Ryan, T., Ingram, B. A., Woakes, A. J., Butler, P. J. & Frappell, P. B. (2005). Factorial aerobic scope is independent of temperature and primarily modulated by heart rate in exercising Murray cod (*Maccullochella peelii peelii*). *Physiological and Biochemical Zoology* **78,** 347-355.

Dewar, H. & Graham, J. B. (1994). Studies of tropical tuna swimming performance in a large water tunnel I. Energetics. *Journal of Experimental Biology* **192,** 13-31.

Fielder, D. S. & Bardsley, W. (1999). A preliminary study on the effects of salinity on growth and survival of mulloway *Argyrosomus japonicus* larvae and juveniles. *Journal of the World Aquaculture Society* **30,** 380-387.

Fry, F. E. J. (1971). The effect of environmental factors on the physiology of fish. In *Fish Physiology* (Hoar, W. S. & Randall, D. J., eds), pp. 1-99: Academic Press

Gray, C. A. & McDonal, V. C. (1993). Distribution and growth of juvenile mulloway, *Argyosomus hololepidotus* (Pisces : Sciaenidae), in the Hawkesbury River, south-eastern Australia. *Australian Journal of Marine and Freahwater Research* **44,** 401-409.

Griffiths, M. H. & Heemstra, P. C. (1995). A contribution to the taxonomy of the marine fish Genus *Argyrosomus* (Perciformes: Sciaenidae), with descriptions of two new species from southern Africa. *Ichthyological Bulletin* **65,** 1-34.

Griffiths, M. H. (1997a). Influence of prey availability on the distribution of dusky knob *Argyrosomus japonicus* (Sciaenidea) in the great river estuary, with note on the diet of early juveniles from three other estuarine systems. *South African Journal of Marine Science* **18,** 137-145.

Griffiths, M. H. (1997b). Feeding ecology of South African *Argyrosomus japonicus* (Pisces: Sciaenidae), with emphasis on the eastern cape surf zone. *South African Journal of Marine Science* **18,** 249-264.

Hecht, T. & Mperdempes, A. (2001). Screening of *Argyrosomus japonicus* (Sciaenidea) and *Pomadasys commersonnii* (Haemulidea) as candidates for aquaculture in South Africa. In *Aquaculture 2001: Book of Abstracts* eds), pp. 286: World Aquaculture Society

Hong, W. & Zhang, Q. (2003). Review of captive bred species and fry production of marine fish in China. *Aquaculture* **227,** 305-318.

Hughes, G. M. (1973). Respiratory responses to hypoxia in fish. *American Zoologist* **13,** 475-489.

Korsmeyer, K. E. & Dewar, H. (2001). Tuna metabolism and energetics. In *Fish Physiology: Tuna Physiology, Ecology, and Evolution* (Block, B. A. & Stevens, E. D., eds), pp. 35-78: Academic Press

Lefrancois, C. & Claireaux, G. (2003). Influence of ambient oxygenation and temperature on metabolic scope and scope for heart rate in the common sole *Solea solea*. *Marine Ecology Progress Series* **259,** 273-284.

Mallekh, R. & Lagardere, J. P. (2002). Effect of temperature and dissolved oxygen concentration on the metabolic rate of the turbot and the relationship between metabolic scope and feeding demand. *Journal of Fish Biology* **60,** 1105-1115.

Neill, W. H. & Bryan, J. D. (1991). Responses of fish to temperature and oxygen, and response integration through metabolic scope. In *Aquaculture and Water Quality* (Brune, d. E. & Tomasso, J. R., eds), pp. 30-57: The World Aquaculture Society

Neill, W. H., Miller, J. M., Van Der Veer, H. W. & Winemiller, K. O. (1994). Ecophysiology of marine fish recruitment: a conceptual framework for understanding interannual variability. *Netherlands Journal of Sea Research* **32,** 135-152.

Ott, M. E., Heisler, N. & Ultsch, G. R. (1980). A re-evaluation of the relationship between temperature and the critical oxygen tension in freshwater fishes. *Comparative Biochemistry and Physiology* **67A,** 337-340.

Pichavant, K., Person-Le-Ruyet, J., Le Bayon, N., Severe, A., Le Roux, A. & Boeuf, G. (2001). Comparative effects of long-term hypoxia on growth, feeding and oxygen consumption in juvenile turbot and European sea bass. *Journal of Fish Biology* **59,** 875-883.

Randall, D. J. (1982). The control of respiration and circulation in fish during exercise and hypoxia. *Journal of Experimental Biology* **100,** 275-288.

Schurmann, H. & Steffensen, J. F. (1997). Effects of temperature, hypoxia and activity on the metabolism of juvenile Atlantic cod. *Journal of Fish Biology* **50,** 1166-1180.

Sepulveda, C. & Dickson, K. A. (2000). Maximum sustainable speeds and cost of swimming in juvenile kawakawa tuna (*Euthynnus affinis*) and chub mackerel (*Scomber japonicus*). *Journal of Experimental Biology* **203,** 3089-3101.

Thetmeyer, H., Waller, U., Black, K. D., Inselmann, S. & Rosenthal, H. (1999). Growth of European sea bass (*Dicentrarchus labrax* L.) under hypoxic and oscillating oxygen conditions. *Aquaculture* **174,** 355-367.

Thomas, P., Arnold, C. & Holt, J. (1996). Aquaculture of red drum (*Sciaenops ocellatus*) and other sciaenids. *Biotecnologia Aplicada* **13,** 285-286.

Webb, P. W. (1998). Swimming. In *The Physiology of Fishes* (Evans, D. H., eds), pp. CRC Press

White, C. R., Phillips, N. F. & Seymour, R. S. (2006). The scaling and temperature dependence of vertebrate metabolism. *Biology Letters* **2,** 125-127.

Chapter 4: Modelling of nitrogen and phosphorus loads from yellowtail kingfish (*Seriola lalandi*) aquaculture

Milena Fernandes* and Jason Tanner
SARDI Aquatic Sciences, PO Box 120, Henley Beach SA 5022, Australia

*corresponding author, Phone: +61 (8) 8207 5306, Fax +61 (8) 8207 5481,
E-mail: fernandes.milena@saugov.sa.gov.au

4.1 Abstract

Farming of yellowtail kingfish (*Seriola lalandi*) in coastal waters of South Australia is a relatively new aquaculture industry and little is known about the magnitude of nutrient discharges from individual pens. In this work we modelled the flow of nitrogen and phosphorus for each of two commercial pens in Fitzgerald Bay, upper Spencer Gulf, South Australia. The fish were fed commercial pellets with feed conversion ratios (FCR) between 3.0 and 3.2 (dry weight feed/wet weight growth). These high values of FCR were reflected in high nitrogen and phosphorus loads to the environment (179-198 kg N and 44-47 kg P tonne^{-1} growth) and a small retention of both in fish growth (14-15% & 7% of feed inputs respectively). Considering an annual production of 2,000 tonnes, total loads to Fitzgerald Bay can reach 396 tonnes N and 94 tonnes P per year. Eighty-three percent of this N load is expected to be lost to the water column as dissolved wastes, whereas less than 1% of P will be lost in dissolved form. The high nutrient loads and the importance of dissolved wastes compared with other aquaculture species such as salmon and trout, reflect the more active lifestyle of this pelagic predatory species. The nature of the wastes suggests low localized impacts at current stocking densities and holding periods, but regional effects remain unknown.

4.2 Introduction

The mainstay of the marine fish farming industry in Australia has been the cultivation of southern bluefin tuna (*Thunnus maccoyii*) and Atlantic salmon (*Salmo salar*). The lack of suitable coastal sites, declining prices of both species, and limited quota of southern bluefin tuna, have led the industry to seek diversification. As a result, interest has risen in the development of yellowtail kingfish (YTK) (*Seriola lalandi*) farming in the Spencer Gulf of South Australia. YTK is the second most popular sashimi product in Japan

and attracts a high market value in both Asia and Europe (Love & Langenkamp, 2003). The ready availability of fingerlings from two local hatcheries, and its fast growth rate, make this marine species an attractive alternative for the sector (PIRSA, 2002).

YTK are farmed in South Australia off the Eyre Peninsula in Fitzgerald Bay, Cowell and Port Lincoln (PIRSA, 2002). This emerging industry is the second most valuable aquaculture industry in the state, with commercial production in 2004/2005 estimated at more than 2,000 tonnes (Chambers & Ernst, 2005), showing potential to reach 4,000 tonnes over the next few years (Love & Langenkamp, 2003). Five-gram hatchery fingerlings are typically transferred into sea-cages in October to maximize early growth during summer. The maximum allowable stocking density is 10 kg m^{-3} (PIRSA, 2002). These fish are fed on pelleted diets, graded and redistributed twice before harvest at 2 years when whole weights reach 3-3.5 kg.

The development and sustainability of this new industry requires quantification of nutrient discharges to the water column and sediments, and definition of its potential for impact on the surrounding marine ecosystem. Nitrogen, in particular, is usually considered the limiting nutrient for primary productivity in the oligotrophic coastal waters of South Australia, where an increase in concentrations could have a disproportionately large impact on local ecosystems (Russell et al., 2005). Previous modelling exercises that attempted to quantify the impacts of YTK farming on the environment (Oceanique Perspectives, 1998) lacked accurate estimates of nitrogen and phosphorus flows in the footprint of the pens. In this study we address this gap by developing a mass-balance model to predict the release of dissolved and particulate nitrogen and phosphorus from YTK pens. For this purpose, we determined the amount of both elements that is lost directly to the water column as soluble wastes, the rate of accumulation of solid wastes in the sediments, and the regeneration of nutrients at the sediment-water interface. These results were combined with estimates of fish metabolism to define nitrogen and phosphorus pathways, which were ultimately built into models for nitrogen and phosphorus flows from individual pens. The loads calculated here constitute the first quantification of nitrogen and phosphorus losses from YTK farming in South Australia. The amount of nitrogen released per tonne of production is compared to the loads reported for other finfish aquaculture industries and discussed in terms of the magnitude of discharges considering current production levels and other anthropogenic inputs.

4.3 Methods

4.3.1 Characterization of feed, faeces and fish tissues

Feed samples were obtained from commercial operators and stored frozen at -30 °C in zip lock bags. The pellets were manufactured by Skretting (Hobart, Australia) from fish-meal, fish oil and plant protein meal, with added vitamins, minerals and antioxidants. These pellets were approximately 9 mm long and 9 mm in diameter, weighing 0.8 ± 0.05 g (SD, n=15). Ten YTK were caught on lures, brain spiked using a knife and stored on ice. These fish had an average fork length of 59 ± 3 cm and weighed 2.8 ± 0.3 kg. Fish tissues were sampled below the dorsal fin, placed into a pre-combusted glass jar and stored frozen at -30 °C. Faeces were collected by gentle stripping of the distal section of the intestine of the fish to minimize contamination from epithelial cells. Samples showed no visible contamination from blood or mucous and were stored frozen at -30 °C in glass jars.

4.3.2 Nitrogen, phosphorus and water contents

Pellets, fish tissues and faeces (n=10) were freeze-dried and the water content calculated from the difference between wet and freeze-dried weights. Aliquots were homogenised in a ball mill and TN & TP concentrations determined in a LECO TruSpec CNS Elemental Analyser. TN & TP concentrations are reported in mg g^{-1} dry weight (dw).

4.3.3 Leaching simulations

To determine dissolved nutrient release from solid wastes, leaching simulations were conducted in a controlled environment room where temperature was maintained at 19.1 ± 0.3 ^{o}C to approximate conditions typical of YTK farming in South Australia. A data logger recorded air temperatures every 5 min during the experimental period. Seawater was vacuum filtered through an isopore polycarbonate filter (Millipore, 0.4 µm, 47 mm diameter) and kept in the controlled environment room overnight. A WTW 340i conductivity meter measured a salinity reading of 37.2.

Frozen pellets and faeces were thawed at room temperature. Four replicates of approximately 1.5 g of pellets, and four replicates of approximately 500 mg of faeces (all wet weight), were weighed, placed into beakers containing 300 mL of the filtered seawater and stirred with a glass rod. After 2 min a 20 mL aliquot was taken and the beaker stirred again. This procedure was repeated at 5, 30, 60 and 240 min. Experiments were conducted over a period of 4 h to minimize microbiological growth. Each

sampled aliquot was filtered (0.45 µm) and stored frozen (-30 ºC). The syringe, filter and storage bottles used to collect the samples were pre-rinsed with the experimental seawater.

For determination of total nitrogen and phosphorus, filtered samples were digested for 45 min in an autoclave with an alkaline persulphate solution to convert N-containing compounds to nitrates (APHA-AWWA-WPCF, 2001). The digestion process was repeated twice. The persulphate solution was prepared by dissolving 4.5 g of NaOH in 200 mL of MilliQ-water, this solution was cooled to room temperature, 20 g of $K_2S_2O_8$ added and the volume adjusted to 500 mL. Total nitrogen & TP concentrations were corrected for background concentrations in the seawater, collected from each beaker at the start of the experiment and measured in the same way as the samples.

4.3.4 Settling rates

Settling rates of both pellets and faeces were determined using a clear acrylic tube (diameter: 20 cm, length: 183 cm) fitted into an aquaculture fish tank (diameter: 455 cm, depth: 202 cm) filled with seawater. The acrylic tube was open at the top and bottom, and the bottom fitted with an exchangeable plastic collector. The water depth in the tube was 140 cm. All experiments were run at an ambient water temperature of 21 ^{o}C and salinity of 37.2.

Samples were defrosted and pre-weighed. One feed pellet at a time was gently placed on the water at the top of the acrylic tube and allowed to sink. A diver visually established the time necessary for the pellet to reach the end of the acrylic tube. This procedure was repeated 15 times and the settling rate of pellets is reported as the average value.

Faeces aliquots were gently poured at the water surface. The settling rates of average and slow sinking material were recorded in two different runs. In the first run a diver visually established the time necessary for the majority of the sample to reach the bottom. This was considered as the average sinking time and the material reaching the collector kept for gravimetric analyses. The slow settling material was measured by recovering the material reaching the collector in 180 s. Each run was repeated twice.

Faeces samples reaching the collector were filtered onto pre-weighed glass fibre filters (MFS GF-75, 0.7 µm, 47 mm diameter) under vacuum. Filters were placed in separate glass petri dishes, covered with a glass lid and oven dried at 50ºC. Before gravimetric analysis, the petri dishes containing the dried filters were placed in an oven at 50 ^{o}C for at least 3 h and placed in a desiccator with silica gel for 1 h to cool. The filters were weighed using

an electrobalance to five decimal places. Results were corrected for salt that impregnates the filters.

4.3.5 Study area

Fitzgerald Bay is a microtidal (3 m) marine system (salinity 40-45) located in upper Spencer Gulf, South Australia (PIRSA Aquaculture, 2004). Study sites included two commercial pens located in two of the five 20 ha finfish leases in the area. The pens were 25.5 m in diameter with a net wall depth of 6 m, moored in water depths between 17 and 20 m. Feed input, growth and feed conversion performance of YTK in these pens are summarized in Table 4.1. Pen P1 in southern Fitzgerald Bay was stocked with 13,066 fish in September 2004. The grow-out period between stocking and harvest of this pen lasted for 288 days with feeding rates averaging 283 kg d^{-1}. Pen P2 in northern Fitzgerald Bay was stocked with 11,493 fish in July 2004. These fish were fed an average of 187 kg d^{-1} for 324 days. The estimated initial weight of fish in both pens was 1.3 kg, determined from a sample of 50-70 fish. Fish were harvested from both pens in June 2005 with an average whole weight of 3.3 kg (P1) and 2.9 kg (P2).

Table 4.1. Feed input, growth and feed conversion performance of YTK in commercial pens P1 and P2 (raw data obtained from SA Aquaculture Management).

	P1	P2
Mean initial weight (kg)	1.3	1.3
Mean final weight (kg)	3.3	2.9
Number of fish stocked	13,066	11,493
Number of mortalities	332	358
Stocking (days)	288	324
Feeding (days)	169	108
Mean feed input (kg d^{-1})	283	187
SGR (%)[1]	0.32	0.25
FCR[2] (wet weight)	3.1	3.4
FCR[3] (dry weight)	3.0	3.2

[1]Specific growth rate, or weight gain per day.
[2]Feed conversion rate (wet weight feed/wet weight gain).
[3]Feed conversion rate (dry weight feed/wet weight gain).

4.3.6. Sampling

Environmental samples were collected in May 2005 at the edge of the commercial pens and at two control sites located at least 1 km from any aquaculture lease. Sediments were collected by divers using 67 mm (i.d.) PVC tubes capped with rubber bungs. Upon retrieval, the overlying water in the tube was carefully discarded to minimise surface disturbance and the

sediment extruded onto a clean stainless steel table. Four cores were collected for the analysis of total nitrogen and total phosphorus (TN & TP). The top layer (0-1 cm) of each core was sliced, transferred into a pre-combusted glass jar and stored frozen (-30 ^{o}C). Two cores were collected for the determination of wet density. The top layer (0-2 cm) of each core was sliced, transferred into a pre-weighed centrifuge tube of known volume and stored refrigerated (4 ^{o}C) for up to 3 h before transfer to the laboratory.

For determination of nutrient fluxes at the sediment-water interface and sediment water content, we collected sediments in 105 mm (i.d.) opaque PVC tubes impervious to light (Lauer, 2005). The cores used for determination of nutrient fluxes were fitted with a bottom seal with double O-rings and a top seal with a single O-ring. Six replicates were transferred into an incubation system for determination of nutrient fluxes. These cores had a visibly undisturbed sediment surface, a minimum of 800 mL of clear overlying *in situ* bottom seawater and at least 10 cm depth of sediment. Two additional cores used for the determination of water content were sealed with rubber bungs and refrigerated onboard (4 °C) for up to 3 h before transfer to the laboratory.

Sediment traps were placed 1 m above the seafloor. Each trap consisted of two PVC tubes with a height to width ratio of 4.7 (height 400 mm, diameter 85 mm), lead weighted on the bottom (40 g) to ensure correct vertical orientation. Three pairs of sediment traps separated by 30 m were deployed at each site. This design gave us sedimentation rates at 0, 30 and 60 m from the edge of the pens with two replicates per distance. Sediment traps were moored for at least 47 h but no more than 53 h. Upon retrieval, traps were spiked with $HgCl_2$ to a final concentration of 10 mg L^{-1} to prevent microbial degradation.

4.3.7 Analytical procedures

4.3.7.1 Sediments

Sediment samples were freeze-dried, sieved to 500 μm to remove large shell fragments, and homogenized with a mortar and pestle. Aliquots were weighed into foil capsules and analysed for TN & TP by Continuous-Flow stable Isotope Ratio Mass Spectrometry (CF IRMS) using a Europa Scientific ANCA-SL elemental analyser coupled to a Geo 20-20 Mass Spectrometer. TN & TP concentrations are reported as a percentage of total dry sediment. The samples collected for determination of wet density were weighed and results are reported as g (wet weight) cm^{-3}. The samples collected for determination of water content were extruded onto aluminium foil, the top 0-1 cm sectioned, homogenised and any visible macroinfauna removed. 30 g of each homogenised section was transferred to an aluminium tray and oven-dried at 60 ^{o}C until constant weight. Results are expressed as the percentage of water in the wet sediment.

4.3.7.2 Sedimentation fluxes

The contents of sediment traps were sieved (1 mm mesh size) to remove material not part of the passive flux (e.g. mobile organisms such as zooplankton). Sieved samples were vacuum filtered through pre-combusted (450 ºC overnight) and pre-weighed glass-fibre filters (MFS GF-75, 0.7 µm, 47 mm diameter). Filters were placed in separate pre-combusted glass petri dishes, covered with a glass lid and oven dried at 50 ºC. Before gravimetric analyses, the petri dishes containing the dried filters were placed in an oven at 50 ^{o}C for at least 3 h and placed in a desiccator with silica gel for 1 h to cool. The filters were then weighed using an electrobalance to five decimal places. Results were corrected for salt that impregnates the filters and sedimentation rates expressed in units of g (dw) m^{-2} d^{-1}. The material collected in the traps deployed at the edge of the pens was gently scraped off the filters with a spatula, homogenized in a mortar and pestle, and analysed for TN & TP according to the method described above for sediment samples. Nitrogen and phosphorus sedimentation rates were calculated using sedimentation rates and nitrogen and phosphorus contents for each site and sampling time, and are expressed in units of mg N/P m^{-2} d^{-1}.

4.3.7.3 Benthic fluxes

Nutrient fluxes were measured with a manually operated incubation system immediately after sampling (Lauer, 2005). Incubations were designed to last for 2 to 4 hours to limit the likelihood of non-linear nutrient changes. The incubation system consisted of two temperature sensors connected to a data logger (DT 50, Datataker), six seawater stirrers to prevent stratification (single blade, 7 mm wide, 4 mm long) and a temperature-controlled water bath, thus allowing six sediment cores to be incubated at once. The magnetic stirrers were fitted with an O-ring and penetrated through the top seal of the cores. The water bath consisted of a 200 L PVC outer container filled with ice and a 60 L polystyrene inner container filled with freshwater. The PVC barrels sealed at both ends were placed in the inner container, which had a pump to circulate the water and an aquarium heater to maintain water temperature. The temperature was set at ambient bottom seawater temperature measured at the time of collection. The system maintained temperatures to ± 0.8 ºC of the set value. Samples of the overlying seawater were taken in duplicate from each core at the start and end of the incubation, filtered (0.45 µm) and stored frozen (-30 ºC). Nutrient fluxes were determined from the change between initial and final concentrations in the overlying seawater. Nitrates/nitrites (NO_x) and total phosphorus were determined spectrophotometrically at 520 nm by flow injection analysis with a QuickChem 8000 Automated Ion Analyser (APHA-AWWA-WPCF, 1998a). Ammonium was also determined spectrophotometrically by flow injection

analysis using the automated phenate method with detection at 630 nm (APHA-AWWA-WPCF, 1998b). The duplicate samples were averaged and the change in nutrient concentration was then adjusted to account for the sediment surface area, the duration of incubation, and the volume of overlying seawater to determine the rate of nutrient release or uptake. The resultant rate of change was expressed in units of mg N/P m^{-2} d^{-1}.

4.4 Model development

4.4.1 Feed input

Total and daily feed inputs were calculated using the amount of pellets fed to each pen per day (data supplied by farmers) and their average water and nitrogen contents. Fish were fed 1 to 7 times a week, with highest frequencies in the warmer months between November and February. Feeding rates varied between 0.02 and 5.6 % of body weight, with a mean value for both pens of 0.8 %. The TN content of pellets was 71 ± 2 mg N g^{-1} dw, and the TP content 14.8 ± 0.5 mg P g^{-1} dw, whereas the water content was 5.8 ± 1.1 %. The average nitrogen input from fish feed varied between 13 and 19 kg N d^{-1}, the cumulative value over the grow-out period reaching 4.1-5.4 tonnes N. For phosphorus, these values are 2.6-3.9 kg P d^{-1} and 0.84-1.13 tonnes P respectively. These modelled ranges of nitrogen feed input as well as YTK retention, excretion and environmental flows are depicted in Figure 4.1 as the minimum and maximum values observed for both pens. Similar values for phosphorus are in Figure 4.2.

Although the fraction of uneaten feed is unknown, video footage under the pens suggested low values (Fernandes and Tanner, unpublished results). We used an estimate of 3 % of the total feed input for this component of the model, a value in the range reported for other marine fish fed manufactured diets (Gillibrand et al., 2002; Davies & Slaski, 2003; Doglioli et al., 2004). This corresponds to an environmental loss of 0.4-0.6 kg N d^{-1}, or 0.1-0.2 tonnes N over the grow-out period. For phosphorus, these values are 0.08-0.12 kg and 25.3-33.0 kg respectively

4.4.2 Fish retention and excretion

In order to calculate YTK daily retention of nitrogen and phosphorus, we estimated the amount of each in fish biomass for each day of the grow-out period based on fish weights, water, TN and TP contents. Monthly estimates of fish weights were based on industry measurements of 50-70 YTK. The specific growth rate (SGR) for each month was then calculated from mean initial (W_i) and final weights (W_f):

$$SGR = \frac{\ln W_f - \ln W_i}{t} \quad (4.1)$$

where *t* corresponds to time in days. Fish weights for each day were estimated based on W_i and W_f and SGR for each period. The latter attained maximum values between 0.73 and 0.85 % weight gain per day, while values for the whole grow-out period were lower, between 0.25 and 0.32 % (Table 4.1). We assumed that the water, TN and TP contents of YTK remained constant, with mean TN content in muscle tissues of 112 ± 8 mg N g^{-1} dw, TP content 11 ± 1.2 mg P g^{-1} dw and water content 72 ± 2 %. Nitrogen retained daily for growth was calculated as the change in the total amount of nitrogen in each pen for any specific day in comparison to the previous day. Retained nitrogen averaged 2-3 kg N d^{-1}. The cumulative value was estimated as the difference between the nitrogen recovered at harvest and with recorded mortalities, and the nitrogen in the initial stock. The cumulative value retained for growth over the period accounted for 0.6-0.8 tonnes N. The values for phosphorus are 0.17-0.28 kg and 56.6-80.5 kg respectively.

To calculate faecal nitrogen excretion, we used protein digestibility values. Although no estimates are available for yellowtail kingfish, apparent protein digestibility of pelleted diets has been reported for related species such as yellowtail (*Seriola quinqueradiata*) and Mediterranean yellowtail (*Seriola dumerili*) (Masumoto et al., 1996; Kofuji et al., 2005; Tomás et al., 2005; Kofuji et al., 2006). These can vary between 60 and 95 % depending on pellet composition and method of faeces collection. Based on values from these studies, we estimated a mean protein digestibility of 76 % for yellowtail kingfish. Therefore, nitrogen released with faeces was calculated as 24 % of nitrogen in ingested feed, with an average of 3-4 kg N d^{-1} leading to a total of 0.9-1.3 tonnes of faecal nitrogen over the grow-out period. We assumed that the amount of ingested nitrogen that is not retained for growth, or excreted with faeces, was metabolised and excreted as soluble excretion products. This corresponded to 7-11 kg N d^{-1}, with a cumulative total of 2-3 tonnes N. For phosphorus, it was assumed that 3.5% of feed inputs were excreted to the environment (from Datoh et al., 2004), which is equivalent to 0.088-0.133 kg P d^{-1}, or 28.6-38.4 kg over the growout period. It was further assumed that the difference between feed inputs on the one hand, and fish gain and excretion on the other, was lost in faeces. This results in values of 2.26-3.40 kg d^{-1} being lost as faeces.

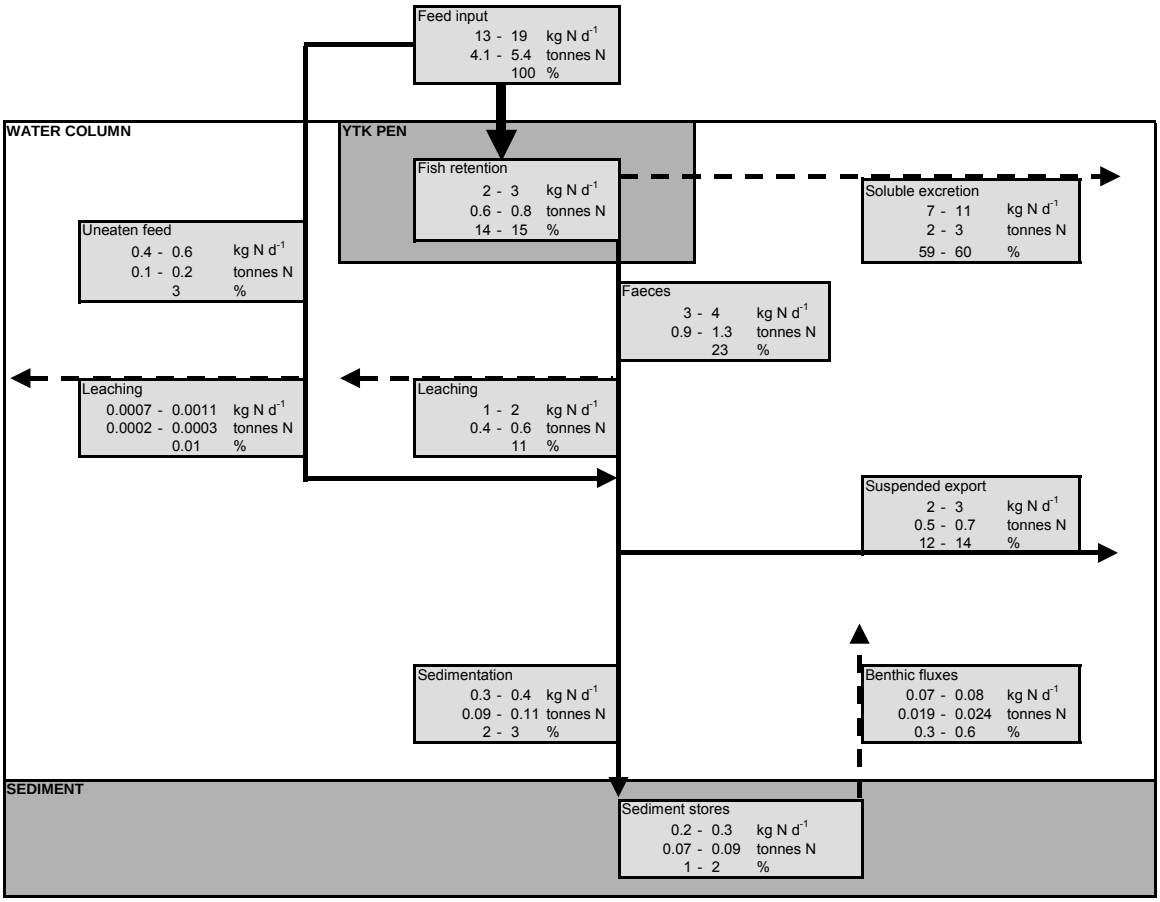

Figure 4.1. Model of environmental flows for nitrogen supplied with feed to farmed YTK in coastal waters off Fitzgerald Bay, South Australia. Values correspond to the range calculated for two commercial pens and are reported as daily (kg N d^{-1}) and cumulative totals (tonnes N over the stocking period), as well as a fraction of total feed inputs (%). Particulate flows are depicted as solid arrows and dissolved flows as dashed arrows.

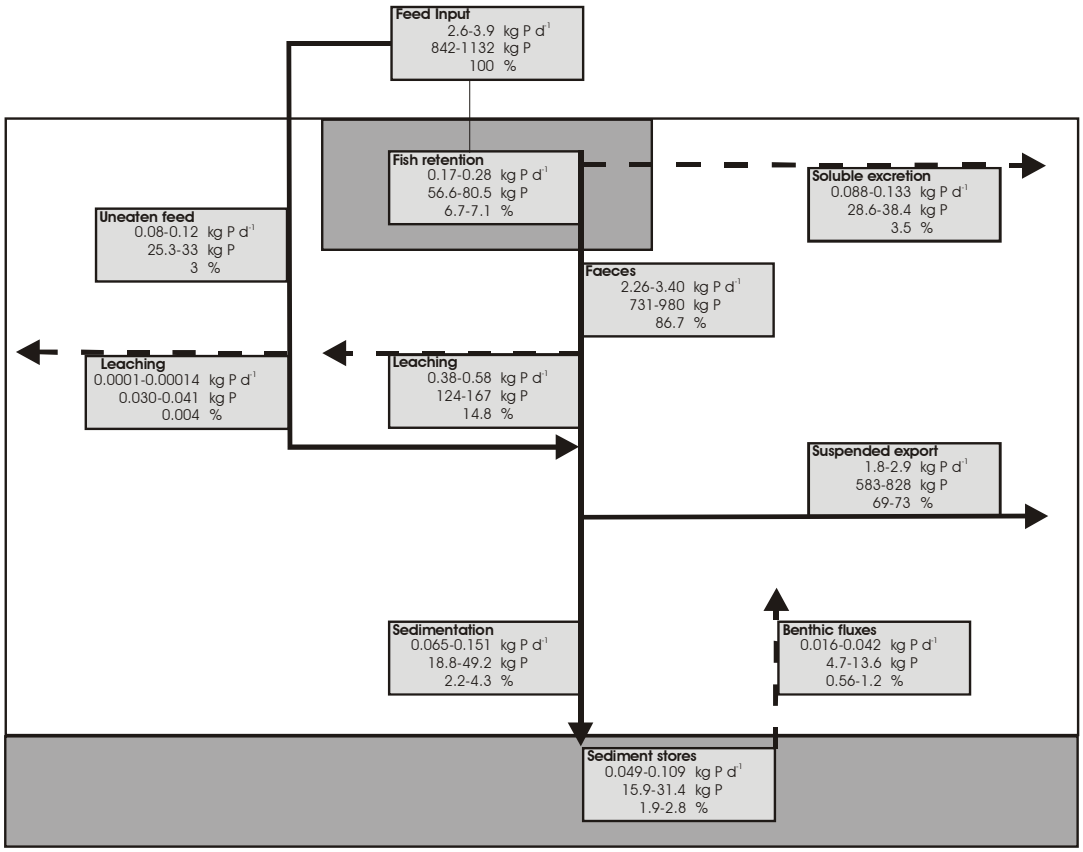

Figure 4.2. Model of environmental flows for phosphorus supplied with feed to farmed YTK in coastal waters off Fitzgerald Bay, South Australia. Values correspond to the range calculated for two commercial pens and are reported as daily (kg P d^{-1}) and cumulative totals (kg P over the stocking period), as well as a fraction of total feed inputs (%). Particulate flows are depicted as solid arrows and dissolved flows as dashed arrows.

4.4.3 Leaching, dispersion and settling of wastes in the water column

Approximately 4 % of the nitrogen in pellets and 47 % in faeces was soluble and available to leach into seawater after an immersion time of 4 hours (Table 4.2), with the values for phosphorus being 2.7 and 54% respectively. With an average settling rate of 12 ± 1 cm s^{-1}, it would take close to 3 min for uneaten pellets to reach the seafloor in a 20 m water column typical of YTK farms. In this timeframe, approximately 0.2 % of the nitrogen and 0.05% of phosphorus in uneaten pellets would leach into the water column (Table 4.2). Settling rates of faeces were much lower. It took approximately 90 s for 14 % of faecal matter to sink through a water depth of 140 cm, implying maximum sinking rates of or above 1.6 cm s^{-1}. The percentage recovered after 180 s was marginally higher, at 16 %. Therefore, faeces would reach the seafloor after at least 20 min in the water column, when all of the soluble nitrogen would have leached into seawater, but only about

17% of soluble phosphorus would have leached (Table 4.2, note that the ~50% of each that did not leach out in the 240 min trial is regarded as non-soluble). We used these values to estimate the amount of nitrogen and phosphorus that would leach from solid wastes into the water column before deposition. The combined daily average for leaching from both uneaten feed and faeces was 1-2 kg N d^{-1} and the cumulative total 0.4-0.6 tonnes N. The values for phosphorus were 0.38-0.58 kg and 124-167 kg respectively.

The first step in determining the flux of nutrients settling through the water column and reaching the sediments is to estimate the area of impact of sedimentation fluxes from the pens. Gowen & Bradbury (1987) suggested that the radius of impact around fish pens (*D*) can be determined from the following equation:

$$D = \frac{d \times V}{v} \qquad (4.2)$$

where *d* is water depth, *V* is current speed and *v* is settling velocity of the waste. The average water column depth of YTK sites is 20 m and the maximum faecal settling velocity was estimated at 1.6 cm s^{-1}. The settling velocity of faeces was used as a proxy for the settling velocity of wastes because it is much lower than the settling velocity of pellets and therefore will give the maximum area of impact. Although no detailed information is available for currents in the area, values of 1 cm s^{-1} were reported close to shore in Fitzgerald Bay (Hone et al., 1996; PIRSA Aquaculture, 2004). These values were used in equation 4.2 to give a radius of impact of 13 m. Indeed, sedimentation rates at the edge of the pens (79-83 g m^{-2} d^{-1}) were significantly higher than at 30 or 60 m (63-69 g m^{-2} d^{-1}) (Figure 4.2). The latter are in the same range as long-term background sedimentation rates of 65 ± 9 g m^{-2} d^{-1} measured in Fitzgerald Bay between December and May by Hone et al. (1996). For modelling purposes, we thus considered the area affected by sedimentation of farm wastes extending up to 13 m from the edge of the pens. We then calculated the average daily input of nitrogen and phosphorus with feed from the day prior to deployment until the day of retrieval of sediment traps using daily values of feed input. This average was used to estimate the fraction of the total input accounted for by sedimentation fluxes in the area of impact. Average sedimentation rates varied from 170 to 260 mg N m^{-2} d^{-1} and 36-55 mg P m^{-2} d^{-1} in the footprint of stocked pens (Table 4.3). Considering the radius of impact up to 13 m from the pens, these sedimentation rates accounted for a maximum of 2 to 3 % of feed inputs, delivering 0.3-0.4 kg N d^{-1} and 0.065-0.151 kg P d^{-1} to the sediments up to 13 m from the pens, or 0.09-0.11 tonnes N and 0.0188-0.0492 tonnes P over the grow-out period.

To calculate the amount of sinking matter dispersed away from the area of impact by currents or scavenger consumption, we assumed that the

difference between the total input of faeces and uneaten feed and the amount leached into the water column, and settling to the seafloor, was exported out of the system as fine suspended matter or consumed feed. Exports out of the system varied between 2 and 3 kg N d^{-1} and 1.8-2.9 kg P d^{-1}, with the total reaching a maximum value of 0.5-0.7 tonnes N and 0.58-0.83 tonnes P.

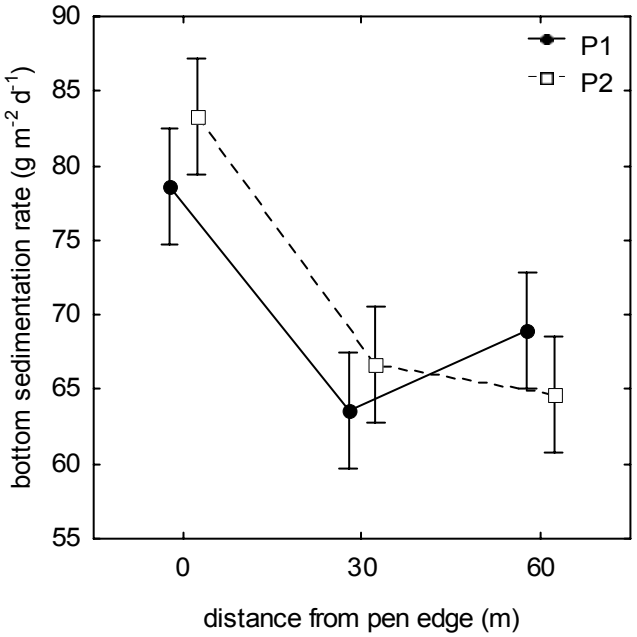

Figure 4.2. Dry matter sedimentation rates as a function of distance from the edge of pens P1 and P2. Values are reported as the mean, vertical bars denote 95 % confidence intervals.

Table 4.2. Percentage of total nitrogen in YTK faeces and pellets that leached into seawater as a function of immersion time. Values are reported as the mean (SD).

Time (min)	Soluble N (% of total)		Soluble P (% of total)	
	Faeces	Pellets	Faeces	Pellets
2	47 (4)	0.1 (0.0)	7.4 (2.3)	0.02 (0.005)
5	45 (6)	0.3 (0.0)	11.5 (3.6)	0.13 (0.03)
30	46 (5)	0.9 (0.4)	16.7 (7.4)	0.51 (0.22)
60	50 (4)	1.4 (0.2)	34.3 (7.6)	0.83 (0.18)
240	48 (1)	3.7 (0.5)	53.9 (6.6)	2.68 (0.27)

4.4.4 Remineralization and accumulation of wastes in the sediments

The sum of ammonia and NO_x benthic fluxes was used to estimate total inorganic nutrient fluxes from the sediments, which varied from 32 to 74 mg N m^{-2} d^{-1} and 8.0-20.5 mg P m^{-2} d^{-1} in the footprint of stocked pens (Table 4.3). With the lack of additional data points, we assumed for modelling purposes that these rates remained constant up to 13 m from the edge of the pens throughout the stocking period. Based on these assumptions, the daily amount of nitrogen remineralised in the sediments and released with benthic fluxes averaged 0.07-0.08 kg N d^{-1} and 0.0163-0.042 kg P d^{-1} over the grow-out period, with a cumulative total of 0.02 tonnes N and 0.0047-0.0136 kg P. The amount of nitrogen and phosphorus that actually accumulated in the sediments at the end of the grow-out period was then estimated from the difference between the total reaching the seafloor with sedimentation fluxes and the amount released from the sediments with benthic fluxes. Using this approach, < 0.1 tonnes N and 35 kg P accumulated in sediments up to 13 m from the pens during the grow-out period, with a daily average of less than 0.3 kg N d^{-1}, and 0.049-0.109 kg P d^{-1}.

Table 4.3. Mean sedimentation and benthic fluxes (± SD) measured at pens P1 and P2.

	Sedimentation fluxes (mg N m^{-2} d^{-1})	**Benthic fluxes (mg N m^{-2} d^{-1})**	**Sedimentation fluxes (mg P m^{-2} d^{-1})**	**Benthic fluxes (mg P m^{-2} d^{-1})**
P1	170 (1)	32 (10)	36 (0.2)	8.0 (4.2)
P2	260 (15)	74 (21)	55 (3)	20.5 (6.4)

4.5 Discussion

The standard metabolic rates of predatory pelagic fish need to be high to support the physiological systems underlying a high aerobic capacity. This elevated aerobic scope is necessary to maximize the potential for high energy returns in prey capture (Korsmeyer & Dewar, 2001). However, the maintenance of high metabolic rates requires large amounts of energy, derived primarily from proteins. For the genus *Seriola*, and YTK in particular, standard metabolic rates are close to those reported for tuna and at least double values for other non-tuna species considered to be of high performance (Korsmeyer & Dewar, 2001; Clark, 2006). These high rates explain the small fraction of nitrogen retained for growth in YTK (14-15 % of feed inputs) compared to other well-studied aquaculture species (e.g. 20-40 % for salmonids) (Table 4.4).

The high protein turnover associated with high standard metabolic rates also explains why soluble excretion products accounted for the largest environmental loss, releasing 59-60 % of nitrogeneous feed inputs directly into the water (Figure 4.1). Similar values have been reported for other active carnivorous fish, such as areolated grouper (*Epinephelus areolatus*) (46-64 %) (Leung et al., 1999) and southern bluefin tuna (*Thunnus maccoyii*) (59-64%) (Fernandes et al., 2006a). Losses from leaching of solid wastes and remineralization at the sediment-water interface delivered comparatively smaller amounts of nitrogen to the water column. Although smaller, losses from leaching of faeces during settling to the seafloor corresponded to the second most important source of dissolved nutrients, releasing 11 % of feed inputs to the water column. When combined with branchial and urinary excretion losses, these dissolved flows indicate that most (70-72 %) of the nitrogen in feed inputs is released directly into the water column in dissolved form (Table 4.4).

Particulate wastes accounted for a comparatively smaller fraction of losses to the environment, or approximately 15 % (Table 4.4). These losses were associated with sediment accumulation and, more importantly, exports out of the system (Figure 4.1). Despite significant leaching, faecal matter comprised 80 % of nitrogeneous particulate wastes. Given its low settling rate, faecal matter is likely to make up the majority of nitrogen exports out of the system with currents. In contrast, uneaten feed is expected to accumulate locally, up to 2 m from the edge of the pens according to equation 4.2.

Between 89 and 94 % of nitrogeneous particulate wastes did not reach the seafloor, leading to sediment accumulation rates of less than 0.1 tonnes N. These values suggest low localized impacts, confirmed by video footage of the seafloor (Fernandes and Tanner, unpublished results). Although small, modelled sediment accumulation rates were higher than calculated from *in situ* values. Using TN concentrations, water content and wet density of sediments (Table 4.5), we calculated the amount of nitrogen in sediments of the impacted area assuming that the depth of impact is restricted to the first cm of the sediment profile. Subtracting from this value the average amount of nitrogen in sediments of controls located in the same area, we found that the total accumulation of TN was negligible, between 0.001 and 0.005 tonnes N. If we increase the depth of impact to 5 cm, maximum values were still below 0.024 tonnes N. The difference between maximum accumulation calculated from the model and from *in situ* values may be related to resuspension and/or consumption by scavengers. If resuspension was the only factor accounting for differences, it would affect more than 50 % of nitrogeneous wastes reaching the seafloor. However, scavenger activity is considered high in Spencer Gulf (Ib Svane, personal communication). If the accumulation of uneaten feed was restricted to the immediate vicinity of the pens and all of it was consumed by benthic scavengers, virtually no nitrogen

would accumulate in the sediments, potentially explaining the discrepancy between calculated and modelled values.

According to the flows modelled above, more than 85 % of nitrogen in pellets fed to YTK is expected to be lost to the environment, leading to environmental loads between 179 and 198 kg N tonne^{-1} growth (Table 4.4). Similarly high loads, generally above 170 kg N tonne^{-1} growth, have been reported for other active predatory fish, a reflection of their high standard metabolic rates and associated FCRs, particularly when fed on baitfish (Table 4.4). In comparison, the loads for less active species with lower FCR generally fall below 100 kg N tonne^{-1} growth (Table 4.4).

Considering a production of 2,000 tonnes, the total release of nitrogen from aquaculture of YTK in Fitzgerald Bay would vary between 358 and 396 tonnes N for values of FCR between 3.0 and 3.2. This discharge is significantly lower than the 1,137 tonnes N estimated to be released from southern bluefin tuna farms in lower Spencer Gulf (Fernandes et al., 2006b). However, if we take into account the area leased for farming, loads are 2.7-3.0 tonnes N per leased ha for YTK, but less than 1.2 tonnes N per leased ha for southern bluefin tuna (Fernandes et al., 2006b). Similar discharges of 1.2 tonnes N per leased ha are associated with salmon farms in the Bay of Fundy, Canada (Department of Agriculture Fisheries and Aquaculture, 2002; Strain & Hargrave, 2005). The consequences of these loads are site specific and need to be considered in terms of flushing regimes and local carrying capacity for effective comparisons to be made.

Eighty three percent of nitrogen loads from aquaculture into Fitzgerald Bay would be delivered in dissolved form, or a minimum of 295 tonnes of dissolved N and 62 tonnes of particulate N. To put these data in perspective, the nitrogen standing stock in the water column of the Western Fitzgerald Bay aquaculture management zone is only 41 tonnes N taking into account an area of 17.04 km^2 (PIRSA Aquaculture, 2004), an average water depth of 20 m and background total nitrogen concentrations of 0.12 mg L^{-1} (Fernandes and Tanner, unpublished results). In terms of other anthropogenic inputs to the region, the local Whyalla wastewater treatment plant, which serves a population of 27,000, discharges 48 tonnes N per year into the marine environment (SA Water, 2003), while discharges from the Whyalla steelworks are 210 tonnes N per year (DEH, 2003). Although the nitrogen loads from aquaculture are apparently high, the impacts in a regional context are difficult to ascertain given the little information available on the magnitude of flux rates between natural nitrogen pools in the system.

Table 4.4. Partition of nitrogen feed input into retention, soluble and particulate waste streams, and nitrogen loads per tonne of YTK production, as compared with data for some other species.

Species	Fate of nitrogen in feed inputs (%)			Nitrogen loads (kg N tonne^{-1} growth)			Diet	FCR	Source
	Fish retention	Solid wastes	Soluble wastes	Solid	Soluble	Total			
Southern bluefin tuna	7	8	86	40	462	502	Baitfish	4.9[a]	Fernandes et al., 2006a
SBT	12	12	76	35	224	260	Baitfish	2.7[a]	As above
Areolated grouper	12	42	46	153	168	321	Baitfish	---	Leung et al., 1999
Yellowtail	---	---	---	---	---	177	Baitfish	2.3[a]	Watanabe et al., 1993
Yellowtail	---	---	---	---	---	265	Pellets	3.1[a]	As above
YTK	15	15	70	31	148	179	Pellets	3.0[a]	This work
YTK	14	14	72	33	164	198	Pellets	3.2[a]	This work
Atlantic halibut	30	19[b]	50[b]	18	48	66	Pellets	1.3	Davies & Slaski, 2003
Atlantic salmon	38	15[b]	47[b]	14	43	57	Pellets	1.2	Gillibrand et al., 2002
Atlantic salmon	40	26[b]	34[b]	9	33	42	Pellets	1.1	Strain & Hargrave, 2005
Salmonids	20	28	52	43	80	123	Pellets	2.0	Gowen & Bradbury, 1987
Salmonids	28	16[b]	56[b]	17	61	78	Pellets	1.5	Ackefors & Enell, 1990
Rainbow trout	25	21	54	28	73	102	Pellets	2.1	Hall et al., 1992
Rainbow trout	19	7	74	11	114	125	Pellets	1.8	Foy & Rosell, 1991a, b
European seabass	---	---	---	---	---	65[c]	Pellets	1.2	Kaushik, 1998
Gilthead Seabream	---	---	---	---	---	52[c]	Pellets	1.1	As above
Gilthhead seabream	22	10[b]	68[b]	13	90	103	Pellets	1.8	Lupatsch & Kissil, 1998

[a]dry weight feed/wet weight gain.
[b]these values do not account for remineralization of solid wastes at the sediment-water interface.

[c]maximum estimates.

Table 4.5. Mean (± SD) total nitrogen, wet density and water content of sediments collected under pens P1 and P2 and their respective controls, C1 and C2.

	Total nitrogen (%)		Wet density (g cm^{-3})		Water content (%)	
P1	0.13	(0.02)	1.55	(0.01)	38	(6)
C1	0.11	(0.01)	1.65	(0.05)	34	(3)
P2	0.20	(0.01)	1.53	(0.01)	48	(2)
C2	0.19	(0.01)	1.44	(0.01)	49	(0.4)

4.6 Conclusions

The loads calculated here constitute a first estimate of nitrogen and phosphorus losses from YTK farming in South Australia using actual management and environmental data. Although the model relies on many simplifications, the level of uncertainty of total loads is small as these were based on inputs (stock and feed) and outputs (mortalities and harvested fish) supplied by the industry. However, the loads were calculated from data obtained for the last year of the grow-out period, and may need to be adjusted if additional information becomes available for earlier stages. The calculation of daily loads during the course of the grow-out period would greatly benefit from more data detailing how excretion and deposition rates, and benthic fluxes, vary seasonally with water temperature and current speeds. This level of detail would allow calculation of loads on more suitable time scales (e.g. months) to pinpoint periods of increased susceptibility of disturbance to natural processes.

Nitrogen losses per tonne of YTK growth were found to be at least double values for other aquaculture species fed manufactured pellets. The high metabolic rates of these predatory fish not only account for high nutrient loads to the environment, but also for a different partition between solid and dissolved wastes. High rates of nitrogen excretion in urine and through the gills explain the low nitrogen retention in fish tissues and high losses of dissolved wastes to the water column. These processes, combined with the low settling velocity of faeces, and the effects of scavenger feeding, lead to minimal impacts to the benthos. The nature of the wastes (dissolved or faecal with low settling velocity) however, suggests that these effects will not be confined to the footprint of the pens and might spread over a large area. Regional effects are currently unknown.

4.7 Acknowledgements

This work received funds from PIRSA Aquaculture and the Fisheries R&D Corporation. We wish to thank Brad Mansell (SA Aquaculture Management)

and farm operators for help in accessing sites and management data. Sonja Venema, Gen Mount, Peter Lauer, Bruce Miller-Smith and Michael Guderian (SARDI Aquatic Sciences) are acknowledged for sample collection, preparation and analyses. We also wish to thank Stuart McClure (CSIRO Land & Water) for nitrogen IRMS analyses and Tina Hines (Water Studies Centre, Monash University) for dissolved nitrogen analyses.

4.8 References

Ackefors, H. & Enell, M. (1990). Discharge of nutrients from Swedish fish farming to adjacent sea areas. Ambio, 19, 28-35.

APHA-AWWA-WPCF (1998a). Method 4500-NO3-I. In Standard methods for the examination of water and wastewater (pp. 4-121). Washington: American Public Health Association.

APHA-AWWA-WPCF (1998b). Method 4500-NH3-I. In Standard methods for the examination of water and wastewater (pp. 4-111). Washington: American Public Health Association.

Chambers, C.B. & Ernst, I. (2005). Dispersal of the skin fluke *Benedenia seriolae* (Monogenea: Capsalidae) by tidal currents and implications for sea-cage farming of *Seriola* spp. Aquaculture, 250, 60-69.

Clark, T.D. (2006). Energy expenditure of the yellowtail kingfish (*Seriola lalandi*) at different swimming speeds: developing a bioenergetics model for Australian aquaculture. In Innovative solutions for aquaculture planning and management – Project 2a, Spatial impacts and carrying capacity: Further developing, refining and validating existing models of environmental effects of finfish farming (Draft final report). Adelaide: SARDI Aquatic Sciences.

Davies, I.M. & Slaski, R.J. (2003). Waste production by farmed Atlantic halibut (*Hippoglossus hippoglossus* L.). Aquaculture, 219, 495-502.

DEH (2003). Focus: A Regional Perspective of Spencer Gulf. Department of Environment and Heritage, Coast and Marine Branch, Adelaide, 70 pp.

Department of Agriculture Fisheries and Aquaculture (2002). Agriculture, Fisheries and Aquaculture Sectors in Review 2002. Government of New Brunswick, New Brunswick, Canada, 10 pp.

Doglioli, A.M., Magaldi, M.G., Vezzulli, L. & Tucci, S. (2004). Development of a numerical model to study the dispersion of wastes coming from a marine fish farm in the Ligurian Sea (Western Mediterranean). Aquaculture, 231 215–235.

Fernandes, M., Lauer, P., Cheshire, A. & Angove, M. (2006a). Modelling of nitrogen environmental flows in southern bluefin tuna aquaculture. In Aquafin CRC - Southern Bluefin Tuna Aquaculture Subprogram: tuna environment subproject - evaluation of waste composition and waste mitigation (draft final report for Aquafin CRC Project 4.3.2 and FRDC

Project 2001/103) (pp. 217-242). Adelaide: Aquafin CRC, SARDI Aquatic Sciences and FRDC.

Fernandes, M., Lauer, P., Cheshire, A., Putro, S., Svane, I., Mount, G., Tanner, J. & Fairweather, P. (2006b). Aquafin CRC – Southern Bluefin Tuna Aquaculture Subprogram: Tuna Environment Subproject – Evaluation of Waste Composition and Waste Mitigation. Draft technical report, Aquafin CRC Project 4.3.2, FRDC Project 2001/103. Aquafin CRC, SARDI Aquatic Sciences and FRDC, Adelaide, 344 pp.

Foy, R.H. & Rosell, R. (1991a). Loadings of nitrogen and phosphorus from a Northern Ireland fish farm. Aquaculture, 96, 17–30.

Foy, R.H. & Rosell, R. (1991b). Fractionation of phosphorus and nitrogen loadings from a Northern Ireland fish farm. Aquaculture, 96, 31-42.

Gillibrand, P.A., Gubbins, M.J., Greathead, C. & Davies, I.M. (2002). Scottish Executive locational guidelines for fish farming: predicted levels of nutrient enhancement and benthic impact. Scottish Fisheries Research Report No. 63/2002. Scottish Fisheries Research Services, Aberdeen, 53 pp.

Gowen, R.J. & Bradbury, N.B. (1987). The ecological impact of salmonid farming in coastal waters: a review. Oceanography and Marine Biology Annual Review, 25, 563–575.

Hall, P.O.J., Holby, O. & Kollberg, S.-O. (1992). Chemical fluxes and mass balances in a marine fish cage farm. IV. Nitrogen. Marine Ecology Progress Series, 89, 81-91.

Hone, P., Vandepeer, M., Clarke, S. & Nichols, J. (1996). Fitzgerald Bay snapper aquaculture baseline environmental monitoring program (collected for the Whyalla Industrial Development Executive). July 1996. SARDI Aquatic Sciences, Adelaide, 16 pp.

Kaushik, S.J. (1998). Nutritional bioenergetics and estimation of waste production in non-salmonids. Aquatic Living Resources, 11, 211-217.

Kofuji, P.M., Akimoto, A., Hosokawa, H. & Masumoto, T. (2005). Seasonal changes in proteolytic enzymes of yellowtail *Seriola quinqueradiata* (Temminck & Schlegel; Carangidae) fed extruded diets containing different protein and energy levels. Aquaculture Research, 36, 696-703.

Kofuji, P.M., Hosokawa, H. & Masumoto, T. (2006). Effects of dietary supplementation with feeding stimulants on yellowtail *Seriola quinqueradiata* (Temminck & Schlegel; Carangidae) protein digestion at low water temperatures. Aquaculture Research, 37, 366-373.

Korsmeyer, K.E. & Dewar, H. (2001). Tuna metabolism and energetics. In B.A. Block and E.D. Stevens, Tuna: Physiology, Ecology and Evolution (pp. 35-78). San Diego: Academic Press.

Lauer, P. (2005). Benthic metabolism adjacent to Southern Bluefin Tuna (*Thunnus maccoyii*) pontoons in South Australia. PhD Thesis, Flinders University, Adelaide, 210 pp.

Leung, K.M.Y., Chu, J.C.W. & Wu, R.S.S. (1999). Nitrogen budget for the areolated grouper *Epinephelus areolatus* cultured under laboratory conditions and in open-sea cages. Marine Ecology Progress Series, 186, 271–281.

Love, G. & Langenkamp, D. (2003). Australian Aquaculture: Industry Profiles for Related Species, ABARE eReport 03.8. Abareconomics, Fisheries Resources Research Fund, Canberra, 135 pp.

Lupatsch, I. & Kissil, G. (1998). Predicting aquaculture waste from gilthhead seabream *Sparus aurata* culture using a nutritional approach. Aquatic Living Resources, 11, 265– 268.

Masumoto, T., Ruchimat, T., Ito, Y., Hosokawa, H. & Shimeno, S. (1996). Amino acid availability values for several protein sources for yellowtail (*Seriola quinqueradiata*). Aquaculture, 146, 109-119.

Oceanique Perspectives (1998). Estimate of the environmental carrying capacity of the Fitzgerald Bay aquaculture management zone. Primary Industries and Resources SA, Adelaide, 15 pp.

PIRSA (2002). Yellowtail kingfish aquaculture in SA (Fact Sheet). Primary Industries and Resources SA, Adelaide, 10 pp.

PIRSA Aquaculture (2004). Fitzgerald Bay aquaculture management policy. Primary Industries and Resources SA, Adelaide, 34 pp.

Russell, B.D., Elsdon, T.S., Gillanders, B.M. & Connell, S.D. (2005). Nutrients increase epiphyte loads: broad-scale observations and an experimental assessment. Marine Biology (Berlin), 147, 551-558.

SA Water (2003). Sustainability report. Water, for growth, development and quality of life for all South Australians. SA Water, Adelaide, 67 pp.

Strain, P.M. & Hargrave, B.T. (2005). Salmon aquaculture, nutrient fluxes and ecosystem processes in southwestern New Brunswick. In B. Hargrave, The Handbook of Environmental Chemistry, Vol. 5, Part M: Environmental Effects of Marine Finfish Aquaculture (pp. 29-57). Berlin: Springer-Verlag.

Tomás, A., La Gándara, F.d., García-Gomez, A., Pérez, L. & Jover, M. (2005). Utilization of soybean meal as an alternative protein source in the Mediterranean yellowtail, *Seriola dumerili*. Aquaculture Nutrition, 11, 333-340.

Watanabe, T., Takeuchi, T., Okamoto, N., Viyakarn, V., Sakamoto, T., Satoh, S. & Matsuda, M. (1993). Feeding experiments of yellowtail with a newly developed soft-dry pellet. Journal of the Tokyo University of Fisheries, 80, 1-17.

Chapter 5: Carbon deposition modelling for yellowtail kingfish in Fitzgerald Bay

Jason Tanner, Greg Collings and Anthony Cheshire

SARDI Aquatic Sciences, PO Box 120, Henley Beach SA 5022 & Aquafin CRC

Note: The model described here was originally developed as part of a project for PIRSA Aquaculture, and subsequently further developed for SBT through funding from Aquafin CRC. The SBT model was then adapted for YTK as a part of the current project. This chapter is based on Collings *et al.* 2006.

5.1 Executive Summary

To help predict the pattern of benthic impacts around a yellowtail kingfish pontoon, and in particular to examine the potential for impacts of neighbouring pontoons to overlap, as well as broader scale pelagic impacts, a model of what can loosely be termed 'carrying capacity' was developed. While the model has not been fully calibrated and validated, and therefore cannot provide an absolute estimate of deposition loads, it does provide a useful qualitative picture of the pattern of carbon deposition that is likely to occur based on stocking densities, feeding rates and current flows. In the short term, this information can be used by farm operators to examine the likely consequences of different pontoon arrangements within a lease, and it can help structure monitoring programs as it predicts the positions of maximal impact, even if the numeric estimate of loading is not currently verified. The model can also be used to guide increases in production in an adaptive management framework. In the longer term, the model will provide a framework to direct future research and assist in the integration and synthesis of field results and the identification of gaps in current knowledge.

The model, "*Farmér*", is a simulation of the increased carbon loading to the seabed caused by finfish farming. From estimates of feeding rates and chemical composition of food and fish, the path of carbon in both faecal material and uneaten food is simulated to the seafloor to estimate the pattern of organic deposition on the seabed. This involves two components of movement in the water column – a current induced movement (advection) and diffusion independent of water motion (dispersion). The magnitude of both effects is determined, at least in part, by the time taken to sink to the seafloor. Once deposited, the carbon can either accumulate over the period of the simulation, or it can be utilised at least in part by the benthos, depending on the options selected. The resultant output is a two dimensional surface plot of loading across the area of the seabed covered by the waste materials. Currently, the model is set up to operate at the lease scale, although a single pontoon can also be simulated, as could interactions between 2 neighbouring leases.

5.2 Introduction

"Carrying capacity" has multiple definitions in the ecological literature. In terms of traditional population ecology, it refers to the number of organisms of a given species that can be supported by the level of resources available (Fernandes *et al.* 2001). Aquaculture operations necessarily involve a waste stream that has the potential to impact on the surrounding environment (Gowen *et al.* 1994). These changes to the surrounding environment may result in conditions that are deleterious to the fish being raised or have an unacceptable effect on the natural biota (Pearson and Black 2001; Read *et al.* 2001). Thus the "environmental carrying capacity" represents the level of production that can be maintained without a loss of habitat quality that is unacceptable because of an effect on stock or other biota (Fernandes *et al.* 2001).

Carrying capacity is not determined by a single variable, but rather by any one of a suite of potential factors operating at different scales (Silvert 1992). At the most localised of scales, the stocking rate of the fish within a pontoon will have ramifications on oxygen levels in the immediate water column (Silvert and Cromey 2001) and the likelihood of disease transmission. At a larger, but still quite local scale, organic deposition, of either uneaten food or faecal material, can have a profound influence on the benthos (Findlay and Watling 1994; Silvert and Sowles 1996). At the regional scale, the release of soluble nutrients becomes a more important issue (Silvert 1992, Silvert and Cromey 2001). This chapter deals with the intermediate scale, modelling patterns of carbon deposition around yellowtail kingfish pens.

5.2.1 The overall modelling approach

The modelling strategy used here investigates carrying capacity in terms of organic deposition (a near-field effect) while the release of soluble nutrients (a far-field effect) is covered in chapter 6. It is important to note that while other issues, (e.g. oxygen stress, disease transmission, physiological response to environmental conditions such as temperature and salinity, behavioural issues, etc) may act to limit productivity, these effects are not within the scope of the models detailed here. Such issues should be dealt with based on the cumulative experience of industry.

The carbon deposition model simulates the deposition of carbon onto the seafloor around an individual pontoon or a small group of pontoons. This model is designed primarily to be used at the lease scale, allowing an examination of how deposition from neighbouring pontoons may overlap, but it could also be used to examine interactions between two neighbouring leases or deposition around a single pontoon. The carbon deposition model cannot be used at the scale of the entire farming region in its current implementation. While there are no theoretical restrictions to running the model at this larger scale, the computational effort required would be excessive, and unless wastes disperse large distances before settling out, little would be gained. The model is based on the best available data, but our understanding of many processes, particularly hydrodynamics, in the Fitzgerald Bay area is incomplete, and thus the model has not been fully calibrated or validated. Thus, while the patterns predicted are likely to be reasonably

accurate, the absolute values of the predictions should be treated with caution. In the short term, this information can be used to help structure monitoring programs as it predicts the positions of maximal impact, even if the numeric estimate of loading is not currently verified. In the longer term, the model will provide a framework to direct future research and assist in the integration and synthesis of field results and the identification of gaps in current knowledge.

Carbon deposition is modelled using a Gowen-type model (see Gowen *et al.* 1994) developed by SARDI. This allows a prediction of the pattern of organic deposition around each pontoon. Again, due to uncertainties in some parameters, the model is more useful as a predictor of the qualitative pattern of carbon deposition and of the *relative* impact on different sites than it is as an indicator of the absolute rates of deposition. This model cannot be used to predict the carrying capacity of a region, but can be used to assess likely consequences of different stocking rates and pontoon arrangements at the lease scale.

5.2.2 Farmér – predicting carbon loading to the seafloor

One of the principal factors to be considered in assessing the waste stream generated by a marine pontoon aquaculture system is the deposition of carbon to the seabed (Bergheim *et al.* 1991; Ervik *et al.* 1997; Panchang *et al.* 1997). The deposition of organic material, either in the form of uneaten food or faeces, creates a biological oxygen demand, and this may lead to a level of deoxygenation in the overlying water column which is detrimental to the health of both the farmed fish and any natural biota. The fact that this material is particulate rather than dissolved dictates that this problem is a near-field, or local issue, in contrast to the issue of dissolved nutrients, which is a far-field issue (Silvert 1994a). Thus, the output of the Farmér model is restricted to the area of seafloor in close proximity to an individual lease. The assumption is made that leases are separated by a great enough distance that the carbon deposition of a given lease is not going to interact appreciably with that of any other lease.

Farmér is a composite model that performs mass balance calculations on the carbon flow through the system, and then applies diffusion and current displacement functions to the carbon loads represented by faecal matter and uneaten food. These two components are modelled separately as they are likely to have very different sinking rates. However, they are treated in a similar manner.

Food is assumed to be evenly distributed across the surface of the pontoon, as are faeces. Both components are subject to two separate influences that affect the pattern of deposition. The first is a current induced movement that is defined by current speed and direction and the time taken to sink to the seafloor. The second influence is a natural diffusion that occurs independent of the current, and in still water results in inputs from a point source being deposited in a circular area centred on the point of input (Figure 5.1). The combination of these two provides a pattern of deposition for a given time period over which the current is assumed to be uniform.

The time step used in the model is hourly across the course of a year. Note that the fall time is calculated from the *bottom* of the pontoon rather than the top, as the presence of the pontoon walls is claimed by some sources to substantially restrict water movement. The assumption is thus that no material is dispersed through the sides of the pontoons, and that it all falls through the bottom. While this claim may be an oversimplification, this produces the most conservative estimates as decreasing fall time results in a smaller area over which material diffuses and therefore a greater loading to the benthos.

Step 1: Mass Balance Calculations

These calculations are based around the carbon waste stream for a single pontoon for one day.

- **$Weight_{fish}$** = stocking rate (g m^{-3}) x area of pontoon (m^2) x depth (m)
- **$Weight_{food}$** = Feeding Rate (% body weight per day) x $Weight_{fish}$ (g)
- **$Carbon_{input}$** = $Weight_{food}$ (g) x $\%Carbon_{food}$
- **$Carbon_{uneaten\ food}$** = $Carbon_{input}$ (g) x %Food uneaten
- **$Carbon_{respired}$** = O_2 consumption rate (mg O_2 kg^{-1} hr^{-1}) x $Weight_{fish}$ (g) x 16/32 x 24 (hr day^{-1})
- **$WeightGain_{fish}$** = $Weight_{food}$ (g)/ FCR
- **$CarbonGain_{fish}$** = $WeightGain_{fish}$ (g) x $\%Carbon_{fish}$
- **$Carbon_{faeces}$** = $Carbon_{input}$ (g) - $Carbon_{uneaten\ food}$ (g) - $Carbon_{respired}$ (g) - $CarbonGain_{fish}$ (g)

The important end products of this process are $Carbon_{uneaten\ food}$ and $Carbon_{faeces}$. These values are then converted to hourly figures by dividing by 24.

Step 2: Translocation of Carbon Load to Benthos

The diffusion and current-aided transport of the carbon loads associated with the faeces and uneaten food are modelled from the bottom of the pontoon to the seafloor. The two carbon loads are treated separately as they have different sinking rates, which results in them taking different times to reach the seafloor, and subsequently different amounts of time for the actions of diffusion and current movement. For similar reasons, when sinking speeds are represented by a distribution of different speeds (the model will allow particles from each waste stream to be allocated to as many as 10 different sinking rates on a percentage basis) rather than a single average, the fall of each of these components and its distribution on the seafloor is simulated separately. When all components of uneaten food and faeces have been distributed, these loadings are summed to produce an overall distribution. This process is iterated on an hourly basis to take into account the effects of the changing currents. After each hourly iteration, the new distribution is mapped onto the existing one.

The carbon load of the pontoon is uniformly distributed across the area of the pontoon. Diffusion is modelled via the use of a diffusion coefficient that determines the circular area across which the load from a point source will be distributed.

Within this circle of diffusion, a truncated normal distribution is used, with 99% of the load being distributed according to a normal distribution centred on the point of discharge (see Figure 5.1). The 1% that falls further away (i.e. more than 2.58 standard deviations away (Zar 1984)) is, for computational reasons assumed to fall without diffusion. By superimposing the identical patterns of distribution for every point within the pontoon, an overall pattern of distribution of the pontoon could be determined. Essentially this looks like a normal curve flattened toward the centre of the pontoon, as all points in the central area had similar loading, and tailing off some distance outside the area of the pontoon. How flat and how far away the tailing off occurred was dependent on the coefficient of diffusion.

Once the diffusion matrix has been calculated for the pontoon, the effects of currents are introduced. Current data were obtained from a model developed by Petrusevics (in Parsons Brinkerhoff & SARDI Aquatic Sciences, 2003). These data were supplied as an average 15-day tidal cycle for each season, with current speed and direction specified hourly. To produce an annual file, the 15 days of current data for each season were replicated to extend to 3 months, and then data from the four seasons merged into a single file. This procedure was necessary as there are no current data for a full year available from the area.

The effect of the currents was to displace the calculated diffusion matrix away from the pontoon by an amount and direction determined by the current magnitude and direction. This was repeated on an hourly basis across the growout period and the buildup of carbon was recorded as a surface map of the lease area and any additional area that the material diffused or was moved into. A picture of the situation at the end of the growout period was then provided.

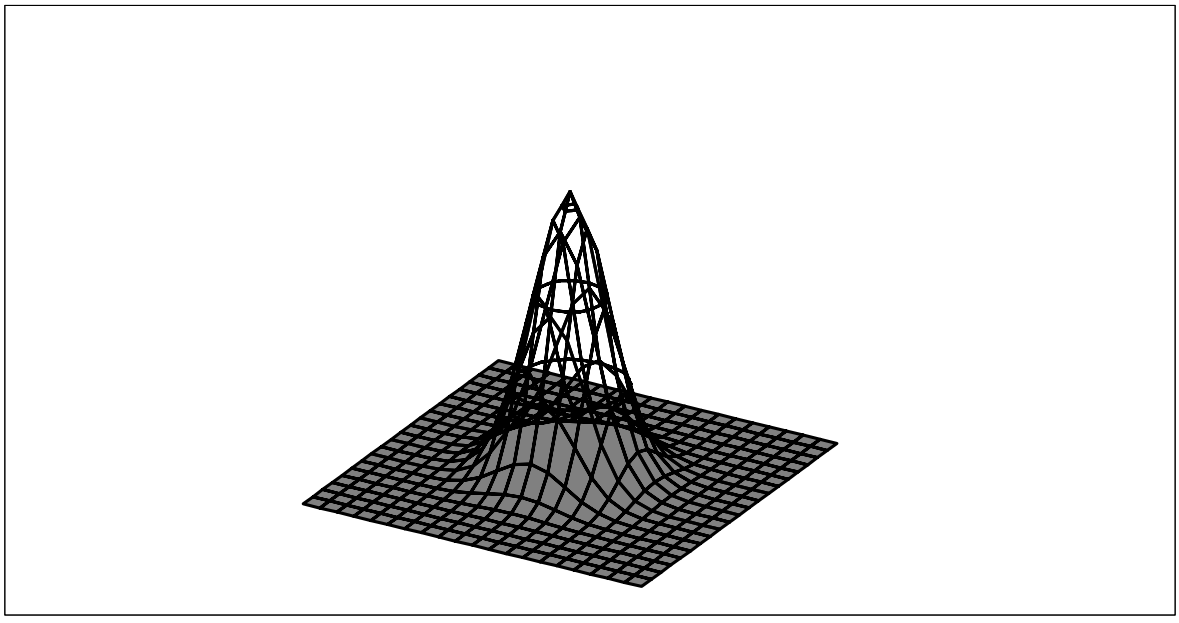

Figure 5.1: Distribution of carbon released from a single point. The width of the circle, and therefore the height, is determined by a diffusion coefficient. The largest proportion of the particles fall directly down, with increasingly smaller proportions falling at distances further from the release point.

Parameterisation

Operational Data:

YTK were fed on a diet of pellets.
The percentage of food *not* ingested was 3% (Chapter 4)
Food Conversion Ratio (wet weight): 3.2:1 (Chapter 4)
Proportion of Carbon in Food (wet weight basis): 43% (Fernandes unpublished data)
Proportion of Water in Food: 5.8% (Chapter 4)
Proportion of Carbon in Fish (wet weight basis): 13% (Fernandes unpublished data)
Fish Respiration rate: 250 mg O_2 kg^{-1} hr^{-1} (Chapter 2 – based on a 2 kg YTK swimming at its optimum speed of 1.2 body lengths per second)
Stocking Rate: 10 kg/m^3 (based on 13,300 2.3 kg fish in a 25.5 m diameter, 6 m deep pontoon). For simplicity, this was assumed to be constant over time and thus will overestimate stocking density early in the season and underestimate it late in the season.
Feeding Rate: 0.9% of body weight per day (from chapter 4).
Sinking Rate of feed and faeces: Table 5.1

The model was run across a 365 day period, beginning January 1, with fish being stocked until December 31.

Table 5.1: Sinking rates for feed and faeces used in the carbon deposition model (obtained from Chapter 4).

Food		***Faeces***	
Settling rate (m sec^{-1})	**% settling**	**Settling rate (m sec^{-1})**	**% settling**
0.12	100	0.01	70
		0.02	30

Assumptions

Like the model dealing with dissolved nutrients (chapter 6), the carbon deposition model relies on several assumptions, and further work is necessary to ascertain their validity.

- The lease is modelled as an individual entity, and is not under the influence of any adjacent lease. With a minimum lease separation of 1 km, and assuming a water depth of 20 m and a net height of 6 m, a particle would

need to be advected 71 m for every 1 m it sank through the water column to reach an adjacent lease. Assuming a high current speed of 39 cm sec^{-1} (the maximum from the hydrodynamic model produced by Petrusevics in Parsons Brinkerhoff & SARDI Aquatic Sciences 2003), this would require particle settling rates <0.55 cm sec^{-1}, which is extremely slow, and 455% of the minimum settling rate assumed in the model, based on laboratory measurements of faecal settling. However, it is not unrealistic that some fine material is transported this distance (see Fernandes 2006, Chapter 4), and with bidirectional currents, it is likely that areas of deposition would overlap if leases are placed directly in line with each other, as material from each lease would then only have to be advected 500 m.

- All carbon contained in both faecal matter and uneaten feed is assumed to be in the solid rather than the dissolved form. Any carbon in the latter state would clearly not add to the loading on the seafloor. Thus the assumption that all the carbon is solid is a conservative one as it produces the highest values of deposition.
- The nets surrounding the pontoon, any fouling on these, and the presence of the fish themselves, act to reduce currents within the pontoon quite markedly (Cronin 1995). This would act to restrict carbon within the pontoon, rather than allowing it to disperse through the nets. For this reason it was assumed that the distance over which diffusion and current movement could occur was the distance between the bottom of the pontoon and the seafloor, rather than from the surface of the water. This would lead to a decreased area of dispersion and therefore increased density of deposition, so it is an assumption that provides a more conservative estimate of seabed souring.
- It is assumed that carbon is released uniformly over time, i.e. each hour, $1/24^{th}$ of the daily load is released. While there is anecdotal evidence that evacuation from the fish occurs less uniformly, without either verification or quantification, it is difficult to model this satisfactorily. Feed is input evenly over 24 hours.
- Post-depositional changes, whereby the sediments and benthic community recycle the organic matter, are not taken into consideration. Other models such as that of Fox (1990) (cited by Gowen *et al.* 1994) have modules that deal with this aspect. Although our model does itself have a capacity for introducing the removal of carbon through benthic respiration, it is not well enough calibrated at present to use it for predictive purposes.
- The sea floor is assumed to be a uniform depth, equal to the average depth of the lease. This may be unrealistic, as there is considerable variation in water depth within and around the farming zone in Fitzgerald Bay.
- Current speeds and directions are calculated on a depth-averaged basis (i.e. are assumed constant throughout the water column) rather than at different levels within the water column. This is likely to be less of a problem in these open coastal situations than in the fjordic systems of some other countries (Silvert and Cromey 2001).
- The diffusion coefficient used has assumed that a sinking time of 400 seconds would result in 99% of the particulate matter falling in a normal distribution within a circle of diameter 80 metres. This figure requires empirical validation.

- No effects of temperature on fish physiology are integrated within the model.
- Lack of quantification of the effects of scavenging of carbon by the natural biota dictates that this factor has not been taken into account. Again, this follows the precautionary principle required when our data are poor.

All parameters detailed above are subject to change through further measurements and research, as well as changes in the operation of leases and food technology.

Output

Output from the model is in the form of a surface plot of carbon loading. A record is also made of total loading and the point on the map where maximum loading occurs along with the value of that load. The output in all cases reflects the *additional* load imposed by the aquaculture operation. It does not take into account background rates of deposition. Figure 5.2 represents an example output from the model, and demonstrates how carbon deposition changes on a monthly basis through a 12-month farming season.

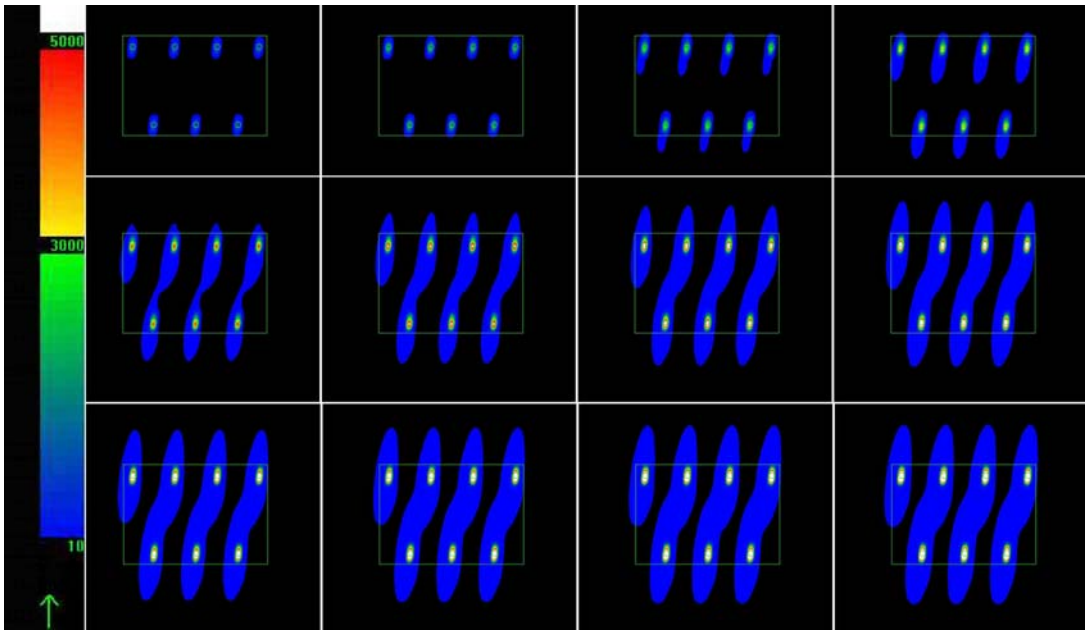

Figure 5.2: An example output from the Farmér (carbon deposition) model, showing monthly (January top left to December bottom right) development of carbon deposition (note: there are no removal processes operating in this simulation). Scale bar shows total deposition over time in g m^{-2}.

5.2.3 Finfish carbon deposition model – sensitivity analysis

A sensitivity analysis was performed on the finfish carbon deposition model (Farmér) to test the sensitivity of the model predictions of maximum carbon loading and the pattern of spread from finfish aquaculture pontoons to respiration rate, food conversion ratio (FCR), and feeding rate. This analysis shows how carbon deposition changes with changes in these parameters. Similar sensitivity analyses could be conducted for any other parameter desired, although the other parameters that have high uncertainty (sinking rates and currents) are complex and are not just introduced into the model as a single parameter. Thus a sensitivity analysis would have to be based on comparing different scenarios, rather than simply stepping through different values of a parameter.

Respiration rate sensitivity analysis

The initial model simulations of carbon deposition were based on a YTK swimming respiration rate of 250 mg O_2 kg^{-1} hr^{-1}, although rates of 660 mg O_2 kg^{-1} hr^{-1} have been recorded during intense activity (chapter 2). The sensitivity analysis involved repeated simulations of the carbon deposition model using a range of respiration rates. The respiration rates used for the sensitivity analysis were 150, 200, 250, 300 & 350 mg O_2 kg^{-1} hr^{-1}, hence, a total of 5 simulation runs were performed.

Food Conversion Ratio (FCR) sensitivity analysis

The food conversion ratio (FCR) is the amount of food fed per kg to achieve a 1 kg increase in fish body weight (Jover *et al*, 1999). Within the current model, an FCR value of 3.2 is used.. Repeated model runs were conducted with FCRs ranging from 2.6 to 3.8, in steps of 0.2 (i.e. 7 separate runs).

Feeding rate sensitivity analysis

To examine the effects of varying feeding rate, a sensitivity analysis was also conducted of this parameter. Based on data in chapter 4, feeding rates are ~0.9% of body weight per day on average. The sensitivity analysis involved model runs with feeding rate varying from 0.6 to 1.2% of body weight, in 0.1% increments (7 model runs).

5.3 Results and Discussion

5.3.1 Respiration

The model output is sensitive to the value of respiration rate chosen (Figure 5.3). It is obvious that as respiration rate increases, the amount of carbon deposited on the seafloor decreases if the other parameters remain constant. This decrease is due to increased amounts of carbon being respired as carbon dioxide. Assuming an FCR of 3.2 (wet weight), and a feeding rate of 0.9% of body weight per day, respiration rates above 389 mg O_2 kg^{-1} hr^{-1} produce a carbon deficit (i.e. the fish would lose mass if respiration rates greater than this were maintained). The pattern of carbon deposition around a series of pontoons is very similar at the different respiration rates (Figure 5.4), although obviously the area of high deposition decreases as respiration increases.

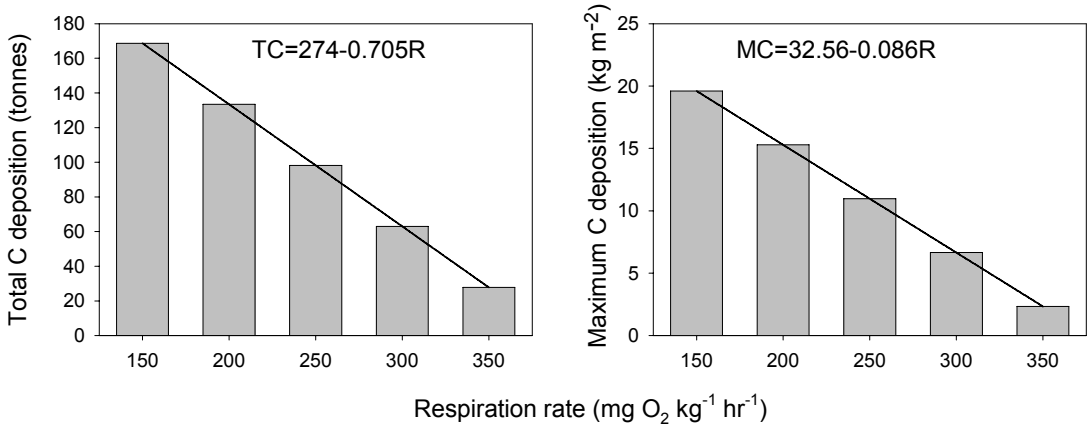

Figure 5.3: Sensitivity analysis of respiration rate on total and maximum carbon deposition (FCR=3.2, feeding rate = 0.9%). Both linear fits have r^2=1.

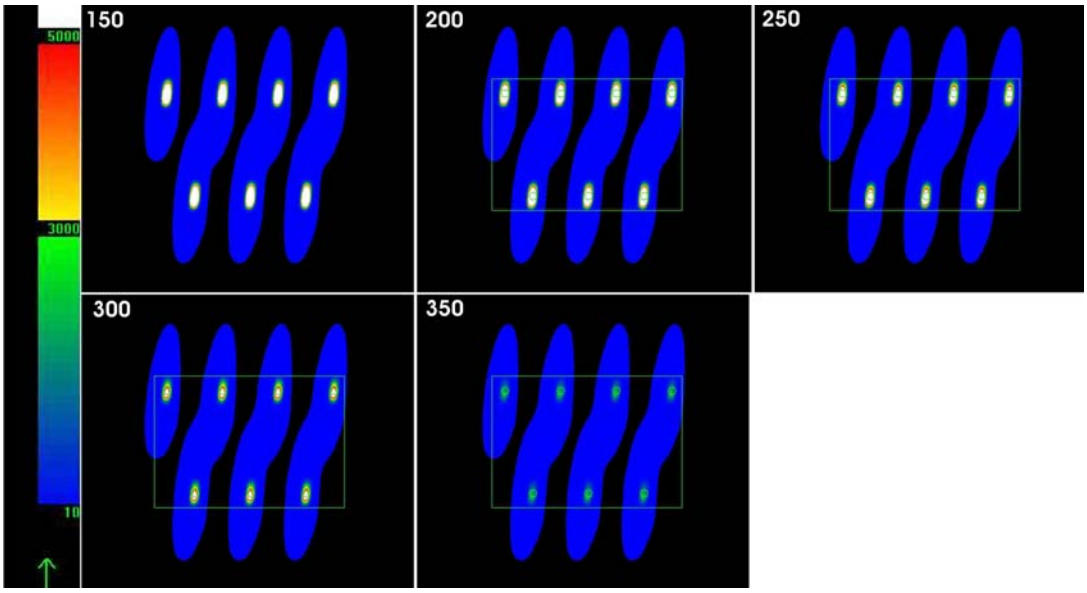

Figure 5.4: Sensitivity analysis of respiration rate (varying from 150-350 mg O_2 kg^{-1} hr^{-1}) on carbon deposition pattern (note: there are no removal processes operating in this simulation). Scale bar shows total deposition over time in g m^{-2}.

5.3.2 Food conversion ratio

The model was much less sensitive to FCR than it was to respiration rate (Figure 5.5). As the FCR improves (gets lower), the amount of carbon assimilated by the fish increases, and obviously the amount deposited on the seafloor decreases. At a respiration rate of 250 mg O_2 kg^{-1} hr^{-1}, and feeding rate of 0.9% of body weight per day, none of the FCRs tested resulted in the carbon demand of the fish being greater than supply. Again, FCR appeared to have little effect on the actual pattern of carbon deposition (Figure 5.6).

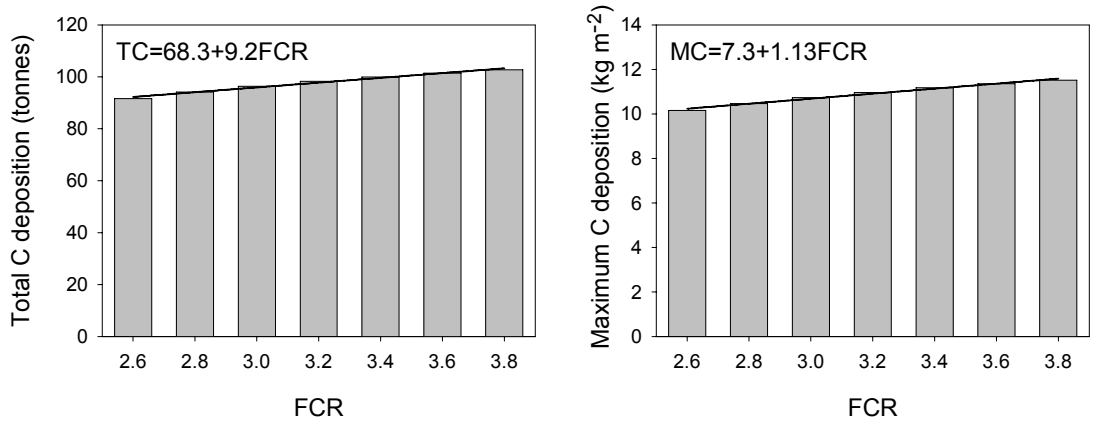

Figure 5.5: Sensitivity analysis of FCR on total and maximum carbon deposition (respiration rate = 250 mg O_2 kg^{-1} hr^{-1}, feeding rate = 0.9%). The linear fits for both total carbon deposited maximum carbon loading at a point have r^2 of 0.99.

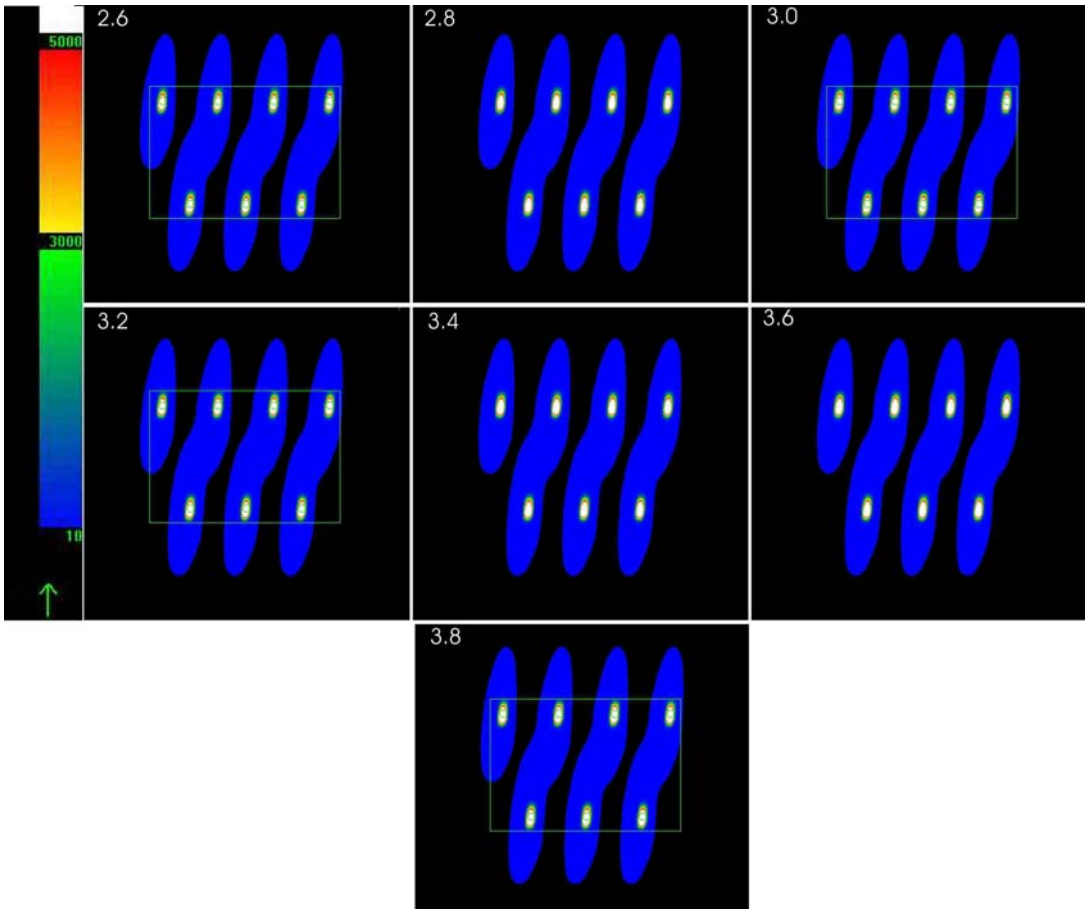

Figure 5.6: Sensitivity analysis of FCR (varying from 2.6-3.8) on carbon deposition pattern (note: there are no removal processes operating in this simulation). Scale bar shows total deposition over time in g m^{-2}.

5.3.3 Feeding rate

The model displayed similar sensitivity to feeding rate as it did to respiration rate (Figure 5.7). Obviously, lower feeding rates led to lower carbon deposition. Carbon demand by the fish equalled carbon supply at a feeding rate of 0.577% of fish body weight per day. That is, this feeding rate supplied just enough carbon to the fish for it to maintain its basal respiration, without any carbon being deposited as faecal material, and without any scope for fish growth. At low feeding rates, the carbon spread is less than at high feeding rates (Figure 5.8).

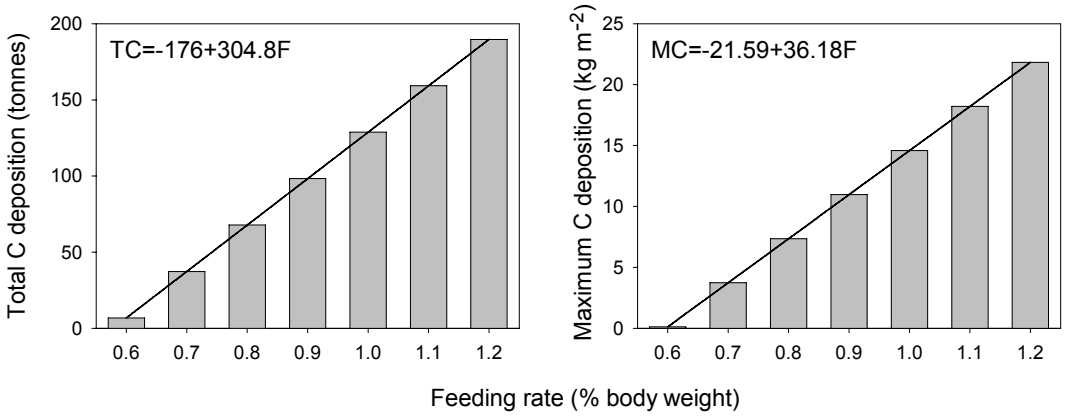

Figure 5.7: Sensitivity analysis of feeding rate on total and maximum carbon deposition (respiration rate =250 mg O_2 kg^{-1} hr^{-1}, FCR=3.2). Both linear fits have r^2=1.

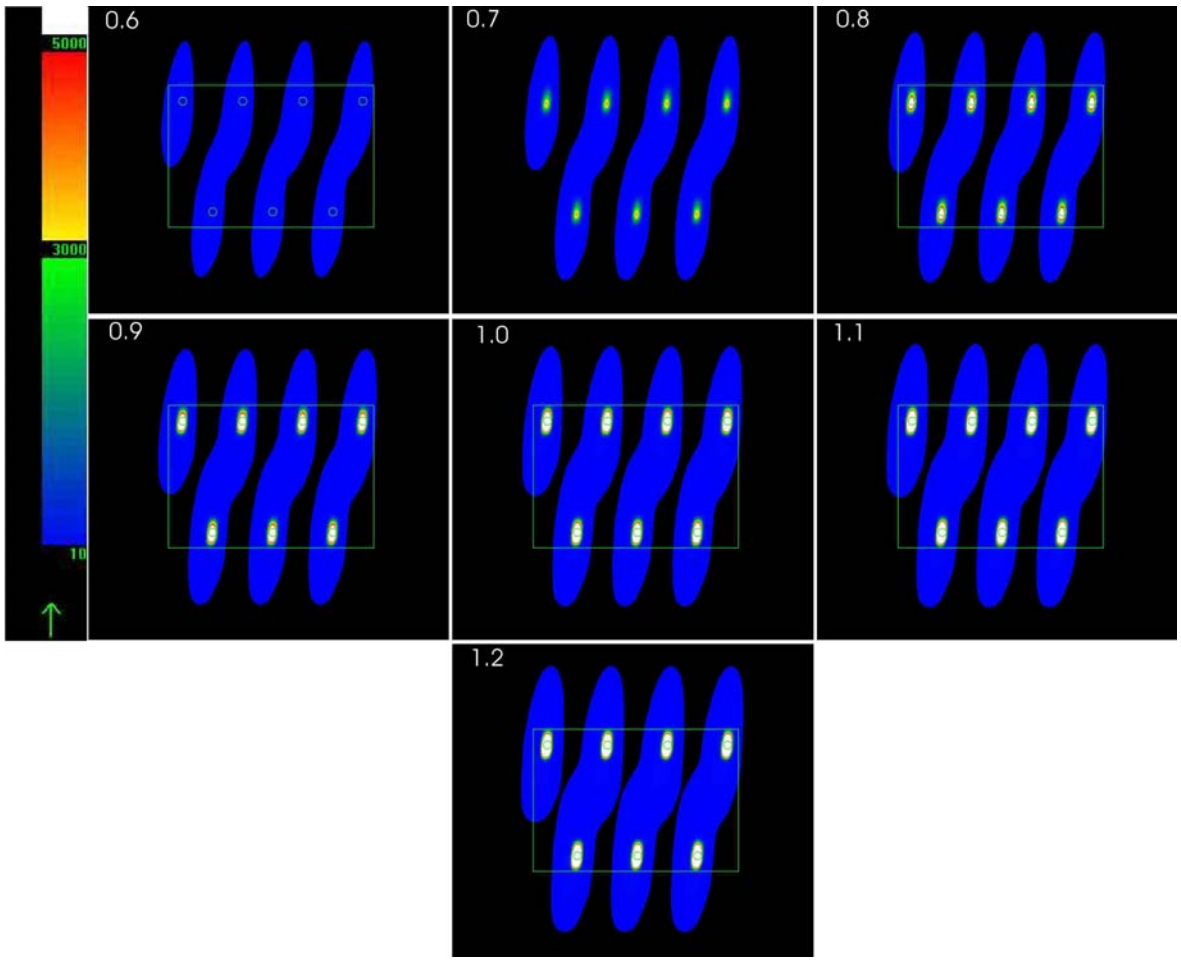

Figure 5.8: Sensitivity analysis of feeding rate (varying from 0.6-1.2% of body weight) on carbon deposition pattern (note: there are no removal processes operating in this simulation). Scale bar shows total deposition over time in g m^{-2}.

The results from this simple sensitivity analysis have shown that the respiration rate and feeding rate must be accurately measured or estimated to yield conclusive and confident model predictions. Exact knowledge of the FCR is considerably less important. The respiration rate used in the model of 250 mg O_2 kg^{-1} hr^{-1} is that for a yellowtail kingfish swimming at its optimum speed in 20^{o}C water, and that has not recently fed.

5.3.4 Implications of the results

The application of the model described above has allowed a range of useful outcomes. Farmér, whilst not used directly for the enumeration of carrying capacity, has provided useful information on likely patterns of carbon deposition, and with future calibration efforts and research on the environmental effects of different levels of deposition, is likely to become an even more useful tool.

Where possible, this model has been designed and parameterised with the precautionary principle in mind, i.e. where uncertainty exists, parameters are chosen to produce the worst possible outcome. Areas which require particular attention are the issue of water movement in terms of current speed and direction. In particular, the model assumes that the cages and other physical infrastructure on the lease have no influence on water movement, and thus carbon deposition patterns, with the exception that there is no flow across the cage walls. The sinking rates and diffusion coefficients of uneaten food and faeces also need further

attention. While some data are available on these factors, they are not comprehensive. The sensitivity analysis of the carbon deposition model also indicates that it is important to have good estimates of respiration and feeding rate, while FCR is less important in predicting carbon outputs. The model also tracks total inputs, assuming that these inputs remain in the system, and are not processed by other components such as scavengers and phytoplankton.

The results of this model should be seen, not as an endpoint of the process, but as a part of a cycle of improvement (Henderson *et al.* 2001; Read *et al.* 2001). Adaptive management is the principle that makes use of models to make preliminary predictions that are then adopted along with a careful monitoring strategy. The object of this monitoring is essentially to test the predictions of the model. In doing this, it serves two purposes – it acts to safeguard stock, and importantly, it is used to improve the model. Thus it becomes a recursive process, with the model becoming increasingly accurate and the monitoring acting to test the model and indicate further areas for improvement.

The immediate benefits of the creation of this modelling system are indications of the likely pattern of carbon loading around the lease area. However, there are other benefits of the creation of an "in-house" model that will be realised with time. Unlike proprietary models such as DEPOMOD (Cromey *et al.* 2000), we have developed a model that can be continually re-engineered in-house to reflect a system that we understand increasingly well. This model is in place, being used for preliminary predictions, and is deployed in an environment that is eager to monitor its results, recalibrate and continually improve its output, both in terms of accuracy and function.

5.3.5 Validation of model outputs

Fernandes & Tanner (chapter 4) measured sedimentation rates at the edge of YTK pens on the order of 75-90 g m^{-2} day^{-1}, as compared to background rates of ~ 65 g m^{-2} day^{-1}. Assuming that these rates are typical of the entire year, the sedimentation rates at the edge of a pen due to fish farming are on the order of 3,650-9,125 g m^{-2} $year^{-1}$. This compares with the maximum deposition predicted by the base model (with FCR=3.2, feeding rate at 0.9% of body weight a day and respiration of 250 mg O_2 kg^{-1} hr^{-1}) of 10,965 g C m^{-2} $year^{-1}$. Assuming that this is all faeces, which has a C content of 30% (Fernandes unpublished), then this translates to an actual sedimentation rate of 36,550 g m^{-2} $year^{-1}$, 4-10 times higher than that observed at the edge of the pen. Given that the sediment traps ran in a north-south direction from the pen edges, they would have been ideally located to sample areas predicted to have a C deposition of up to 9,000 m^{-2} $year^{-1}$ by the model, which is equivalent to a total deposition of 30,000 m^{-2} $year^{-1}$, or 3-8 times what was observed.

There appear to be three main areas of uncertainty in the model that could account for the discrepancy between model predictions and observed sedimentation rates:

1. The respiration rate used assumes that there is no increase in respiration due to feeding. This assumption was necessary because feeding trials in the respirometer were unsuccessful. However, it is well established that the act of feeding in itself involves an increase in metabolic rate. Thus, average respiration rate is likely to be higher than the value used. Based on the response of fish metabolism reviewed by Fitzgibbon (chapter 1), it can be assumed that average YTK metabolic rate is between 9 and 20% above the rate used here, and thus an average respiration rate of 300 mg O_2 kg^{-1} hr^{-1} is not unrealistic. Based on this assumption, maximum C deposition over the course of a year would be considerably lower (6646 g C m^{-2} $year^{-1}$ maximum, or ~ 6000 g m^{-2} $year^{-1}$ where the sediment traps were deployed, equivalent to an actual sedimentation rate of 20,000 g m^{-2} $year^{-1}$, only 2.2-5.5 times higher than that observed at the edge of the pen). In addition, the value of 250 mg O_2 kg^{-1} hr^{-1} is based on a 2 kg fish, as used by Clark (chapter 2), whereas fish in the pens on which the model is based

ranged between 1.3 and 3.3 kg. Given metabolic rate increases exponentially with body size (Fitzgibbon chapter 1), this is again likely to underestimate the average respiration rate over the course of one year.

2. The current vector used under-represents current speeds, and thus sediments are more widely dispersed than predicted, resulting in a lower maximum load. However, it is more likely that cages and other lease infrastructure impede water movement immediately around the pens.

3. Faecal settling rates (chapter 4) are slower than those used in the model. While these rates were measured empirically, this was done in the confines of a tank, with no turbulence. It was also not possible within the restrictions of the experiment conducted to determine how much carbon did not settle, and how much is typically removed by consumers other than YTK before it reaches the bottom. These consumers would include net fouling organisms and wild fish.

The sensitivity analysis indicates that mis-specification of the FCR is unlikely to account for the observed discrepancies, as changes in this parameter had very little influence on C deposition rates. While changes in feeding rate produced even greater changes in C deposition than did changes in respiration, it is considered that this parameter is known well enough that any errors are likely to be less than 0.1% BW, and therefore will have relatively little influence on the model results. It is also considered that major errors in the chemical composition of the model components (feed, faeces and YTK) are unlikely, and therefore would not account for the discrepancies.

While the model indicates higher deposition rates than those observed, if a base respiration rate of 300 mg O_2 kg^{-1} hr^{-1} is used, the degree of concordance is still good, and the overestimate means that using the model as is will automatically invoke the precautionary principle. Thus, it is considered that the model provides a useful indication of likely patterns of C deposition around a YTK lease.

Care would need to be taken if the model was used in areas outside of Fitzgerald Bay. For use anywhere else, a local current data file would be needed. If the farming practises were similar to those used in Fitzgerald Bay, it is likely that the other parameters used would be transferable. Substantially different farming practises, or environmental conditions (e.g. water temperature) are likely to invalidate the outputs of the model, however.

5.4 Future directions for the finfish carrying capacity models

There are many factors that need to be considered in the refining of the carbon deposition model. Important areas of improvements are listed below:

5.4.1 Improvements to program structure and function

Adding in a benthic-processing module to the model will allow the rate of accumulation of carbon in the sediments to be modelled. Currently, the model simulates total deposition, and does not allow for removal of carbon that is utilised by the benthic fauna. With measurements of benthic respiration, which have now been obtained for Fitzgerald Bay, it would be possible to estimate this carbon utilisation, and subtract it from the loading at each iteration.

Also, it would be beneficial to develop the simulation output as a 3-D view of the contour map showing the concentration of carbon loading.

5.4.2 Improvements to calibration

Adequate calibration of the model has not currently been achieved and this is probably the most important issue to be considered at this stage of development. There are several factors that need either a more complete data set to give better predictions, or more information and knowledge is needed to further build the model structure to make the simulations more realistic.

The empirical measurements of falling rates of faeces need to be improved. Currently, there is one settling rate for uneaten feed, which is considered to have a high level of accuracy, and two for faeces, with settling rates of faeces needing to be resolved in finer detail. Use of a broader range of particle sizes is likely to result in a more even distribution than that indicated. More importantly, field/laboratory measurements of diffusion distance for each particle size/type need to be included. The diffusion coefficient used has assumed that a sinking time of 400 seconds would result in 99% of the particulate matter falling in a normal distribution within a circle of diameter 80 metres. This figure requires empirical validation, although this will be difficult to achieve.

At this stage of the model development, temperature has not been incorporated within the structure. This is an area that needs to be revised and parameterised accordingly. Temperature is likely to influence respiration rate, which the sensitivity analysis indicates is important for the carbon deposition model.

The understanding of hydrodynamics within Fitzgerald Bay also needs to be improved, and is probably the highest priority need at this stage. The current vector used was based on a 2-dimensional hydrodynamic model that was parameterised based on typical wind and temperature conditions in each of the 4 seasons. A single 15 day current vector was then supplied for each season, and these were replicated to obtain a current vector for an entire year. Model predictions would benefit from either in situ measurements of currents over a one-year period, or extraction of a current vector from a hydrodynamic model of the area that has been parameterised using a full-year of data.

While good data have been obtained on yellowtail kingfish respiration in this project, it was not possible to obtain respiration rates of fish after feeding. As a result, the base respiration rate used (250 mg O_2 kg^{-1} hr^{-1}) is likely to underestimate average respiration rate. Thus, considerable further improvements could be made by obtaining a better average respiration rate that takes into account feeding.

Finally, the results need to be validated against long-term field measurements. This is a very important consideration in the model's development. If the model predictions can be compared to long-term field situations, then a greater understanding and confidence in model predictions can be achieved.

5.5 Acknowledgements

This work received funds from PIRSA Aquaculture & FRDC. We wish to thank Milena Fernandes, Jeff Buchanan, Peter Petrusevics and Steve Clarke for useful discussions and provision of data and Andrew Collings for assistance with programming of the model.

5.6 References

ANZECC/ARMCANZ (2000). Australian and New Zealand Guidelines for Fresh and Marine Water Ecology. Canberra.

ANZECC (1992) Australian and New Zealand Guidelines for Fresh and Marine Water Ecology – DRAFT. Canberra.

Bergheim, A., Aabel, J. P., Seymour, E. A. (1991) Past and present approaches to aquaculture waste management in Norwegian net pen culture operations. In. 'Nutritional strategies and aquaculture waste'. (Eds. C. B. Cowey, C. Y. Cho). Pp 117-136. University of Guelph, Guelph.

Beveridge, M. C. M. (1987) Cage Aquaculture. Fishing News Books Ltd, Surrey, England.

Campbell, D. E. & Newell, C. R. (1998). MUSMOD©, a production model for bottom culture of the blue mussel, *Mytilus edulis* L. *Journal of Experimental Marine Biology and ecology*, 219: 171-203.

Cho, C. Y., Hynes, J. D., Wood, K. R., Yoshida, H. K. (1991) Quantification of fish culture wastes by biological (nutritional) and chemical (limnological) methods; the development of high nutrient dense (hnd) diets. In. 'Nutritional Strategies & Aquaculture Waste'. (Eds. C. B. Cowey, C. Y. Cho). Pp 37-50. University of Guelph, Guelph.

Collings, G., Cheshire, A. & Tanner, J. E. (2006) Carrying capacity modelling. In. 'Aquafin CRC – Southern Bluefin Tuna Aquaculture Subprogram: Tuna environment subproject – Development of regional environmental sustainability assessments for tuna sea-cage aquaculture'. (Ed. J. E. Tanner). Pp 230-251. SARDI Aquatic Sciences, Adelaide.

Cromey, C. J., Nickell, T. D., Black, K. D. (2000) A model for predicting the effects of solids deposition from mariculture to the benthos. The Scottish Association for Marine Science (SAMS), Oban.

Cronin, E. (1995) An investigation into the effects of net fouling on the oxygen budget of southern bluefin tuna (*Thunnus maccoyii*) farms. Honours Thesis, University of Adelaide, Adelaide.

Ellis, D. & Rough, K. (2005) Quality and nutritional evaluation of baitfish used for SBT farming (including baitfish profiles). Aquafin CRC, Adelaide.

Ervik, A., Hansen, P. K., Aure, J., Stigebrandt, A., Johannessen, P., Jahnsen, T. (1997) Regulating the local environmental impact of intensive marine fish farming. I. The concept of the MOM system (modelling-ongrowing fish farms-monitoring). *Aquaculture* **158**, 85-94.

Fernandes, M. (2006). Tuna Waste Mitigation. Aquafin CRC/FRDC final report in preparation (FRDC 2001/103). SARDI Aquatic Sciences, Adelaide.

Fernandes, T. F., Eleftheriou, A., Ackefors, H., Eleftheriou, M., Ervik, A., Sanchez-Mata, A., Scanlon, T., White, P., Cochrane, S., Pearson, T. H., Read, P. A. (2001). The scientific principles underlying the monitoring of the environmental impacts of aquaculture. *Journal of Applied Ichthyology* **17**, 181-193.

Findlay, R. H., Watling, L. (1994) Toward a process level model to predict the effects of salmon net-pen aquaculture on the benthos. In. 'Modelling benthic impacts of organic enrichment from marine aquaculture'. (Eds. B. T. Hargrave). Pp 47-77. Canadian Technical Report of Fisheries and Aquatic Sciences 1949, Canada.

Fox, W. P. (1990). Modeling of particulate deposition under salmon net-pens. In 'Final Programmatic Environmental Impact Statement. Fish Culture in Floating Net-Pens (Technical Appendices)'. Washington State Department of Fisheries, Olympia, USA.

Gowen, R. J., Smyth, D., Silvert, W. (1994) Modelling the spatial distribution and loading of organic fish farm waste to the seabed. In 'Modelling Benthic Impacts of Organic Enrichment from Marine Aquaculture'. (Eds. B. T. Hargrave). Pp 19-30. Canadian Technical Report of Fisheries and Aquatic Sciences 1949, Canada.

Henderson, A., Gamito, S., Karakassis, I., Pederson, P., Smaal, A. (2001) Use of hydrodynamics and benthic models for managing environmental impacts of marine aquauclture. *Jounral of Applied Ichthyology* **17**, 163-172.

Jover, M., García-Gómez, A. Tomás, A., De la Gándara, F. and Pérez, L. (1999). Growth of Mediterranean yellowtail (*Seriola dumerilii*) fed extruded diets containing different levels of protein and lipid. *Aquaculture*, 179: 25-33.

Panchang, V., Cheng, G., Newell, C. (1997) Modeling hydrodynamics and aquaculture waste transport in coastal Maine. *Estuaries* **20**, 14-41.

Parsons Brinkerhoff & SARDI Aquatic Sciences. (2003) Technical review for aquaculture management plans – phase 2. Volume A. Upper Spencer Gulf. Report prepared for PIRSA Aquaculture, Adelaide.

Pearson, T. H., Black, K. D. (2001) The environmental impacts of marine fish cage culture. In. 'Environmental Impacts of Aquaculture'. (Eds. K. D. Black). Pp 1-31. (Sheffield Academic Press, Sheffield, UK).

Petrusevics, P. (1998) Estimate of the carrying capacity of the Fitzgerald Bay aquaculture management zone. Prepared for Primary Industries and Resources of South Australia (Aquaculture Group), by Oceanic Perspectives.

Read, P. A., Fernandes, T. F., Miller, K. L. (2001) The derivation of scientific guidelines for best environmental practice for the monitoring and regulation of marine aquaculture in Europe. *Journal of Applied Ichthyology* **17**, 146-152.

Silvert, W. (1992) Assessing environmental impacts of finish aquaculture in marine waters. *Aquaculture* **107**, 67-71.

Silvert, W. (1994a) Modelling benthic deposition and impacts of organic matter loading. In. 'Modelling benthic impacts of organic enrichment from marine aquaculture'. (Eds. B. T. Hargrave). Pp 1-18. Canadian Technical Report of Fisheries and Aquatic Sciences 1949, Canada.

Silvert, W. (1994b) Modelling environmental aspects of mariculture: Problems of scale and communication. In 'Proceedings of the Canada – Norway Workshop on environmental impacts of Aquaculture'. (Eds. A. Ervik, P. Kupka Hansen, P Wennevik, V. Wennevik). Pp 61-68. Fisken og Havet 13.

Silvert, W., Sowles, J. W. (1996) Modelling environmental impacts of marine finfish aquaculture. *Journal of Applied Ichthyology* **12**, 75-81.

Silvert, W., Cromey, C. J. (2001) Modelling Impacts. In. 'Environmental Impacts of Aquaculture'. (Eds. K. D. Black). Pp 154-181. (Sheffield Academic Press, Sheffield, UK).

Tanner, J. E. & Bryars, S. (2006) Innovative Solutions for Aquaculture Planning and Management – Project 5, Environmental Audit of Marine Aquaculture Developments in South Australia. SARDI Aquatic Sciences, Adelaide.

Zar, J. H. (1984) Biostatistical Analysis (Second Edition). Prentice-Hall International (UK) Limited, London.

Chapter 6: Carrying capacity modelling

Jason Tanner, Greg Collings and Anthony Cheshire

SARDI Aquatic Sciences, PO Box 120, Henley Beach SA 5022 & Aquafin CRC

Note: The model described here was originally developed as part of a project for PIRSA Aquaculture.

6.1 Executive Summary

To help predict broader scale pelagic impacts of yellowtail kingfish farming, and help managers set realistic maximum stocking levels that will minimise the potential for environmental harm, a model of 'carrying capacity' was utilised to predict the level of nutrient build-up that is likely to be experienced with an increased level of production. This model was first utilised in 2003 to provide some preliminary estimates of the carrying capacity of Fitzgerald Bay, in Spencer Gulf, for yellowtail kingfish aquaculture. However, at the time it was acknowledged that our understanding of kingfish physiology and nutrient cycling around kingfish pens was very incomplete, and that many of the parameters used in the model were best guesses, rather than based on hard data. Much of that missing data is provided by the previous chapters in this report, allowing us to calculate more accurate parameters for the model, and remove some of the assumptions that were previously made.

Assuming that the water quality parameters measured in November 2004 are typical of Fitzgerald Bay, the new model suggests that the Fitzgerald Bay aquaculture zone can cope with an additional 1,463 tonnes of production per year, above the current production levels of ~2,000 tonnes per year, before water quality would exceed ANZECC/ARMCANZ (2000) water quality guidelines. This compares to an increase of 2403 tonnes using the new parameters but old model assumptions, and 3927 tonnes based on the original model with original parameters.

6.2 Introduction

"Carrying capacity" has multiple definitions in the ecological literature. In terms of traditional population ecology, it refers to the number of organisms of a given species that can be supported by the level of resources available (Fernandes *et al.* 2001). Aquaculture operations necessarily involve a waste stream that has the potential to impact on the surrounding environment

(Gowen *et al.* 1994). These changes to the surrounding environment may result in conditions that are deleterious to the fish being raised or have an unacceptable effect on the natural biota (Pearson and Black 2001; Read *et al.* 2001). Thus the "environmental carrying capacity" represents the level of production that can be maintained without a loss of habitat quality that is unacceptable because of an effect on stock or other biota (Fernandes *et al.* 2001).

Carrying capacity is not determined by a single variable, but rather by any one of a suite of potential factors operating at different scales (Silvert 1992). At the most localised of scales, the stocking rate of the fish within a pontoon will have ramifications on oxygen levels in the immediate water column (Silvert and Cromey 2001) and the likelihood of disease transmission. At a larger, but still quite local scale, organic deposition, of either uneaten food or faecal material, can have a profound influence on the benthos (Findlay and Watling 1994; Silvert and Sowles 1996). At the regional scale, the release of soluble nutrients becomes a more important issue (Silvert 1992, Silvert and Cromey 2001).

In 2003, Parsons Brinkerhoff & SARDI Aquatic Sciences reported on a carrying capacity model that was developed by Greg Collings and Anthony Cheshire at SARDI, and showed how nutrient concentrations in Fitzgerald Bay would increase in response to increased production of yellowtail kingfish. In developing this model, it was acknowledged that a number of fairly large assumptions had been made both about the model structure and the parameters used, due to a lack of data. In particular, little was known about yellowtail kingfish physiology at the time, or about nutrient cycling around yellowtail kingfish pens. The work of Fitzgibbon, Clark and Fernandes detailed earlier in this report provides hard data on many of the missing parameters, and also allows several assumptions used in developing the model structure to be eliminated. As a consequence, we are now able to provide much more robust estimates of the carrying capacity of Fitzgerald Bay.

6.2.1 The overall modelling approach

The modelling strategy used here investigates carrying capacity in terms of the release of soluble nutrients (a far-field effect). It is important to note that while other issues, (e.g. oxygen stress, disease transmission, physiological response to environmental conditions such as temperature and salinity, behavioural issues, etc) may act to limit productivity, these effects are not within the scope of the models detailed here. Such issues should be dealt with based on the cumulative experience of industry.

A standard mass balance model (Beveridge 1987) was developed to predict how increased inputs from aquaculture would increase nutrient levels within

the water column. Predicted nutrient levels can then be compared to a set of trigger values, such as those provided by ANZECC / ARMCANZ (2000), to estimate the carrying capacity. Due to the uncertainties in some of the parameters of this model, it is important that production be increased incrementally, with the subsequent effects on nutrient levels being compared to model predictions to determine how well the model performs. In this case we do use the ANZECC / ARMCANZ (2000) guidelines for nearshore marine waters in South Australia, which specify ammonia and nitrate thresholds of 50 μg N L^{-1} and a phosphate threshold of 100 μg P L^{-1}.

For comparative purposes, we first describe the original model used in the Parsons Brinkerhoff & SARDI Aquatic Sciences (2003) report, including the parameters used. We then detail the updated parameters, and use these with the original model structure, to determine how they influence our estimation of carrying capacity for the area. Finally, we eliminate assumptions from the model that are no longer necessary, and calculate new estimates of carrying capacity for the Fitzgerald Bay aquaculture zone.

6.3 Methods

6.3.1 Original model description

A mass balance model of the type devised by Beveridge (1987) was utilised to predict the change in dissolved nutrient concentrations in the water body represented by the aquaculture zone. This model was the principal tool utilised to make quantitative predictions of how great a nutrient increase could be expected to be associated with any given level of production, an approach used previously in studies of finfish aquaculture potential in South Australian waters (e.g. Petrusevics 1998).

The dissolved nutrients that were investigated in this model were nitrogen (both as nitrate and ammonia) and phosphorus (as phosphate). The simulations detailed below were parameterised for yellowtail kingfish (*Seriola lalandi*). The model can also be applied to other finfish species including southern bluefin tuna (Tanner 2006) and snapper. Each run of the model requires the operator to develop a specific set of parameters that are applicable to the individual site, species being farmed, and stage of growth.

The central equation of this model is:

$$\Delta N = \frac{L \text{ x } (1 - R_s)}{V \text{ x } F} \qquad (6.1)$$

where: ΔN = the change in dissolved nutrient concentration (kg/m^3)
L = total amount of nutrient released to the environment (kg)

R_s = proportion of nutrient retained by the sediments (denied to water column) (%)
V = volume of water in the proposed zone (m^3)
F = the number of water body changes occurring across the period of interest

Note: R_s can be estimated as a function of flushing rate, whereby

$$R_s = \frac{1}{1 + 0.747 \text{ x } F^{0.507}} \quad (6.2)$$

By adding the present level of the dissolved nutrient to the calculated change (ΔN), a level can be predicted for any given amount of farmed fish growth. These levels can then be compared with appropriate trigger values.

The amount of nutrient lost to the environment is calculated from the amount of nitrogen added in the food (in this case it is assumed yellowtail kingfish are fed entirely on pellets), and the amount assimilated in the growth of the fish. The difference between the two represents loss to the environment. This is a very simplified first order approach, as it does not take into account any feed wastage, and it assumes that all wastes are in a dissolved form. Box 1 demonstrates a worked example of such a calculation.

The flushing rate is calculated from results on particle retention from a hydrodynamic model. The flushing time was taken (conservatively) as the time required for 100% of particles to be flushed, assuming a linear decay rate. This calculation makes the critical assumption that the water body is properly exchanged in this tidal movement, and ignores the possibility of "plug" movement, whereby the nutrients are moved out on an outgoing tide, and then straight back in again on the incoming tide. Without knowledge of the nature of the water exchange, it is not possible to quantify this effect. However, it is worth noting that in this respect, the model is not conservative, and thus underestimates accumulation. It assumes full exchange and no "plug" movement. To run the model conservatively, taking this into account effectively reduces the flushing rate to zero, and consequently, carrying capacity would be reduced substantially. Such sensitivity is a clear indication that the estimates must be treated with caution.

General parameters used in this model are (as % of wet weight)**:**
Pellet (Nova ME) nitrogen content: 7.2% (calculated from Skretting Australia fact sheet; gross protein content 45%)
Pellet (Nova ME) phosphorus content: 1.6% (Skretting Australia fact sheet)
Pellet water content: 8% (Skretting Australia fact sheet Fig 1)

Yellowtail Kingfish nitrogen content: 3.584% (assumed same as southern bluefin tuna supplied by TBOAA)
Yellowtail Kingfish phosphorus content: 0.46% (assumed same as southern bluefin tuna supplied by TBOAA)
Food Conversion Ratio 1: 3.2 (see chapter 5)
Growout period of 12 months

Other required site-specific parameters are:
Average depth (18.2 m)
Flushing Rate (21.8 turnovers/yr, see PB & SARDI 2003)
Current level of dissolved N as ammonium (14 μg N L^{-1}, c see PB & SARDI 2003)
Current level of dissolved N as nitrate (0 μg N L^{-1}, see PB & SARDI 2003)
Current level of dissolved phosphorus (19 μg P L^{-1}, see PB & SARDI 2003)
Zone area (17.04 km^2)

1. Calculate the increase in loading associated with 1kg of production - 1kg of production requires 3.2kg of food (FCR=3.2)
2. This 3.2kg represents 3.2kg x 7.2% = 230.4g of Nitrogen
3. Of this, some is retained in the form of fish growth: 1kg of growth * 3.584% = 35.84g
4. This leaves 230.4g – 35.84g as lost to the environment = 194.56g
5. Of this, a proportion is retained by sediments and not released = $1/(1+ 0.747 * 21.8^{0.507}) = 0.2191$ (or 21.91%)
6. So the amount which *is* released = (1-0.2191)*194560mg =151931mg
7. This amount is divided by the total volume of water that it can be released into (i.e. the standing volume * the number of flushes/yr) So: $151931mg / (17.04*10^6*18.2*21.8) = 2.247*10^{-5}$mg m^{-3} or $2.247*10^{-5}$$\mu$g L^{-1}
8. The above figure represents the increase in nutrient concentration for every kg of production. If (for example) 100 tonnes (100,000kg) of production is proposed then there will be an increase of $10^5 * 2.247 * 10^{-5}$$\mu$g l^{-1} or 2.247 μg L^{-1}.
9. **This increase can be calculated for any proposed level of production, and added to the existing level to predict the new level under that operational regime.**

Box 1: Example calculation of the increased load caused by aquaculture production in a 17.04 km^2 area of average depth 18.2 m, flushing rate of 21.8 yr^{-1}.

6.3.2 Original model assumptions

As with any model, a number of assumptions have had to be made:

1. The area is modelled as an individual entity, and is not under the influence of any adjacent area, nor are any other inputs, other than ambient nutrients, considered. It is assumed that the background nutrient concentrations used take into account all other activities in the area, including existing production, and thus the results show the effects of any increase in aquaculture production.

2. The proportion of nitrogen in both the feed and the fish was equal to 16% of gross protein. This assumption is routinely made when calculating nitrogen content.

3. All pellets fed to the fish were ingested.

4. All nitrogen and phosphorus lost to the environment was lost in soluble form. This is not entirely correct as several sources (Skretting Australia dietary fact sheet; Cho *et al.* 1991) would suggest that up to 20% of the waste nitrogen is in solid form and would therefore not add to the dissolved nitrogen load. However, nitrogen in the solid form is taken up, used by the benthic ecosystem, and utilised within the sediment, resulting in some proportion of this being re-released. Without knowledge of this figure, it was necessary to assume that eventually all of the waste nitrogen was converted to the soluble form in order to produce a conservative result. Similar arguments would apply to phosphorus.

5. The lack of detailed knowledge concerning the nitrogen cycle and the processes of nitrification, denitrification and ammonification also led to the need to make assumptions about the species of nitrogen being dealt with. Although marine fish release ammonium (and associated species, e.g. urea) rather than nitrate, the processes indicated above will convert some proportion of this to nitrate. Without knowledge of what this figure is, it was necessary to assume that all nitrogen released was released as ammonium when basing predictions on ammonium, and all as nitrate when nitrate was the limiting factor.

6. It is assumed that the tidal movement of the water body results in flushing with complete exchange, rather than a “plug” movement of nutrients as they slosh out of the area and then straight back in again.

6.3.3 New model parameters

Based on the data presented earlier in this report, a number of the parameters detailed above were recalculated. In this case, all percentages are expressed as percentage of dry weight, compared to wet weight above, so feed water content is not needed.

Pellet nitrogen content: 7.1%
Pellet phosphorus content: 1.48%
Yellowtail Kingfish nitrogen content: 11.2%
Yellowtail Kingfish phosphorus content: 1.1%
Food Conversion Ratio 1: 3.1

Current level of dissolved N as ammonium (20 μg N L^{-1}, see Tanner & Bryars 2006)
Current level of dissolved N as nitrate (5 μg N L^{-1}, see Tanner & Bryars 2006)
Current level of dissolved phosphorus (5 μg P L^{-1}, see Tanner & Bryars 2006)

6.3.4 New model description

As well as providing new parameter estimates, the work detailed earlier in this report allowed several model assumptions to be eliminated. Equation 6.1, which predicts the change in nutrient concentration, was modified in the new model to take into account the fact that we now know what proportion of nitrogen and phosphorus in the feed is released in dissolved form. The new equation then became:

$$\Delta N = \frac{L_D}{V \text{ x } F} \qquad (6.3)$$

where ΔN = the change in dissolved nutrient concentration (kg/m^3)
L_D = total amount of nutrient released to the environment in dissolved form (kg)
V = volume of water in the proposed zone (m^3)
F = the number of water body changes occurring across the period of interest

In addition, assumptions 2, 3 & 4 above have been dispensed with in this new formulation, although assumptions 1, 5 & 6 still hold.

6.4 Results

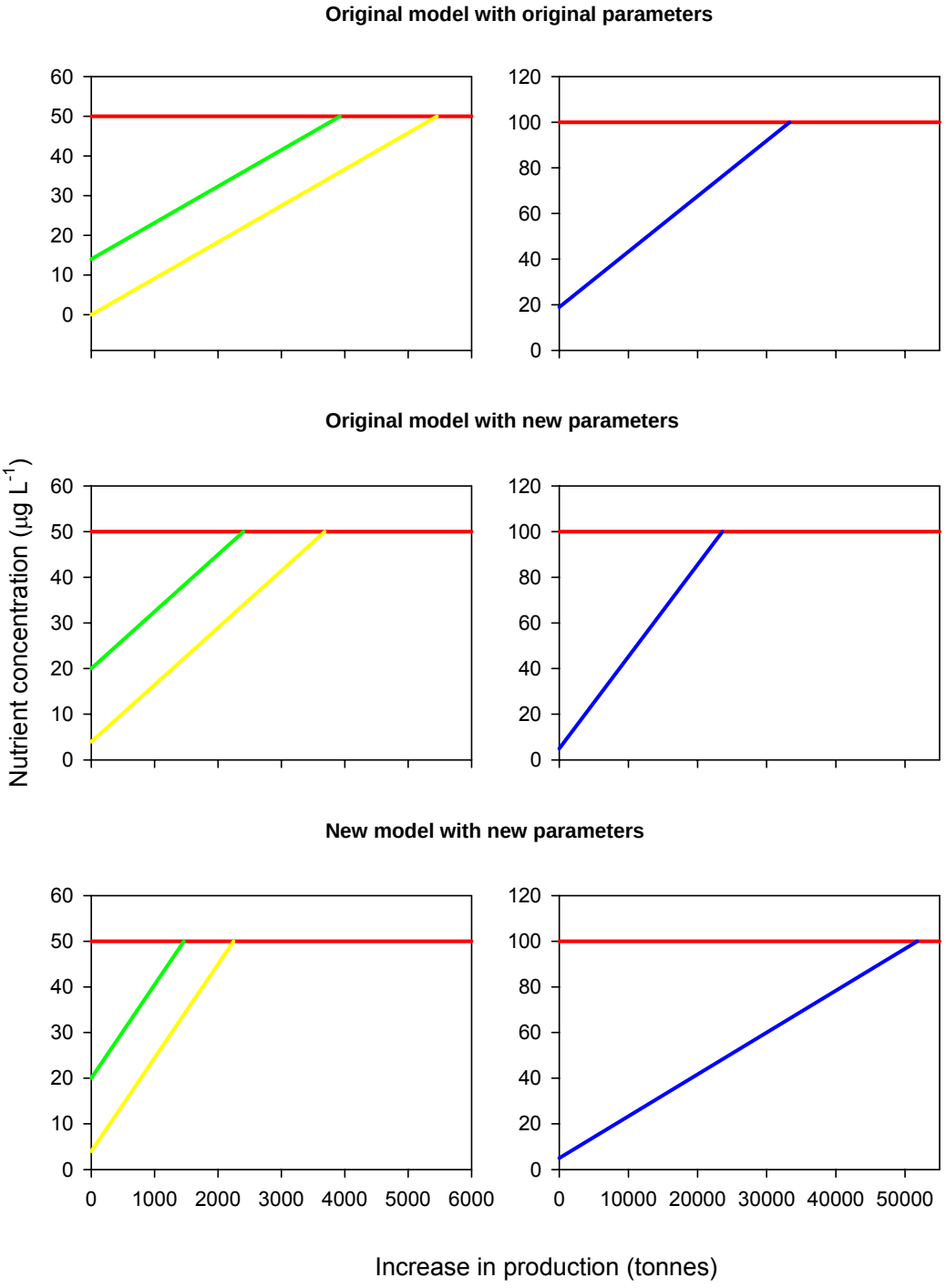

Figure 6.1: Predicted changes in concentration of ammonia, nitrate and phosphate dissolved in the water column as a function of increases in production in the Fitzgerald Bay yellowtail kingfish farming zone. Green represents ammonia, yellow nitrate and blue phosphate. Horizontal red lines indicate threshold values for South Australian waters as per ANZECC / ARMCANZ (2000).

The latest version of the model predicts that a maximum increase of 1463 tonnes over the current annual production of ~ 2000 tonnes is permissible in the Fitzgerald Bay aquaculture zone, before the water quality guidelines are exceeded (based on ammonia, Fig 6.1). It can be seen that at each step in the model's refinement, the predicted carrying capacity of this zone has decreased, with the original model predicting an allowable increase of 3927 tonnes. All nutrients examined follow this pattern, with the exception that reformulating the model led to a decrease in the rate at which dissolved phosphorus accumulates in the water column. This reversal is most likely due to the very high proportion of phosphorus inputs that are released to the water column in a particulate form (69-73%, chapter 5).

6.5 Future directions for the finfish carrying capacity model

There are several factors that need to be addressed and improved to develop a better estimate of likely production based on the build-up of dissolved nutrients around finfish pontoons. A few important points are outlined below:

1. The current nutrient levels in the water column are based on field measurements made at a single point in time. There are several other sets of nutrient data available, each of which is also from a single point in time, and these indicate that nutrient levels can be highly variable. It would thus help to further refine carrying capacity if we had a good understanding of how nutrient levels vary over time, both in the short-term and over an entire year. If the nutrient levels used are indicative of a transient spike, then the carrying capacity indicated may be an underestimate, whereas if it is a transient low it might be an overestimate. Levels of ammonia and nitrate measured by Parsons Brinkerhoff & SARDI Aquatic Sciences (2003), and used here as the 'original' parameters were somewhat lower than the new levels used, whereas phosphate was considerably higher. On the other hand, measurements made by Fernandes & Tanner (unpublished) in May 2005 showed ammonia and nitrate to be 26 & 6 μg N L^{-1} respectively, both somewhat higher than the values used here, while phosphate was < 1 μg P L^{-1}.

2. The lack of detailed knowledge concerning the nitrogen cycle and the processes of nitrification, denitrification and ammonification also led to the need to make assumptions about the chemical species of nitrogen being dealt with. Although marine fish release ammonium (and associated compounds such as urea) rather than nitrate, the processes indicated above will convert some proportion of this to nitrate. Without knowledge of what this figure is, it was necessary to assume that all nitrogen released was released as ammonium when basing predictions on ammonium, and all as

nitrate when nitrate was the limiting factor. This is an area that needs to be further investigated.

3. A better understanding of water movement in the tuna farming zone is needed to allow an improved estimate of flushing rate. Currently it is assumed that any nutrients moved out of the zone do not return, whereas this assumption is unlikely to be correct. The development of a proper hydrodynamic model for the area will allow particle movements to be traced and accurate flushing times to be estimated.

4. The model assumes that production rates are constant. This assumption is needed because fish are grown out over a two-year period. So, for example, a harvest of 1000 tonnes might be achieved through 400 tonees of growth in year one, and 600 tonnes in year 2. If production is constant, there will be 400 tonnes of 1 year old fish produced in year 2, giving a total production of 1000 tonnes for that year, and thus 1000 tonnes harvested equals 1000 tonnes grown that year. If production is increasing rapidly, then more 1-year old fish will be produced in year 2, and the model output will have to be interpreted in terms of amount of fish grown, and not amount harvested. The reverse will occur if production is decreasing rapidly.

6.6 Acknowledgements

This work received funds from PIRSA Aquaculture & FRDC. We wish to thank Jeff Buchanan, Peter Petrusevics and Steve Clarke for useful discussions and provision of data.

6.7 References

ANZECC/ARMCANZ (2000). Australian and New Zealand Guidelines for Fresh and Marine Water Ecology. Canberra.

ANZECC (1992) Australian and New Zealand Guidelines for Fresh and Marine Water Ecology – DRAFT. Canberra.

Bergheim, A., Aabel, J. P., Seymour, E. A. (1991) Past and present approaches to aquaculture waste management in Norwegian net pen culture operations. In. 'Nutritional strategies and aquaculture waste'. (Eds. C. B. Cowey, C. Y. Cho). Pp 117-136. University of Guelph, Guelph.

Beveridge, M. C. M. (1987) Cage Aquaculture. Fishing News Books Ltd, Surrey, England.

Campbell, D. E. & Newell, C. R. (1998). MUSMOD©, a production model for bottom culture of the blue mussel, *Mytilus edulis* L. *Journal of Experimental Marine Biology and ecology*, 219: 171-203.

Cho, C. Y., Hynes, J. D., Wood, K. R., Yoshida, H. K. (1991) Quantification of fish culture wastes by biological (nutritional) and chemical

(limnological) methods; the development of high nutrient dense (hnd) diets. In. 'Nutritional Strategies & Aquaculture Waste'. (Eds. C. B. Cowey, C. Y. Cho). Pp 37-50. University of Guelph, Guelph.

Cromey, C. J., Nickell, T. D., Black, K. D. (2000) A model for predicting the effects of solids deposition from mariculture to the benthos. The Scottish Association for Marine Science (SAMS), Oban.

Cronin, E. (1995) An investigation into the effects of net fouling on the oxygen budget of southern bluefin tuna (*Thunnus maccoyii*) farms. Honours Thesis, University of Adelaide, Adelaide.

Ellis, D. & Rough, K. (2005) Quality and nutritional evaluation of baitfish used for SBT farming (including baitfish profiles). Aquafin CRC, Adelaide.

Ervik, A., Hansen, P. K., Aure, J., Stigebrandt, A., Johannessen, P., Jahnsen, T. (1997) Regulating the local environmental impact of intensive marine fish farming. I. The concept of the MOM system (modelling-ongrowing fish farms-monitoring). *Aquaculture* **158**, 85-94.

Fernandes, M. (2006). Tuna Waste Mitigation. Aquafin CRC/FRDC final report in preparation (FRDC 2001/103). SARDI Aquatic Sciences, Adelaide.

Fernandes, T. F., Eleftheriou, A., Ackefors, H., Eleftheriou, M., Ervik, A., Sanchez-Mata, A., Scanlon, T., White, P., Cochrane, S., Pearson, T. H., Read, P. A. (2001). The scientific principles underlying the monitoring of the environmental impacts of aquaculture. *Journal of Applied Ichthyology* **17**, 181-193.

Findlay, R. H., Watling, L. (1994) Toward a process level model to predict the effects of salmon net-pen aquaculture on the benthos. In. 'Modelling benthic impacts of organic enrichment from marine aquaculture'. (Eds. B. T. Hargrave). Pp 47-77. Canadian Technical Report of Fisheries and Aquatic Sciences 1949, Canada.

Fox, W. P. (1990). Modeling of particulate deposition under salmon net-pens. In 'Final Programmatic Environmental Impact Statement. Fish Culture in Floating Net-Pens (Technical Appendices)'. Washington State Department of Fisheries, Olympia, USA.

Gowen, R. J., Smyth, D., Silvert, W. (1994) Modelling the spatial distribution and loading of organic fish farm waste to the seabed. In 'Modelling Benthic Impacts of Organic Enrichment from Marine Aquaculture'. (Eds. B. T. Hargrave). Pp 19-30. Canadian Technical Report of Fisheries and Aquatic Sciences 1949, Canada.

Henderson, A., Gamito, S., Karakassis, I., Pederson, P., Smaal, A. (2001) Use of hydrodynamics and benthic models for managing environmental impacts of marine aquauclture. *Journal of Applied Ichthyology* **17**, 163-172.

Jover, M., García-Gómez, A. Tomás, A., De la Gándara, F. and Pérez, L. (1999). Growth of Mediterranean yellowtail (*Seriola dumerilii*) fed extruded diets containing different levels of protein and lipid. *Aquaculture*, 179: 25-33.

Panchang, V., Cheng, G., Newell, C. (1997) Modeling hydrodynamics and aquaculture waste transport in coastal Maine. *Estuaries* **20**, 14-41.

Parsons Brinkerhoff & SARDI Aquatic Sciences (2003) Technical review for aquaculture management plans – phase 2: Volume A Upper Spencer Gulf. Produced for PIRSA Aquaculture, Adelaide.

Pearson, T. H., Black, K. D. (2001) The environmental impacts of marine fish cage culture. In. 'Environmental Impacts of Aquaculture'. (Eds. K. D. Black). Pp 1-31. (Sheffield Academic Press, Sheffield, UK).

Petrusevics, P. (1998) Estimate of the carrying capacity of the Fitzgerald Bay aquaculture management zone. Prepared for Primary Industries and Resources of South Australia (Aquaculture Group), by Oceanic Perspectives.

Read, P. A., Fernandes, T. F., Miller, K. L. (2001) The derivation of scientific guidelines for best environmental practice for the monitoring and regulation of marine aquaculture in Europe. *Journal of Applied Ichthyology* **17**, 146-152.

Silvert, W. (1992) Assessing environmental impacts of finish aquaculture in marine waters. *Aquaculture* **107**, 67-71.

Silvert, W. (1994a) Modelling benthic deposition and impacts of organic matter loading. In. 'Modelling benthic impacts of organic enrichment from marine aquaculture'. (Eds. B. T. Hargrave). Pp 1-18. Canadian Technical Report of Fisheries and Aquatic Sciences 1949, Canada.

Silvert, W. (1994b) Modelling environmental aspects of mariculture: Problems of scale and communication. In 'Proceedings of the Canada – Norway Workshop on environmental impacts of Aquaculture'. (Eds. A. Ervik, P. Kupka Hansen, P Wennevik, V. Wennevik). Pp 61-68. Fisken og Havet 13.

Silvert, W., Cromey, C. J. (2001) Modelling Impacts. In. 'Environmental Impacts of Aquaculture'. (Eds. K. D. Black). Pp 154-181. (Sheffield Academic Press, Sheffield, UK).

Silvert, W., Sowles, J. W. (1996) Modelling environmental impacts of marine finfish aquaculture. *Journal of Applied Ichthyology* **12**, 75-81.

Tanner, J. E. (2006) Aquafin CRC – Southern bluefin tuna aquaculture subprogram: Tune environment subproject – Development of regional environmental sustainability assessments for tuna sea-cage aquaculture. SARDI Aquatic Sciences, Adelaide.

Zar, J. H. (1984) Biostatistical Analysis (Second Edition). Prentice-Hall International (UK) Limited, London.

Chapter 7: Conclusions

7.1 Benefits and adoption

The nutrient budgets and carbon deposition and carrying capacity model presented here will allow PIRSA Aquaculture to make decisions on lease allocations and total allowable stocking densities in Fitzgerald Bay with greater confidence. This information can also be used in other areas of South Australia where yellowtail kingfish are farmed, providing that farming practises are similar to those on which the data given here were based. In the case of the carbon deposition model, a current vector will have to be obtained that is specific for the area being considered, but all other parameters should be transferable. The current vector used here was derived from data provided for an earlier project that considered a number of potential aquaculture areas around the state, so it would be easy to derive current vectors for these areas.

The South Australian EPA and DEH have also indicated an interest in the nutrient model in particular, with the intention of using it for assessing new applications. Both have requested that this model be further developed by incorporating a user-friendly interface. Similarly, the WA Department of Fisheries have indicated that they would be interested in using these models to assist in informing the development of the aquaculture industry in their state.

As well as PIRSA Aquaculture, farm managers will be able to utilise the carbon deposition model to investigate patterns of carbon deposition within a lease. This information will allow them to make decisions on how to arrange pens so as to minimise areas of overlap, and thus of high sedimentation. This model is available in a user firiendly format, which can be provided by the author to managers and/or industry if they are interested.

The metabolic data are potentially useful to industry also, in that it will give them a greater understanding of the oxygen requirements of their fish. This understanding could enable industry to reduce stress imposed on their fish through reduced oxygen levels.

7.2 Further development

Perhaps the most useful further development of both the carbon deposition model and the nutrient budgets presented here would be to combine them with a hydrodynamic model. If such a model was used to obtain a continuous 1-year current vector, instead of the one used here, which was derived from 15-day current vectors typical of each season, it will allow a more precise prediction of carbon deposition patterns. Combining the

hydrodynamic model with the nutrient budgets will allow the build-up of nutrients within Fitzgerald Bay to be predicted, as well as an understanding of where they are dispersed to.

A range of government management agencies (PIRSA Aquaculture, DEH & EPA in South Australia, and Department of Fisheries in Western Australia), have also requested that both of these models be developed further. In the case of the carbon deposition model, the incorporation of a benthic processing module has been requested, allowing carbon to be removed from the system and the effects of fallowing to be predicted. For the nutrient model, desired enhancements include the development of a user-friendly interface, the ability to compare several scenarios at once, and the ability to farm a mic of species in a single zone (including finfish, abalone, bivalves and macroalgae). By incorporating macroalgae, nutrients can actually be extracted from the system. With this development, it would be possible to set a nutrient cap on a zone, and the model would provide a tool for investigating a range of trade-offs that can be used to increase production while remaining within the cap. The small amount of funding required to pursue these developments is being sought from the Aquafin CRC technology transfer program, as both models have been applied to tuna as part of Aquafin CRC projects.

It may also be useful for farm managers to develop an oxygen model for individual pens. Such a model is currently being developed for the tuna industry as part of the Aquafin CRC, and will allow farmers to understand how different tidal conditions, net fouling loads, and feeding regimes could contribute to fish stress through decreased oxygen availability.

7.3 Planned outcomes

1. An understanding of how wastes produced by yellowtail kingfish are partitioned in the environment.

This project has greatly increased our understanding of how the key constituents of the wastes produced by YTK farming are partitioned in the environment. The nitrogen and phophorus budgets presented in chapter 4 show how both of these elements are partitioned between dissolved, suspended and sedimented fractions, and what components they are likely to accumulate in. The carbon deposition model shows how solid wastes are likely to be distributed on the seafloor around a series of pens (or a single pen).

2. An understanding of nutrient outputs from yellowtail kingfish cages, and how they relate to natural spatial and temporal variation in nutrient levels.

The nutrient budgets presented here provide us with a much greater understanding of the nutrient outputs from YTK cages. These outputs are placed into the context of other anthropogenic sources of nutrients, as well as current standing stocks in the Fitzgerald Bay aquaculture zone.

3. A refined model of nutrient loads in aquaculture zones, enabling better management of these zones in an environmentally sustainable fashion.

The nutrient budgets and model developed here provide a much better model of nutrient loads than what has been available previously. While they are specific to Fitzgerald Bay, providing farming practises are similar, they should be transferable to other coastal areas of South Australia. The better understanding of nutrient inputs that these budgets give has allowed refinement of the carrying capacity model, and will allow improved management by allowing PIRSA Aquaculture to specify maximum stocking levels for a zone with greater certainty.

Appendix 1: Intellectual property

The distribution of this report is restricted, and approval is required from PIRSA Aquaculture for access.

The Carbon deposition model (Farmér) is jointly owned by SARDI and Aquafin CRC, although the IP associated with the parameterisation file for YTK is a part of this project.

Appendix 2: Staff

SARDI:
Dr Jason Tanner (Principal investigator)
Dr Milena Fernandes (Co-investigator)
Ms Sharon Drabsch
Ms Yvette Eglinton
Mr Michael Guderian
Dr Peter Lauer
Mr Bruce Miller-Smith
Ms Genevieve Mount
Mr Arron Strawbridge
Ms Sonja Venema

Adelaide University:
Mr Quinn Fitzgibbon (Co-investigator)
Dr Roger Seymour (Co-investigator)
Dr Timothy Clark